III International Conference on Applications of Optics and Photonics

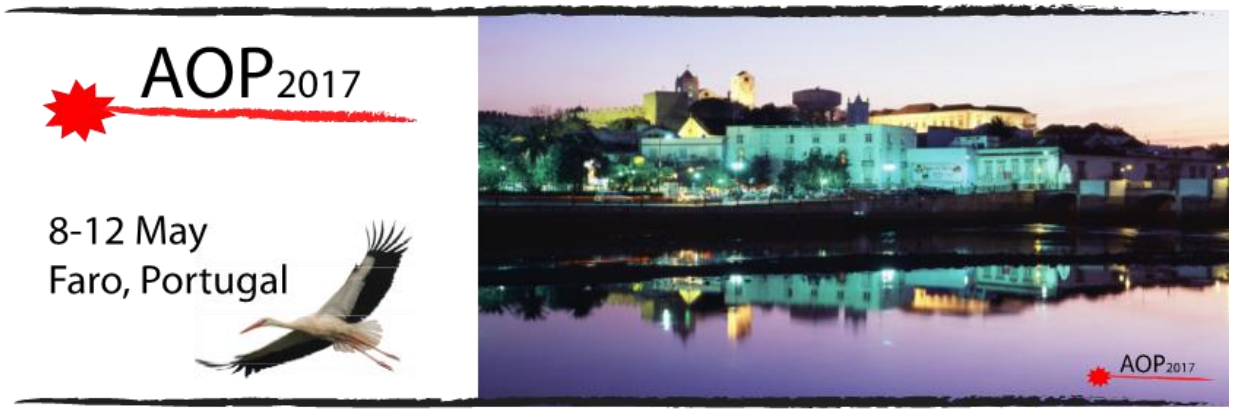

Booklet of Abstracts

SPOF

SPOF, Portuguese Society for Optics and Photonics *www.optica.pt*

AOP2017 Program Overview

Monday (May 08)	Tuesday (May 09)	Wednesday (May 10)	Thursday (May 11)	Friday (May 12)
8:30 - 9:00 Registration	8:30 - 9:00 **Registration**	8:30 - 9:00 Registration	8:30 - 9:00 Registration	8:30 - 9:00 Registration
	9:00 - 9:45 Plenary session **Fabrice Laussy**	9:00 - 9:45 Plenary session **Jürgen Jahns**	9:00 - 10:45 Plenary session **Robert Lieberman**	9:00 - 10:45 Parallel sessions **Fr.1.a | Fr.1.b | Fr.1.c**
	9:45 - 10:45 Parallel sessions **Tu.1.a | Tu.1.b | Tu.1.c**	9:45 - 10:45 Parallel sessions **We.1.a | We.1.b | We.1.c**	9:45 - 10:45 Parallel sessions **Th.1.a | Th.1.b**	
10:30 - 11:00 Opening Ceremony	10:45 - 11:15 Coffee break	10:45 - 11:15 Coffee break	10:45 - 11:15 Coffee break	10:45 - 11:15 Coffee break
11:00 - 12:30 Plenary session **Rainer A. Leitgeb** and **Humberto Michinel**	11:15 - 12:30 Parallel sessions **Tu.2.a | Tu.2.b**	11:15 - 12:30 Parallel sessions **We.2.a | We.2.b | We.2.c**	11:15 - 12:30 Parallel sessions **Th.2.a | Th.2.b**	11:15 - 12:30 Awards & Closing Ceremony
12:30 - 14:00 Lunch	12:30 - 14:00 Lunch	12:30 - 14:00 Lunch	12:30 - 14:00 Lunch	
14:00 - 15:30 Parallel sessions **Mo.1.a | Mo.1.b | Mo.1.c**	14:00 - 14:45 Plenary session **Pramod Rastogi**	14:00 - 18:00 **Excursion** **(Ria Formosa)**	14:00 - 14:45 Plenary session **Jesús Lancis**	
15:30 - 16:00 Coffee break	14:45 - 16:00 Parallel sessions **Tu.3.a | Tu.3.b**		14:45 - 16:00 Parallel sessions **Th.3.a | Th.3.b | Th.3.c**	
16:00 - 18:00 Parallel sessions **Mo.2.a | Mo.2.b | Mo.2.c**	16:00 - 17:00 Coffee break & Poster session - **Tu.P**		16:00 - 17:00 Coffee break & Poster session - **Th.P**	
	17:00 - 18:00 Parallel sessions **Tu.4.a | Tu.4.b | Tu.4.c**		17:00 - 18:00 SPOF' General Assembly or Parallel Session	
19:30 - 21:00 **Welcome Reception**			19:30 - 22:00 **Conference Dinner**	

AOP2017 - Provisional Program (*abstract #*)

Day	Parallel session' designation	*Plenary lectures (45 min)*	*Keynote lectures (30 min)*	*Invited lectures (20 - 25 min)*	*Orals (15 min)*
May 8	Pl1	Rainer A. Leitgeb			
May 8	Pl2	Humberto Michinel			
May 8	Mo.1.a			169	47, 76, 162, 7
May 8	Mo.1.b				57, 222, 97, 20, 202
May 8	Mo.1.c				13, 23, 58, 135, 203
May 8	Mo.2.a		163		15, 21, 27, 30, 133
May 8	Mo.2.b		64	235, 96	35, 241, 139
May 8	Mo.2.c			65	6, 137, 196, 114, 199, 105
May 9	Pl3	Fabrice Laussy			
May 9	Tu.1.a		242		28, 22
May 9	Tu.1.b		182		87, 179
May 9	Tu.1.c				170, 174, 52, 54
May 9	Tu.2.a			56	5, 98, 125
May 9	Tu.2.b			44,46	20, 25
May 9	Pl4	Pramod Rastogi			
May 9	Tu.3.a			164, 66	59, 74, 93

May 9	Tu.3.b			158	108, 171
May 9	Tu.4.a		166	186	208
May 9	Tu.4.b			155	177, 223
May 9	Tu.4.c				124, 145, 150, 192
May 10	Pl5	Jürgen Jahns			
May 10	We.1.a				219, 220, 221, 210, 232
May 10	We.1.b				50, 8, 14, 111
May 10	We.1.c		175		11, 12
May 10	We.2.a			146, 138	68, 115
May 10	We.2.b			190	45, 95, 180, 103
May 10	We.2.c				24, 101, 226, 231, 159
May 11	Pl6	Robert Lieberman			
May 11	Th.1.a.				75, 213, 110, 200
May 11	Th.1.b		239		3, 234, 238
May 11	Th.2.a				26, 63, 152, 191, 230
May 11	Th.2.b		173	38, 228	
May 11	Pl7	Jesús Lancis			
May 11	Th.3.a				117, 118, 120, 153
May 11	Th.3.b				141, 142, 83, 224, 144, 131
May 11	Th.3.c/iBROW		211	194, 209	

May 12	Fr.1.a		132	136, 188	204, 205, 74
May 12	Fr.1.b			116	62, 79, 82, 92 , 94, 113
May 12	Fr.1.c/iBROW		216	193	9, 10

		Posters (60 min)
May 9		32, 40, 81, 91, 125, 201, 148
May 9		41, 51, 154, 160, 161, 167, 183, 198
May 9		17, 37, 43, 49, 53, 55, 67, 112, 127, 143, 156, 165, 185, 233, 237
May 9		176, 240, 217, 218
May 11		36, 60, 214, 215
May 11		48, 210, 225, 236, 243
May 11		34, 77, 78, 80, 126, 84, 90
May 11		39, 61, 88, 168, 178, 197, 54
May 11		42, 104, 107, 109, 119, 187, 189, 195
May 11		2, 19, 86, 99, 100, 102, 121, 122, 134, 140, 151, 207

Provisional schedule of parallel sessions

Keynote, invited and regular talks
Abstract # and main author (Invited and keynote lectures are underlined)

Monday 8		
Mo.1.a	Mo.1.b	Mo.1.c
169 M. T. Flores-Arias	057 V. F. Duma	013 L. S. Supian
047 H. Pires	222 A. Popov	023 D. Wawrzynczyk
076 C. P. João	097 A. F. Pérez	058 C. M. Vicente
162 A. Boyle	020 F. Wahaia	135 F. Almabouada
007 N. Suhaimi	202 V. Kumar	203 F. R. Lorenzo
Mo.2.a	Mo.2.b	Mo.2.c
163 Y. P. Rakovich (*Keynote*)	064 B. T. Barrett (*Keynote*)	065 J. Vazquez-Dorrio
015 I. Fuks-Janczarek	235 P. M. Serra	006 F. Velosa
021 A. Fantoni	096 S. M. Franco	137 D. Hincapie-Zuluaga
027 C. R. Bernardo	035 S. M. Perinchery	196 D. Rodriguez
030 M. Ghafoor	241 K. Panke	114 J. F. Kuhne
133 J. Borges	139 V. Pereira	199 Y. Arosa
		105 I. Radkowska

Tuesday 9		
Tu.1.a	Tu.1.b	Tu.1.c
242 W. T. Rhodes (*Keynote*)	182 P. T. Fiadeiro (*Keynote*)	170 J. C. L. Carreño
028 T. Döhring	087 E. Acosta	174 E. Rivera-Pérez
022 D. C. Alves	179 A. M. Ionescu	052 P. Smid
		054 Y. O. Barmenkov
Tu.2.a	Tu.2.b	
056 M. Melgosa	044 H. Terças	
005 I. Silva	046 J. D. Rodrigues	
098 A. F. G. Ferreira	025 A. L. Aragón	
125 L. J. Herrera	085 N. A. Silva	
Tu.3.a	Tu.3.b	
164 E. del Valle	158 H. Bértolo	
066 A. Guerreiro	108 A. R. R. Tuna	
059 A. Souto	171 A. F. Macedo	
093 Y. G. Vela		

Tu.4.a	Tu.4.b	Tu.4.c
166 I. Meglinski (*Keynote*) 186 M. M. P. Gómez 208 S. Agarwal	155 B. Romeira 177 G. G. M. Fernandes 223 J. M. V. Ortiz	124 R. I. Martin 145 A. D. Gomes 150 J. H. Osório 192 G. Chesini

Wednesday 10		
We.1.a	We.1.b	We.1.c
210 A. I. C. Machado 219 K. Raja 220 K. Raja 221 Y. Sheikhnejad 232 N. S. M. Rojo	050 D. Benedicto 008 F. C. Moreira 014 R. Miedzinski 111 S. M. G. Rodrigues	175 M. C. R. Medeiros (*Keynote*) 011 M. Vieira 012 M. A. Vieira
We.2.a	We.2.b	We.2.c
146 H. J. Kalinowski 138 W. Margulis 068 M. M. P. Gómez 115 L. Beltran	190 J. Javaloyes 045 D. Benedicto 095 H. Abbasi 180 A. V. Kir'yanov 103 M. A. Bani	024 M. Żelechower 101 S. G. Stanciu 226 L. R. Pereira 231 P. Brągiel 159 S. V. Pasechnik

Thursday 11		
Th.1.a	Th.1.b.	
075 L. Coelho 213 H. Vilhena 110 U. J. Dreyer 200 M. S. Nascimento	239 M. Martínez-Corral (*Keynote*) 234 A. Reyes 3 M. Costa 238 P. Rodríguez-Montero	
Th.2.a	Th.2.b	
026 P. L. Antunes 063 P. Lourenço 152 J. M. V. Ortiz 191 J. Sabino 230 L. Pereira	173 L. Plaja (*Keynote*) 228 E. Solarte-Rodriguez 038 J. M. Vieira	
Th.3.a	Th.3.b	Th.3.c

117 N. A. Carvajal 118 G. Rodríguez 120 T. E. C. Magalhães 153 J. M. V. Ortiz	141 A. D. Gomes 142 P. L. Inácio 083 M. F. Domingues 224 G. Sagias 144 C. S. Monteiro 131 S. Silva	211 M. Naftaly (*Keynote*) 194 H. I. Cantu 209 J. Wang

Friday 12		
Fr.1.a	Fr.1.b	Fr.1.c
132 O. Frazão (*Keynote*) 136 M. S. Ferreira 188 H. F. Martins 074 R. A. Alves 204 S. Novais 205 M. F. S. Ferreira	116 A. Guzman 062 A. V. Mazhukin 079 M. B. T. Gomes 082 V. P. Minkovich 092 R. A. de la Osa 094 P. Palevicius	216 F. Hartmann (*Keynote*) 193 S. Watson 009 G. C. Rodrigues 010 J. F. M. Rei

Posters

Tuesday 9		
017 P. Solarz	080 J. C. Costa	165 L. J. Miranda Díaz
032 U. Bazylinska	081 N. Ornelas-Soto	167 S. M. Franco
037 R. Lisiecki	091 M. Rodríguez-Delgado	176 N. Majewska
040 M. Aymerich	*112 M. Labidi*	183 D. H. Zuluaga
041 H. Pena-Verdeal	123 M. Salas	185 A. Khodko
043 Á. Sanz-Felipe	127 M. Nespereira	198 O. O. Myakinin
049 V. P. Minkovich	143 R. Lima	201 W. Gao
051 C. García-Resúa	148 E. Benjumea	217 A. Arellanes
053 E. Dunaeva	154 M. Aymerich	218 J. A. Rodrigues
055 S. Labidi	156 J. Sniķeris	229 E. E. R. Vera
067 I. Aguilar	160 S. M. Franco	233 M. Kumar
	161 S. M. Franco	237 E. E. R. Vera
		240 A. Arellanes
Thursday 11		
002 F. Diaz-Otero	086 N. A. Silva	140 J. C. G. Sande
019 R. Martínez-Herrero	088 M. B. T. Gomes	151 J. M. V. Ortiz
034 M. P. Cardoso	090 M. B. T. Gomes	168 V. Hariton
036 A. Shinde	099 A. Guerreiro	178 A. Boyle
039 D. Maluenda	100 J. Fernandes	187 V. G. Krasilenko
042 B. Vázquez-Dorrío	102 R. Martinez-Herrero	189 E. Tcarenkova
048 C. Rodrigues	104 D. A. A. Padilla	195 W. D. Furlan
054 Y. O. Barmenkov	107 F. A. Donado	197 F. Cambronero-López
060 L. A. D. Marulanda	109 D. A. A. Padilla	207 S. M. G. Rodrigues
061 V. I. Mazhukin	119 G. Dutra	214 X. Roselló-Mechó
077 J. C. Costa	121 J. C. Pérez	215 L. Poveda-Wong
078 R. A. Alves	122 C. J. J. Ruiz	225 J. M. V. Ortiz
084 N. A. Silva	126 H. Vilhena	236 J. M. V. Ortiz
	134 S. Horta	243 P. Lopez-Higuera

AOP2017' Plenary Lectures

Modern trends in optical coherence tomography

Rainer A. Leitgeb, Christian Doppler Lab., Medizinische Univ. Wien (Austria)

Optical Coherence Tomography (OCT) has been the most successful optical medical imaging technique in the last decades that has been rapidly developing and gained by many orders of magnitudes in performance. As an optical technique it is limited in penetration to the first millimetres of tissue, but effectively compensates for this drawback by its optical resolution close to the level of histology, its non-invasiveness, cost-effectiveness, imaging speed of already several volumes per second, and easy operation. In terms of resolution and penetration depth it can be seen as link between standard microscopic techniques, that need in general elaborate sample preparation and are limited in penetration to a few 100 micrometres and below, and full-body imaging techniques which provide in general inferior resolution, or employ ionizing radiation. Today, OCT has already become the standard technique for retinal diagnostics. Novel applications are following up with commercial instruments in dermatology, dentistry, endoscopy, and intravascular imaging. In-situ tissue assessment with microscopic resolution and high specificity, i.e., non-invasive optical biopsy, is still an important goal in OCT. Extensive research is therefore directed to exploit the rich functional imaging capabilities of OCT, including needle/lable-free OCT angiography, polarization sensitive OCT, spectroscopic OCT, and optical elastography. On the technology side, integrated optics and new compact light source development show already today exciting capabilities of miniaturizing complex optical systems. OCT on a chip - enabling OCT of the size of a pen or a modern cell phone, or even adapted to it- might be soon reality leading to easy and cheap point of care diagnosis.

Simulating dark matter with photonic systems

Humberto Michinel, Angel Paredes, Univ. de Vigo (Spain)

A model of dark matter is present, assuming that it takes the form of a coherent matter wave of ultralight axions. The mathematical description is obtained in terms of a system of nonlinear Schrodinger-Poisson equations, which are well-known in Optics and other fields of Physics. A split-step pseudospectral numerical calculation method is used to compute the evolution in time of dark matter clumps and to explain the so-called "offsets" between dark matter and galaxies in cosmic clusters. Formal connections to laser beam propagation in thermo-optical media are stablished, leading to proposals of tabletop photonic analogues of cosmological phenomena such as the connection between supermassive black holes and dark matter distributions.

Quantum effects with polaritons

Fabrice P. Laussy, Universidade Autónoma de Madrid (Spain)

Polaritons are superpositions of light and matter that combine their antagonist properties, endowing them with unique properties thanks to which they have demonstrated to be on par with cold-atoms physics, from displaying Bose-Einstein condensation (up to room temperature) to implementing metamaterials and black hole analogues. A major prospect for polaritons is quantum-based technology, as strongly-interacting photons. I will show how, by exciting polaritons directly with quantum light [PRL, 115:196402, 2015 & PRA, 94:063826,2016], we have succeeded in creating the first non-classical state of the polariton field [arXiv:1609.01244, 2016], robust to dephasing, and how we probed polariton interactions down to the single particle level. Our results suggest that a polariton qubit would be able to undergo a pi phase-shift induced by its interactions with one other polariton only, thus providing an on-chip nonlinear CNOT gate.

Multidimensional deformation measurements using holographic interferometry

Pramod Rastogi, Ecole Polytechnique Fédérale de Lausanne (Switzerland)

The applicability of the state-of-the-art optical methods for multi-dimensional deformation measurements is strongly limited by their reliance on sequential operations and complex experimental configurations. Hence, it is essential to develop vastly more targeted ways to address this issue. This has primarily lead to research focused on understanding and implementing processes needed for supporting information embedded in multi-wave interferometers. This talk presents an overview of estimation techniques based on spectral decomposition that have been proposed by the authors to address the problem, and summarizes various aspects based on accuracy and data frames.

Spatio-temporal processing of ultra-short pulses with micro optics

Jürgen Jahns, Fern-Univ. Hagen (Germany)

Ultrashort pulses with time durations on the femtosecond scale can be suitably processed by microoptical devices. The temporal impulse response of an element is determined by its spatial structure, its action in the temporal domain can be conveniently described by its impulse response. All categories of elements can be used: refractive, diffractive and reflective. Here, the basic concepts are discussed and several examples for shaping and filtering short pulses are presented.

Optical waveguide sensors: submicron to supra-kilometer

Robert A. Lieberman, Lumoptix LLC (United States)

The advancement of optical waveguide technology has been driven by interplay between the development of techniques for sensing and for communications. This interplay has resulted in sensors capable of measuring physical and chemical properties at length scales comparable to entire railroad tunnels, comparable to cellular organelles, and a panoply of point sensors, distributed sensors, and sensor arrays for every length scale in between. As new waveguide-related technologies emerge, exciting new opportunities are arising to extend this range even further.

Computational imaging with a single-pixel photosensor

Jesús Lancis, Enrique Tajahuerce, Pere Clemente, Fernando Soldevila, Univ. Jaume I (Spain)

The single-pixel imaging (SPI) scheme introduced in 2007 at Rice University has gained considerable attention during the past few years thanks to the advent of spatial light modulators with remarkable features in terms of spatial resolution and frame speed. In this talk, we will show the ability of the computational single-pixel camera for multidimensional imaging by use of dedicated sensors. Also, we will exploit the unique features of this device to develop an optical camera for seeing objects completely embedded inside a turbid medium with high-resolution. Finally, applications in optical microscopy and the design of an ophtalmoscope for imaging the retina of the living eye will be presented.

AOP2017' Keynote Papers

An overview of the rationale and evidence for vision training in elite sports players and officials *(Keynote Presentation)*
Paper AO100-64
Author(s): Brendan T. Barrett, Univ. of Bradford (United Kingdom)

In this lecture I will briefly examine the strength of the evidence from the literature to support the rationale and claims supporting vision training in elite level sports players and officials. I will also present some of our results from studies of vision and elite-level sports performance/officiating. This research area is of interest to many because of the huge potential that vision training may present, e.g. to enable elites to perform even better or to identify elite potential in promising young athletes. This is reflected in the many online programs which are now offered to sports players/coaches (e.g. EyeGym, Neurotracker). The literature provides clear evidence that experts are better than non-experts in picking up perceptual cues and that they exhibit different visual search behaviours. However, evidence that clinical measures of vision are better in experts or that vision training is beneficial is less robust. Overall, therefore this is an unfolding story.

New challenges in Fabry-Perot cavity for sensing applications *(Keynote Presentation)*
Paper AO100-132
Author(s): Orlando Frazão, Ricardo André, Susana Silva, José Santos, INESC Porto (Portugal)

A brief review on optical fiber-based fabry-perot interferometry is presented. with the emergence of new microstructured fibers or specialty fibers, it has been possible to work in the development of new Fabry-Perot cavity configurations for different applications. It will be reported in the conference several new sensor designs based on Fabry-Perot cavities developed by INESC TEC in collaboration with international institutes.

Strong coupling effects in hybrid plexitonic systems *(Keynote Presentation)*
Paper AO100-163
Author(s): Yury P. Rakovich, Ctr. de Física de Materiales (Spain), IKERBASQUE, Basque Foundation for Science (Spain), National Research Nuclear Univ. MEPhI (Russian Federation); Dzmitry Melnikau, Ctr. de Física de Materiales (Spain); Ruben Esteban, Donostia International Physics Ctr. (Spain), IKERBASQUE, Basque Foundation for Science (Spain); Alexander A. Govyadinov, CIC NanoGUNE (Spain); Diana Savateeva, Ctr. de Física de Materiales (Spain); Thomas Simon, Ludwig-Maximilians-Univ. München (Germany); Ana Sánchez-Iglesias, CIC biomaGUNE (Spain); Marek Grzelczak, CIC biomaGUNE (Spain), IKERBASQUE, Basque Foundation for Science (Spain); Mikolaj K. Schmidt, Ctr. de Fisica de Materiales (Spain); Alexander S. Urban, Ludwig-Maximilians-Univ. München (Germany); Luis M. Liz-Marzán, CIC biomaGUNE (Spain), IKERBASQUE, Basque Foundation for Science (Spain); Jochen Feldmann, Ludwig-Maximilians-Univ. München (Germany); Javier Aizpurua, Ctr. de Física de Materiales (Spain), Donostia International Physics Ctr. (Spain)

We investigated the interactions between localized plasmons in gold nanorods and excitons in J-aggregates and were able to track an anticrossing behavior of the hybridized modes both in the extinction and in the photoluminescence spectra of this hybrid system. We identified the nonlinear optical behavior of this system by transient absorption spectroscopy. Finally using magnetic circular dichroism spectroscopy we showed that nonmagnetic organic molecules exhibit magneto-optical response due to binding to a plasmonic nanoparticles. In our experiments we also studied the effect of detuning as well as the effect of off- and on resonance excitation on the hybrid states.

The opportunity to use angular momentum of light for tissue diagnosis *(Keynote Presentation)*
Paper AO100-166
Author(s): Igor Meglinski, Univ. of Oulu (Finland)

We investigate the opportunity to use the vector Laguerre-Gaussian laser beams for optical biopsy. In current presentation a Monte Carlo based numerical simulation of complex vector Laguerre-Gaussian laser beams propagation in anisotropic turbid tissue-like scattering media is presented in comparison with experiment. Additionally, several basic physical phenomena associated with the anisotropic scattering of vector light beams in turbid media are discussed, including the mutual influence of light's polarization and its directional awareness due to the multiply scattering. The perspectives of use the vector light beams for tissue's biopsy and the results of feasibility studies are presented.

Unconventional scenarios for high-order harmonic generation *(Keynote Presentation)*
Paper AO100-173
Author(s): Carlos Hernández-García, Óscar Zurrón, Laura Rego, Antonio Picón, Julio San Román, Luis Plaja, Univ. de Salamanca (Spain)

In this keynote talk we will discuss the extraordinary degree of control of the XUV radiation using new scenarios in high-order harmonic generation. On one side, we shall explore the different properties of the harmonic emission when the driving field has particular spatial configurations, demonstrating the possibility of generating high-frequency light with elliptical polarization, orbital angular momentum and vector-beam configurations. Secondly, we shall explore high-harmonic generation from unconventional targets, as nano structures or single-layer graphene.

Preferential looking for visual acuity assessment: A human-operator independent approach *(Keynote presentation)*
Paper AO100-182
Author(s): Paulo T. Fiadeiro, João M. O. Alves, André F. F. Machado, Univ. de Beira Interior (Portugal); António M. G. Baptista, Univ. do Minho (Portugal); Pedro M. F. N. Serra, Plymouth Univ. (United Kingdom)

Preferential looking (PL) is a common technique used in clinical settings to determine visual thresholds in people unable to verbalize responses. The method, based on the presentation of cards containing a stimulus and an empty field, is greatly operator (clinician) dependent requiring expertise in identifying the patient's eye movements. Metrics based on eye tracking have been advanced as useful in implementing an objective (clinician independent) PL test. This study aimed to evaluate the utility of different metrics computed from eye-tracking data (experiment 1) and their applicability in a population of normal subjects and subjects with intellectual disability (experiment 2). In experiment 1, a supra-threshold and infra-threshold stimuli (sinusoidal gratings) were presented. In a second experiment, visual acuity (VA) was measured, using a single metric (the RFT). High-pass optotypes were presented; a sigmoidal function modelled the RFT data to determine the VA.

Terahertz metrology: state-of-the-art and challenges *(Keynote presentation)*
Paper AO100-211
Author(s): Mira Naftaly, National Physical Lab. (United Kingdom)

The area of terahertz science and applications has been growing roughly exponentially since the early 1990s as indicated by the number of scientific publications. Moreover, instrumental platforms employed in THz measurements have also proliferated, and now include laser-based, electronic, opto-electronic, and microwave photonics devices. However, it is only in the last few years that the field has matured to the degree that metrology and standardisation have gained focused attention, resulting in an increasing number of publications and a book devoted to the subject. This talk will review THz measurement techniques across various platforms and will discuss the different issues involved in making measurements using these systems. Calibration, verification, and measurement traceability issues are reviewed, along with other major challenges facing these instrument architectures in the years to come.

Resonant tunneling diode photodetectors *(Keynote presentation)*
Paper AO100-216
Author(s): Fabian Hartmann, Andreas Pfenning, Fabian Langer, Georg Knebl, Martin Kamp, Lukas

Worschech, Julius Maximilians Univ. Wuerzburg (Germany); Sven Höfling, Julius Maximilians Univ. Wuerzburg (Germany), Univ. of St Andrews (United Kingdom)

We present different types of resonant tunneling diode photosensors suitable for light detection from the visible (GaAs based) to the mid-infrared (GaSb based) wavelength region. The origin of the nonlinear RTD photocurrent-voltage relation will be discussed and it is shown how to identify optimal working points with ultra-high gain and sensitivities. When biased in the region of negative differential conductance, RTD photodetectors further enable detection schemes which employ a beneficial interplay of noise and nonlinearity. Due to Stochastic Resonance (SR) principles, optimal signal detection can be achieved for non-vanishing noise floors.

Focusing properties of light, point-spread-function engineering in 3D microscopy, and 3D imaging acquisition and display. Three-dimensional integral microscopy based on Fourier-domain capture *(Keynote Presentation)*
Paper AO100-239
Author(s): M. Martínez-Corral, J.C. Barreiro, A. Llavador, E. Sánchez-Ortiga, J. Sola-Pikabea, G. Scrofani and G. Saavedra, Department of Optics, University of Valencia (Spain), B. Javidi, Electrical & Computer Engineering Department, University of Connecticut (USA)

At the beginning of the 20th century a novel technique was reported by Gabriel Lippmann [1] aiming the capture of dense perspective information of 3D scenes. The technique was based in a very simple idea; to insert an array of microlenses in front of a photographic film. The technique was named as Integral Photography (IP), and permitted the capture of a collection of elemental images, each with different view of the 3D object. Later, in 1992, Adelson and Wang [2] provided the formal support to the integral photography. Specifically, they introduced the concept of plenoptic function, which describes the radiance of each luminous ray of light as a function of the angle and position in a given point of its trajectory. Although this function is in strong, unsolvable, conflict with the uncertainty principle, it works reasonably well in the Geometrical Optics domain. The IP concept was applied to microscopy, for the first time, by Jang and Javidi [3], but only with the purpose of displaying microscopic images. It is remarkable the contribution made by Levoy et al. [4] who adapted to microscopy the plenoptic concept. Very recently, the name integral microscopy (iMic) has been coined to refer to this technique. The improvement of the resolution of integral microscopes has aimed many research efforts. In this sense, are noticeable the application of ad-hoc deconvolution tools, the use of 4D interpolation techniques, or, more recently [5], the application of physical interpolation based in time multiplexing. The main drawback of iMics is their poor resolution. Factors that favor the loss of resolution are the limited number of pixels, the vignetting in the collected microimages and the comparable sizes of image PSF and microlens-array pitch.
To avoid the later drawbacks, in this contribution we report advances in a novel a novel architecture in which the lens array is not placed at the image plane, but at the pupil plane. This new realization of the plenoptic concept is named as Fourier-domain integral microscopy (FiMic). The FiMic has some apparent advantages over the iMic. First is the fact that it outputs directly the perspective views of the 3D sample, and therefore much computation time is saved. Second is that there is no conflict between the microscope PSF and the microlenses sizes, and thus, no resolution is lost due to such conflict. Third advantage is the strong reduction in vignetted pixels. Final advantage is a strong gain in compactness (take into account that the FiMic does not need any tube lens). A preliminary realization of FiMic was reported in [6]. In the presentation we show the scheme of the microscope, together with the updated pre-prototype and some examples of 3D images reconstructed from captured microimages.
References
[1] G. Lippmann, "Epreuves reversibles donnant la sensation du relief," J. Phys. 7, 821-825 (1908).
[2] E. H. Adelson and J. Y. A. Wang, “Single lens stereo with plenoptic camera,” IEEE Trans. Pattern Anal. Mach. Intell. 14, 99-106 (1992).
[3] J. S. Jang and B. Javidi, "Three-dimensional integral imaging of micro-objects," Opt. Lett. 29, 1230-1232 (2004).
[4] M. Levoy, R. Ng, A. Adams, M. Footer, and M. Horowitz, "Light Field Microscop", ACM Trans. Graph 25, 934-934 (2006).

[5] A. Llavador, E. Sánchez-Ortiga, J.C. Barreiro, G. Saavedra, and M. Martínez-Corral, "Resolution enhancement in integral microscopy by physical interpolation," Biomed. Opt. Express 6, 2854-2863 (2015).
[6] A. Llavador, J. Sola-Pikabea, G. Saavedra, B. Javidi, and M. Martinez-Corral, "Resolution improvements in integral microscopy with Fourier plane recording," Opt. Express 18, 20792-20798 (2016).

Spatial frequency domain point spread function for Fourier telescopy imaging *(Keynote presentation)*
Paper 242
Author(s): William T. Rhodes, Florida Atlantic University, USA; Yezid Torres Moreno and Omar Javier Tíjaro Rojas, Universidad Industrial de Santander, Colombia

The concept of a point spread function (PSF) is of great value in the understanding of the operation and performance of imaging systems. Resolution criteria can be applied in the evaluation of the "goodness" of the PSF for a given imaging system, and pictorial representations facilitate the understanding of the nature of blurring in image formation. A PSF appropriate for Fourier telescopy and Fourier microscopy can be expected to be of comparable value for those imaging modalities. In this paper three possible spatial-frequency-domain PSFs for Fourier telescopy are proposed. Each is related to the Fourier transform of the object illumination intensity distribution. Most importantly, each, like the conventional space-domain PSF, provides insight into the operation of a Fourier telescopy imaging system, especially when it is operates through atmospheric turbulence.

AOP2017' Invited Papers

High orbital angular momentum harmonics generation in plasmas *(Invited Paper)*
Paper AO100-38
Author(s): Jorge M. Vieira, Instituto Superior Técnico (Portugal)

High harmonic generation (HHG) results from non-linear optical processes by which n photons, with a given frequency ω, combine into a single photon with frequency nω. In recent HHG experiments, where the incident photon beam contained an orbital angular momentum (OAM) ℓ, the upshifted photon contained an OAM level given by nℓ. In these experiments, the OAM and frequency harmonics were coupled. Here we investigate a mechanism to create high OAM harmonics while leaving the laser frequency unchanged, treating the orbital angular momentum as a true independent degree of freedom. Our theoretical calculations and numerical simulations show that the order of the high harmonics obeys a simple algebraic selection rule, which depends only on the initial OAM of the incident laser beams. Our configuration employs stimulated Raman scattering in plasmas, using a pump beam in a fractional OAM state, i.e. containing more than a single OAM level. The physics also occurs in media with Kerr non-linearity

Quantum description of Bose-Einstein condensation of photons in hot plasmas *(Invited Paper)*
Paper AO100-44
Author(s): Hugo Terças, Instituto de Plasmas e Fusão Nuclear (Portugal)

Photons in plasmas behave as slightly massive particles. Together with the fact of having bosonic statistics, photons may undergo Bose-Einstein condensation. In this talk, we review the kinematic processes (Compton and Brillouin scattering) leading to the accumulation of photons near the bottom of the electromagnetic wave dispersion relation. We also provide the quantum description of the photons in the condensed phase, showing that the (repulsive) interaction of the photons, as resulting from four-wave mixing processes, lead to a small depletion of the photon condensate as a consequence of quantum fluctuations. A comparison with atomic BECs and photon condensates in optical cavities is also performed.

Photon bubble turbulence in cold atoms *(Invited Paper)*
Paper AO100-46
Author(s): João D. Rodrigues, Instituto de Plasmas e Fusão Nuclear (Portugal); Jose A. Rodrigues, Univ. do Algarve (Portugal); António V. Ferreira, Hugo Terças, José T. Mendonça, Instituto de Plasma e Fusao Nuclear (Portugal)

In optically thick samples of laser cooled atoms, multiple scattering of light is shown to induce strong light matter coupling. Such intertwine between radiation transport and atom dynamics is at the origin of a photon bubble instability mechanism, previously discussed in the context of turbulent radiation flow in dense astrophysical systems. Here we report on the experimental observation of photon bubble turbulence, as a result of the saturation of the aforementioned instability.

Color-quality control using color-difference formulas: progress and problems *(Invited Paper)*
Paper AO100-56
Author(s): Manuel Melgosa, Luis Gómez-Robledo, Pedro A. García, Univ. de Granada (Spain); Samuel Morillas, Univ. Politècnica de València (Spain); Christine Fernandez-Maloigne, Univ. de Poitiers (France); Noël Richard, Univ. of Poitiers (France); Min Huang, Beijing Institute of Graphic Communication (China); Changjun Li, Univ. of Science and Technology Liaoning (China); Guihua Cui, Univ. of Wenzhou (China)

Color-quality control is one of most relevant industrial applications of color-difference formulas. Color-difference formulas try to predict visually-perceived color differences from objective physical measurements, avoiding the problems related to subjective visual decisions from expert panels or

professional colorists in color-quality control. We will consider the relationship between visual and instrumental measurements of color differences. We will also discuss on the use of power functions as an efficient method to improve the performance of modern color-difference formulas,, and the need of developing color-difference formulas accounting for the increasing use of new materials with different kind of textures and gonioapparent effects.

Wavemeter improvements for laser diode calibration *(Invited Paper)*
Paper AO100-65
Author(s): Ismael Outumuro González, Lab. Oficial de Metroloxía de Galicia (Spain); Javier Diz Bugarin, Univ. of Vigo (Spain); Jose Luis Valencia Álvarez, Lab. Oficial de Metroloxía de Galicia (Spain); Jesús Blanco García, José Benito Vázquez Dorrio, Univ. of Vigo (Spain)

This paper shows the progress made in the wavemeter developed to give traceability to the wavelength of lasers and ECDLs (External Cavity Laser Diode). The improvements are: duplication of the optical path of the laser beams due to a double pass through the interferometer arms [1], the electronic fringe counter [2], the measurement of the refractive index of air and the uncertainty calculations of the wavelength for the case of lasers with frequencies that differs more than 10 THz from laser reference. The new measurements improve the previous results [3].

Space-time refraction of light in time dependent materials *(Invited Paper)*
Paper AO100-66
Author(s): Ariel Guerreiro, INESC TEC, Ctr. of Applied Photonics (Portugal), Universidade do Porto (Portugal); José T. Mendonça, Instituto Superior Técnico (Portugal)

We investigate the generalization of the conventional Fresnel and Snell theory of refraction to describe the transmission, reflection, amplification and attenuation of light in time dependent optical media in terms of the violation of the spatial and temporal symmetries. We present estimates of experimental yields given the current state of the art in epsilon-near-zero materials.

Dynamic and real-time study of the human lens optical and morphological properties during accommodation: preliminary results *(Invited Paper)*
Paper AO100-96
Author(s): Sandra M. Franco, Univ. do Minho (Portugal)

The purpose of this work is to study crystalline lens' optical and geometrical properties during accommodation in order to understand the mechanism of accommodation. We intend to establish the relationship between the geometrical changes of the crystalline lens induced by accommodation and its optical effects on the overall eye aberrations, through the analysis of its wavefront aberrations.

Far field diffraction of optical vortices by a straight edge *(Invited Paper)*
Paper AO100-116
Author(s): Ángela Guzman, Univ. Nacional de Colombia (Colombia); Paula López, Zayda Reyes, Yezid Torres, Jesús Mendoza, Univ. Industrial de Santander (Colombia)

We analyze here the propagation of a beam with well-defined OAM after being diffracted by a circular π-sector or straight edge. The beam's OAM spectrum, as obtained by a Fourier transform, also has a sinc-shaped envelope centered at the OAM value of the incoming OAM wave. The OAM content of the diffracted beam is not well defined, consisting rather of a superposition of OAM waves of different angular momenta. We use spatial light modulators to generate the incoming OAM beam [3] and measure the evolution of the intensity profile of the diffracted beam as it propagates away from the circular sector. A numerical simulation of the Fraunhofer regime propagation [4] of the diffracted beam, described as a superposition of OAM waves, supports the observed rotation of the intensity pattern around the propagation axis.

Fabry-Perot interferometer based on array of microspheres for temperature sensing *(Invited Paper)*
Paper AO100-136

Author(s): Marta S. Ferreira, Univ. of Aveiro (Portugal); Jörg Bierlich, Leibniz Institute of Photonic Technology IPHT (Germany); Jens Kobelke, Leibniz Institute of Photonic Technology (Germany); José L. Santos, Orlando Frazão, INESC TEC, Ctr. of Applied Photonics (Portugal)

A Fabry-Perot interferometer based on an array of soda-lime glass microspheres is proposed for temperature sensing. The microspheres are introduced in a purpose-designed hollow-core silica tube using a tapered fiber tip. It is observed that the reflection spectra visibility increases with the number of microspheres. After the insertion of each microsphere the sensor is subjected to temperature measurements. The sensor exhibits non-linear behavior and a dependence on the number of microspheres is noted. A maximum sensitivity of 11.13 pm/°C is achieved, when there is only one microsphere inside the capillary structure.

Novel optical fiber applications in life-sciences *(Invited Paper)*
Paper AO100-138
Author(s): Walter Margulis, Acreo Swedish ICT AB (Sweden), Royal Institute of Technology - KTH (Sweden); Sebastian Etcheverry, Acreo Swedish ICT (Sweden), Royal Institute of Technology - KTH (Sweden); Muhammad A. Faridi, Harisha Ramachandraiah, Karolinska Institute (Sweden); Aziza Sudirman, Qbtech AB (Sweden); Aman Russom, Karolinska Institute (Sweden); Fredrik Laurell, Royal Institute of Technology - KTH (Sweden)

In this work, we present two proof-of-principle demonstrations of the use of an optical fiber platform in life-sciences. Particles identified by their fluorescence and considered of interest are automatically sucked into fiber holes for analysis. Also, a flow cytometer based on fibers is described, where scattering and fluorescence are used to count particles or cells flowing along a focused stream with high count per second.

Dental resins properties studied by Bragg gratings *(Invited Paper)*
Paper AO100-146
Author(s): Hypolito José Kalinowski, Univ. Federal Fluminense (Brazil); Ana Paula Gebert de Oliveira Franco, Univ. Tecnológica Federal do Paraná (Brazil); Leandro Zen Karam, Pontifical Catholic Univ. of Parana (Brazil)

The development of chemically activated and photo-activated composite materials has revolutionized dentistry because it allows greater preservation of dental tissues and the fixation of artificial parts necessary for the reconstruction of dental structures lost due to the presence of dental caries or fractures. Such resins also permit greater accuracy in the demarcation of occlusal contacts and moulding of multiple implants. These and other dental procedures benefit from the adhesive advantages of composite materials to teeth enamel and dentin, as well as to polymeric materials used to make endodontic posts and prosthetic devices. In spite of the adhesion, there is a great challenge to the manufacturers, which is the development of materials that undergo low polymerization shrinkage. If this property exceeds the value of the adhesive resistance it can generate the formation of gaps, cause the displacement of restorations, prosthetics and endodontics devices, and distortion of moulds. In addition to the contraction, the resinous materials undergo exothermic reaction during cure. High temperatures can lead to tooth sensitivity and pulpal necrosis. The fibre Bragg sensors are used in biomedical research for simultaneous measurement of deformations and temperature. The present study shows results from the characterization of dental resin materials with different composition and applications. The results show that all investigated polymer materials demonstrate a temperature rise within the first few seconds after starting activation procedure. The mode of activation and the material composition influence the polymerization shrinkage values.

Carrier dynamics in metal-dielectric cavity nanoLEDs *(Invited Paper)*
Paper AO100-155
Author(s): Bruno Romeira, Eindhoven Univ. of Technology (Netherlands); Victor Dolores-Calzadilla, Eindhoven Univ. of Technology (Netherlands), Fraunhofer Heinrich-Hertz Institute (Germany); Aura Higuera-Rodriguez, Simone Birindelli, Francesco Pagliano, Renné P. J. van Veldhoven, Barry E. Smalbrugge, Lachlan E. Black, Erwin W. M. M. Kessels, Eindhoven Univ. of Technology (Netherlands);

Dominik Heiss, Eindhoven Univ. of Technology (Netherlands), Infinion Technologies (Germany); Meint K. Smit, Andrea Fiore, Eindhoven Univ. of Technology (Netherlands)

Despite much progress, nanoscale light sources - suitable for photonic integration as required by future optical interconnects - are lacking. Here, the authors present, both theoretically and experimentally, the carrier dynamics in metal-dielectric cavity nanopillar light-emittting diodes (LEDs) on a silicon substrate working at telecommunications wavelengths, coupled to an InP-membrane waveguide, featuring more than 0.3 microWatt waveguide-coupled powers and GHz-range modulation bandwidths. We show that a passivation method using sulfur treatment followed by silicon oxide capping strongly suppresses the surface recombination at the InGaAs surfaces of nanopillars by two orders of magnitude. This will ensure further substantial improvements in the efficiency and output power of nanoLEDs, and reduce the threshold current in nanolasers, which are key requirements for their application in optical interconnects.

Rapid Eye Movements (REMs) and visual dream recall in both congenitally blind and sighted subjects *(Invited Paper)*
Paper AO100-158
Author(s): Helder Bértolo, Instituto Superior de Educação e Ciências (Portugal); Tiago Mestre, The Ottawa Hospital Research Institute / Ottawa Brain and Mind Research Institute (Canada); Ana Barrio, Beatriz Antona, Univ. Complutense de Madrid (Spain)

Our objective was to evaluate rapid eye movements (REMs) associated with visual dream recall in sighted subjects and congenital blind. Polysomnographic recordings were performed at subjects home. REMs were detected by visual inspection on both EOG channels and further classified as occurring isolated or in bursts. Dream recall was defined by the existence of a dream report. The average of REM awakenings per subject and the recall ability were identical in both groups. CB had a lower REM density than CS; the same applied to REM bursts and isolated eye movements. REM bursts and REM density were significantly different for positive dream recall; furthermore for both features significant results were obtained for the interaction of time, recall and diagnosis. Data show that blind have lower REMs density. However the ability of dream recall in Congenital blind and Sighted controls is identical. In both groups visual dream recall is associated with increased REMs activity.

Quantum correlations of colourful photons *(Invited Paper)*
Paper AO100-164
Author(s): Elena del Valle, Univ. Autónoma de Madrid (Spain)

Photon correlations are one of the promising resources to power future quantum technology. Among the most important theoretical characterizations of this resource are correlation functions such as g(2)(t1,t2) through which Glauber established the theory of quantum optical coherence. I present an extension of these functions to take into account correlations of the photons not only in time but also in their colour or frequency [PRL 109, 183601 (2012)]. Our theory provides an efficient computational method that is essential in the unravelling of rich and unexpected landscapes of correlations, and the engineering and optimization of different types of quantum light sources: single photons, polarization-entangled photon pairs, photons with violation of Cauchy-Schwarz and Bell's inequalities and bundles of N photons [Nature Photonics 8, 550 (2014)]. Some of our most fundamental findings have been experimentally observed in a system of exciton polaritons [Sci. Rep. 6, 37980 (2016)].

PET imaging by high power table-top lasers *(Invited Paper)*
Paper AO100-169
Author(s): María Teresa Flores-Arias, Alfredo Iglesias, Manuel Blanco, Carmen Bao-Varela, Pablo Aguiar, Univ. de Santiago de Compostela (Spain); Jesús Silva-Rodriguez, QuBiotech Health Intelligence (Spain); Justo Arines, Ferran Cambronero, Univ. de Santiago de Compostela (Spain)

Table-top lasers, with energies around 50 TW, have shown to be a promising technology for the development of compact acelerators, used in modern facilities to produce radioisotopes for medical applications. One of this applications is the PET (Positron Emission Tomography) imaging. The new scenario and trend is to produce ahort-lived PET isotopes and specific tracers. We are confident that

table-top lasers are a suitable technology to produce radioisotopes in the framework of low capacity local production of small monodose PET tracers activities for medical imaging, instead of the conventional centralized high capacity production and distribution of large activities. This contributions presents the L2A2 (Laser Laboratory for Acceleration and other Applications) at the University of Santiago de Compostela, a new laser facility, being one of its applications to produce radioisotope by laser acceleration for preclinical imaging purposes.

Researching in biomaterials optics *(Invited Paper)*
Paper AO100-186
Author(s): Maria del Mar Pérez Gómez, Ana Maria Ionescu, Ana Yebra, Juan C. Cardona, María José Rivas, Razvan Ghinea, Univ. de Granada (Spain)

The optical properties of a tissue or a biomaterial can be described in terms of the absorption coefficient (μa), the scattering coefficient (μs), the scattering function p(θ,ψ) and the real refractive index of the material. The Inverse Adding-Doubling, IAD, Method and relationship between the Kubelka-Munk parameters and the transport coefficients are used to describe optical properties at different wavelengths for a large variety of tissues and tissue-like biomaterials, such as native cornea, tissue-engineered cornea, tissue-engineered oral mucosa, natural dentin and dental resin nanocomposites, among others.

ΦOTDR with chirped pulses: a new technique for quantitative high sensitivity distributed fiber measurements *(Invited Paper)*
Paper AO100-188
Author(s): Hugo F. Martins, FOCUS SL (Spain); Juan Pastor-Graells, Andres Garcia-Ruiz, Sonia Martín-López, Miguel González-Herráez, Univ. de Alcalá (Spain)

The theoretical and practical implications of using ΦOTDR with linearly chirped pulses is discussed and stat-of-the-art results are presented. By providing a frequency to time mapping, this recent technique allows for the linear measurement of distributed refractive index variations with unprecedented sensitivities (Δn=10^-8) amongst distributed fibre sensors, while maintaining the high bandwidth of detection and long fiber sensing ranges. The technique readily allows for distributed measurement of temperature and/or dynamic strain with resolutions of millikelvin and/or few nε, at kHz rates, with metric spatial resolution over tens of kilometres, but has also important applications in high sensitivity distributed chemical sensing.

Electrical addressing and temporal tweezing of localized pulses in passively mode-locked semiconductor lasers *(Invited Paper)*
Paper AO100-190
Author(s): Julien Javaloyes, Univ. de les Illes Balears (Spain); Patrice Camelin, Mathias Marconi, Massimo Giudici, Univ. Côte d'Azur, CNRS, Institut de Physique de Nice (France)

Localized structures (LSs) in optical resonators have attracted much interest in the last twenty years. LSs can be used as elementary bits of information for all-optical information processing. Recently, we have shown how temporal Localized Structures can evolve from passive mode-locking (PML) in the long cavity regime. Here, the PML pulses become individually addressable and coexist with the off solution. In electrically-biased semiconductor lasers, the current can be easily modulated at several GHz making it a convenient parameter for addressing and manipulating those LSs in view of possible applications. We demonstrate in this work the writing and the erasure operations using positive or negative current pulses that we apply with a period commensurate with the round-trip. In practice, this operation corresponds to the controlled transfer of the state of operation of the laser from one mode-locked regime to another one with a different number of pulses.

Performance characteristics of 1550 nm and 1310 nm detuned ridge waveguide distributed feedback laser diodes *(Invited Paper)*
Paper AO100-194
Author(s): Horacio I. Cantu, Andrew McKee, CST Global (United Kingdom)

In this work we present the performance characterisation results for detuned (>10 nm) in-plane ridge waveguide DFB laser diodes with a peak optical gain centred at a wavelength of 1550 nm, and compare these results to previously published results of a 1310 nm design with a similar topology. Initially, we cover the effect of wavelength detuning on the characteristic temperature (T0), slope efficiency (SE), and maximum optical power available from the laser, but we later extend the discussion to the effect of detuning on the resonance frequency of the lasers (fr) and their maximum 3 dB bandwidth (BW) available for multi-gigabit per second communication applications. This characterisation takes place at the uncooled application specification temperatures of 25 °C and 85 °C.

Resonant tunneling diode oscillators for optical communications *(Invited Paper)*
Paper AO100-193
Author(s): Scott Watson, Jue Wang, Abdullah Al-Khalidi, Weikang Zhang, Univ. of Glasgow (United Kingdom); Horacio Cantu, Compound Semiconductor Technologies Global Ltd. (United Kingdom); José Figueiredo, Univ. do Algarve (Portugal); Edward Wasige, Anthony E. Kelly, Univ. of Glasgow (United Kingdom)

The ability to use resonant tunneling diodes (RTDs) as both transmitters and receivers is an emerging topic, especially with regards to wireless communications. These RTDs have incorporated a small window on top of the device structure and a light absorption layer to allow direct optical access to the oscillator. By modulating the light being sent to the RTD, data can be received and shown in the form of eye diagrams. This idea has been shown using a non-oscillating RTD device acting as a photo-detector, where data was successfully received at a data rate of 1 Gbit/s. The ability to optically modulate the RTD oscillator through the negative differential resistance (NDR) region has also been demonstrated. Data modulation experiments using these oscillators will be shown and the application scenarios discussed. These RTD oscillators will allow for seamless integration of high frequency radio and optical fibre networks.

Resonant tunnelling diode based high speed optoelectronic transmitters *(Invited Paper)*
Paper AO100-209
Author(s): Jue Wang, Abdullah Al-Khalidi, Univ. of Glasgow (United Kingdom); José Figueiredo, Univ. do Algarve (Portugal); Edward Wasige, Univ. of Glasgow (United Kingdom)

As the demand for high speed wireless communication continues to increase exponentially, the need to utilize/match the high speed optic fibre which has been widely employed in most base stations for wireless broadband communications is higher than before. The resonant tunnelling diode (RTD) can provide a low cost solution for the seamless integration of microwave/mm wave radio and fibre networks. The main limitation of RTD transmitter is the low output power. In this paper, high frequency RTD-PD (photo-diode) optoelectronic transmitters with mW output power were demonstrated. It shows the great potential of RTD as high speed optoelectronic transmitter.

Filtering of laser beams with orbital angular momentum *(Invited Paper)*
Paper AO100-228
Author(s): Efrain Solarte-Rodriguez, Julio C. Quiceno, Univ. del Valle (Colombia); Yezid Torres, Univ. Industrial de Santander (Colombia)

Laser beams with orbital angular moment are useful for many applications and in some of them, when beams superposition and interference is desired, stability and softness of the light field are important. Vortex beams production by spatial light modulation can produce spurious structures in the light field and it could be desirable to filter them away. We propose a technique to filter Laguerre Gauss light beams using diffraction to enhance the beam performance. Laser beams with helical front phase and fixed topological charge were generated from laser gaussian beams using standard techniques of computer generated holograms in a spatial light modulator and separating the first diffraction order. Diffractive filtering plates were designed and elaborated using high resolution photographical techniques. The method efficiency was studied by interferometry techniques in a Mach Zehnder type setup. The filtered vortex beams were recorded for different topological charges and filter plates.

Vision in pseudophakia: a short review on pseudoaccommodation *(Invited Paper)*
Paper AO100-235
Author(s): Pedro M. Serra, Univ. of Plymouth (United Kingdom)

Cataract is one of the major causes of visual impairment in the population after the 6th decade of life. Standard treatment consists of implanting a monofocal intraocular lens (IOL) to substitute the cloudy natural crystalline lens, a condition known as pseudophakia. Despite the considerable improvement in the overall visual function, the standard procedure does not prepare the patient to attain functional levels of near vision. The pseudophakic eye is unable to correct the vergence of the light coming from close objects preventing the patient of reading a newspaper at 40 cm distance. There is, however, evidence of patients having functional levels of near vision. This ability known as pseudoaccommodation has been associated to various ocular features such as, pupil size, postoperative refractive error, corneal multifocality ocular aberrations and IOL axial movement. This review will provide a summary of the existing evidence regarding pseudoaccommodation.

AOP2017' Oral Papers

Optical Microtopographic Inspection of Asphalt Pavement Surfaces
Paper AO100-3
Author(s): Manuel F. M. Costa, Elisabete Freitas, Helder Torres, Univ. do Minho (Portugal); Veronic Cerezo, IFSTTAR (France)

Microtopographic and rugometric characterization of surfaces is routinely and effectively performed non-invasively by a number of different optical methods. Rough surfaces are also inspected using optical profilometers and microtopographer. The characterization of tarmac produced in different ways and compositions is fundamental for economical and safety reasons. Having complex structures, including topographically with different ranges of form error and roughness, the inspection of asphalt pavement surfaces is difficult to perform non-invasively. In this communication we will report on the optical non-contact rugometric characterization of the surface of different types of tarmac subjected to wear performed at the Microtopography Laboratory of the Physics Department of the University of Minho.

Spectrophotometric characterization of hemozoin as a malaria biomarker
Paper AO100-5
Author(s): Ivo Silva, Univ. of Minho (Portugal); Rui Lima, Univ. of Minho (Portugal), Univ. of Porto (Portugal); Graça Minas, Susana O. Catarino, Univ. of Minho (Portugal)

Malaria is a parasitic disease mostly widespread in regions with precarious healthcare conditions and resources. This work proposes a malaria diagnostic system based on optical absorption spectrophotometry, presenting a study of hemozoin as a malaria biomarker, since it is an infection sub-product. The optical absorbance of hemoglobin and hemozoin solutions in water was measured in the visible spectrum range using a spectrophotometric setup. The results showed main absorbance peaks at 540 and 574 nm for hemoglobin and at 672 nm for hemozoin. Both hemoglobin and hemozoin, when alone in solution, were detected by absorbance with 0.05 g/L sensitivity. By combining whole blood and hemozoin solutions, it was proved that the absorbance peaks could still be optically detected. The potential for miniaturization was evaluated by detecting hemozoin in blood samples in 3 mm optical path PDMS wells. It was concluded that hemozoin is a viable candidate as a biomarker for malaria detection.

Low cost ellipsometer using a standard commercial polarimeter
Paper AO100-6
Author(s): Filipe Velosa, Manuel A. Abreu, Univ. de Lisboa (Portugal)

Ellipsometry is an optical technique with the purpose of characterizing materials or the phenomena that occurs at an interface or thin film between two different media. In this paper, we present an experimental low-cost version of a photometric ellipsometer, assembled with taipically found material in every Optics laboratory. The polarization parameters measurement was performed using a Thorlabs PAX5710VIS polarimeter. The uncertainty was computed using the Guide to the Expression of Uncertainty in Measurement (GUM) procedures. We measured the thickness of a 10 nm thick SiO_2 thin film deposited upon Si, and the complex refractive index of Gold and Tantalum samples. For the SiO_2 thickness we achieved an experimental deviation of 4.5% with 1.99nm uncertainty. The value complex refractive index of Gold measured agrees with the different values found within the available references. The uncertainty values were found to be mostly limited by the polarimeter's uncertainty.

Generation of five phase-locked harmonics in the continuous wave regime and its potential application to arbitrary optical waveform synthesis
Paper AO100-7

Author(s): Nurul Sheeda Binti Suhaimi, Univ. Pertahanan Nasional Malaysia (Malaysia), Univ. of Electro-Communications (Japan); Chiaki Ohae, Trivikramarao Gavara, Ken'ichi Nakagawa, Univ. of Electro-Communications (Japan); Feng-Lei Hong, Yokohama National Univ. (Japan), ERATO (Japan); Masayuki Katsuragawa, Univ. of Electro-Communications (Japan), ERATO, JST, MINOSHIMA Intelligent Optical Synthesizer Project, Saitama (Japan)

We report the generation of a new broadband coherent light source in the continuous wave (CW) regime which is an ensemble of multi-harmonic radiations (2403, 1201, 801, 600 and 480 nm) with an exact frequency ratio of 1:2:3:4:5 and an extremely wide frequency spacing of 124.7 THz by implementing a frequency dividing technology in the generation process. All five harmonics are generated coaxially with high phase coherence both in time and space, good beam quality and practical power. The highlight of this study is that this light source has a huge potential for the arbitrary optical waveform synthesis in the CW regime which has not been performed yet due to the limitation of the existing CW light source.

Localized modes in saturable Kerr media embedded in non-PT-symmetric complex localized potentials

Paper AO100-8

Author(s): Frederico C. Moreira, Univ. Federal de Alagoas (Brazil)

One-dimensional nonlinear wave propagation in a medium whose refractive index is represented by a local Wadati complex potential of the formG(x)=g2±igx, where g is the generating function is theoretically investigated. We report on the existence of families of stable asymmetric spatial solitons in a saturable nonlinear medium in the presence of a gain/loss asymmetrical profile. The properties of the nonlinear modes bifurcating from the eigenvalue of the underlying linear problem are investigated. While the sign in the front of the imaginary part does not change the spectrum of G(x) even when it is not PT-symmetric, the same cannot be said about the stability of nonlinear functions. We find the remarkable result that the asymmetrical profile of the refractive index is responsible to a split in stability properties of nonlinear branches and explanations are provided.

Resonant tunneling diode photodetectors for optical communications

Paper AO100-9

Author(s): Gil C. Rodrigues, João F. M. Rei, James A. M. Foot, Univ. do Algarve (Portugal); Khalid H. Alharbi, Abdullah Al-Khalidi, Jue Wang, Edward Wasige, Univ. of Glasgow (United Kingdom); José Figueiredo, Univ. do Algarve (Portugal)

Resonant tunneling diodes (RTDs) have been extensively studied due to their potential applications in very high speed electronics, optical communications, and terahertz generation. In this work we report the latest results on the characterization of the resonant tunneling diode photo-detectors (RTD-PDs), incorporating InGaAs light sensitive layers, for light sensing at the telecommunication wavelengths of λ = 1310 nm and λ = 1550 nm, with measured responsivities up 15 A/W.

Simulation of optoelectronic circuits based on resonant tunneling diodes

Paper AO100-10

Author(s): João F. M. Rei, James A. M. Foot, Gil C. Rodrigues, José M. L. Figueiredo, Univ. do Algarve (Portugal)

Resonant tunneling diodes (RTDs) are the fastest pure electronic semiconductor devices, at room temperature. When integrated with optoelectronic devices due to the highly nonlinear properties and electrical gain they can give rise to new optoelectronic devices with novel functionalities and applications for future ultra-wide-band communication systems. The recent coverage on these devices (iBROW H2020 EU Project) led to the needs to have appropriated simulation tools. In this work, we present RTD based optoelectronic circuits simulation packages to provide circuit signal level analysis such as transient and frequency responses. We will present and discuss the models, the simulation results and evaluate the simulation packages with experimental implementations of the above devices and circuits.

Optical bias selector based on a multilayer a-SiC:H optical filter
Paper AO100-11
Author(s): Manuela Vieira, Instituto Superior de Engenharia de Lisboa (Portugal); Manuel Augusto Vieira, Paula Louro, CTS-UNINOVA (Portugal)

A MUX/DEMUX coder/decoder based is presented. The device is a two terminal double pi'n/pin a-SiC:H photodetector under appropriated optical bias . Five visible communication channels are transmitted together. Thirty-two on/off states are detected. The proximity of the magnitude of consecutive levels causes occasional errors in the decoded information. To minimize the errors, four parity bit are generated. Results show that the background works as a selector in the visible range that allows the identification and decoding of the different input channels. A transmission capability of 60 kbps using the generated codeword was achieved.

Visible light communication and indoor positioning using a-SiCH device as receiver
Paper AO100-12
Author(s): Manuel Augusto Vieira, CTS-UNINOVA (Portugal); Manuela Vieira, Instituto Superior de Engenharia de Lisboa (Portugal); Paula Louro, CTS-UNINOVA (Portugal); Pedro Vieira, Instituto das Telecomunicações (Portugal)

An indoor positioning system were trichromatic white LEDs are used as transmitters and an optical processor based on a-SiC:H technology as mobile receiver is presented. The receiver is realized using a double p-i-n photodetector with two UV light biased gates. The relationship between the transmitted data and the received digital output levels is decoded. The received signal is used in coded multiplexing techniques for supporting communications and navigation concomitantly on the same channel. The position is estimated using the visible multilateration metodh using several non-collinear transmitters. The location and motion information is found by mapping position and estimates the location areas.

Low-cost fused taper polymer optical fiber (LFT-POF) splitters for environmental and home-networking solution
Paper AO100-13
Author(s): Latifah S. Supian, National Defence Univ. of Malaysia (Malaysia); Mohammad Syuhaimi Ab-Rahman, Hadi Guna, Hazwan Harun, Malik Sulaiman, National Univ. of Malaysia (Malaysia); Nani Fadzlina Naim, Univ. Teknologi Mara (Malaysia)

In visible optical communication, the overall cost of optical network can be reduced by deploying economical splitters for distributing optical data signals from a point to multipoint in transmission network. The low-cost splitters shall have two main characteristics; good uniformity and high power efficiency. In this study, the most cost-effective and environmental friendly optical splitter having those characteristics have been developed. The device material is purely based on multimode step-index PMMA Polymer Optical Fiber (POF) through fused-taper technique (LFT). The results for uniformity and power efficiency of all splitters have been revealed by injecting 650 nm wavelength into input port while each end of output fibers measured by optical power meter. Final analysis shows that fused-taper splitter has low excess loss 0.53 dB and low insertion loss of average below 7 dB. The splitter has good uniformity that is 32:37:31% in which it is suitably used for demultiplexer.

Nonlinear-optical studies of materials which strongly diffuse the laser Gaussian beam
Paper AO100-14
Author(s): Rafal Miedzinski, Izabela Fuks-Janczarek, Jan Dlugosz Univ. in Czestochowa (Poland)

Third order nonlinear optical susceptibility characterizes the nonlinear optical response of dielectric materials. The real part of the third order nonlinear susceptibility is related to the nonlinear refractive

index and gives an information how the refractive index of the material is change under influence of high intensity light – about GW per square centimetres. The imaginary part is related to the two photon absorption. Both parameters can be easily obtained by classic Z-scan technique. In this method the sample is illuminated by Gaussian profile of a laser beam. The problem starts when the samples strongly distorts the Gaussian profile. In this case the measurement cannot be carried out. In our presentation we proposed the method that solves this problem and can be used for materials with high refractive index. To be able to do that, therefore, it must analysed the scattered laser beam. According on the beam deviation and paraxial optics law the NLO coefficient can be estimated.

Two photon absorption coefficient and nonlinear refractive index of lithium niobate glasses doped by rare-earth elements (Er^{3+}, Gd, Nd)
Paper AO100-15
Author(s): Izabela Fuks-Janczarek, Rafał Miedzinski, Jan Dlugosz Univ. in Czestochowa (Poland)

Optical nonlinearities of lithium niobate glasses doped by rare-earth elements (Er3+, Gd, Nd) glasses were investigated by z-scan method with nanosecond laser pulses at wavelength of 532 nm and 1064 nm. Their dependence on the dopant concentration in melt ranging from 0.1 to 3.5 wt% was investigated. In the present work experimental investigations of the photoinduced changes caused by a 10 Hz Q-switched mode-locked Nd-YAG laser. The two-photon absorption coefficient and nonlinear refractive index are obtained, while the pulse intensity was at the range of 1.1 to 16.2 (GW/cm2). In this paper, the correlation between the observed nonlinearities and the molecular structures is discussed.

Terahertz techniques for gastric cancer diagnosis
Paper AO100-20
Author(s): Faustino Wahaia, Univ. do Porto (Portugal)

Due to sensitivity of terahertz (THz) waves to differences in tissue hydration from normal and abnormal bio-tissue, the present work shows that terahertz time-domain spectroscopy (THz-TDS) can be used to characterize biological tissue for diagnosis of gastric cancer tissue. Healthy (normal) and adenocarcinoma-affected gastric tissue-samples have been measured using transmission THz-TDS in the 0.15–2.00 THz frequency range, where complex optical constants have been determined. Absorption coefficients ( ) and refractive indices ( ) from spectra of both normal and carcinoma-affected tissues have been analyzed. Results demonstrate that THz-TDS is a powerful tool to perform qualitative assessment of bio-tissues, making thus possible the discrimination of abnormal tissue from the normal one, with potential application in gastric cancer diagnosis.

Simulation of localized surface plasmon resonance in metallic nanoparticles embedded in amorphous silicon
Paper AO100-21
Author(s): Alessandro Fantoni, Miguel Fernandes, ISEL-ADEETC (Portugal), CTS-UNINOVA (Portugal); Yuriy Vygranenko, CTS-UNINOVA (Portugal); Paula Louro, ISEL-ADEETC (Portugal); Manuela Vieira, ISEL-ADEETC (Portugal), CTS-UNINOVA (Portugal); Daniela Texeira, ADEQ-ISEL (Portugal); Ana Ribeiro, IST (Portugal); Elisabete Alegria, ADEQ-ISEL (Portugal)

We propose the development and realization of a plasmonic structure, based on the LSP interaction of metal nanoparticles with an embedding matrix of amorphous silicon. Metals of interest for nanoparticles composition are: Aluminium, Gold, Iron and Gallium. The analysis is realized recurring to the Discrete Dipole Approximation method (DDA), using the free software DDSCAT. In this work we study the optical properties of metal nanoparticles embedded in an amorphous silicon matrix, as a function of size, shape, aspect-ratio and metal type. Experimental measurements realized with arrays of metal nanoparticles are compared with the simulations based on the DDSCAT software.

Mode-locked semiconductor laser for long and absolute distance measurement based on laser pulse repetition frequency sweeping: a comparative study between three types of lasers
Paper AO100-22
Author(s): David Castro Alves, Manuel Abreu, Alexandre Cabral, José Rebordão, Univ. de Lisboa (Portugal)

With the goal of using the small, compact and robust mode-locked semiconductors lasers as a primary laser source high precision absolute distance metrology concept based on pulse repetition frequency (PRF) sweep, three types of laser were used in this study. The tested lasers ere one laser with vertical emission and two with transversal emission. Only the vertical emission laser has optical pump, whilst the others operate with electric pumping. One transversal laser does not possess a saturable absorber and relies on a dispersion compensating fiber for generating the pulses. The metrology technique used in this experiment requires values of PRF stabilization, in terms of Allan deviation, better than 10-9. In this study is showed that the hybrid mode, i.e. RF injection, is the best stabilization technique to obtain those values of stabilization and at the same time allowing the laser PRF sweep without degrading the stabilization levels and is showed the advantages of each laser.

Optical properties of up-converting nanoparticles embedded in polyester nanocarriers
Paper AO100-23
Author(s): Dominika Wawrzynczyk, Urszula Bazylinska, Wroclaw Univ. of Science and Technology (Poland)

Optical properties of up-converting nanoparticles co-encapsulated with photosensitizing dyes inside the polyester nanocarriers will be presented. NaYF4 nanoparticles were synthesized with a standard thermal decomposition reaction, while newly designed polyester nanocapsules were used as a container to co-precipitate hybrid cargo: lanthanide doped NaYF4 NPs and organic drugs suitable for photodynamic therapy. The selection of lanthanide doping and type of photosensitizers was made based on the overlap of their emission and absorption spectra, respectively, to further facilitate the energy transfer processes between optically active components of the system. The obtained nanocarriers showed potential for application as multifunctional agents in theranostics.

Erbium and ytterbium co-doped transparent oxyfluoride glass-ceramics optical fibers
Paper AO100-24
Author(s): Michał Żelechower, Elwira Czerska, Silesian Univ. of Technology (Poland); Krzysztof Wiśniewski, Nicolaus Copernicus Univ. (Poland); Elżbieta Augustyn, Silesian Univ. of Technology (Poland), Nicolaus Copernicus Univ. (Poland); Czesław Koepke, Nicolaus Copernicus Univ. (Poland), Silesian Univ. of Technology (Poland)

According to the earlier author’s papers, the erbium/ytterbium co-doped oxyfluoride glass-ceramics fibers should demonstrate better 1550 nm emission under 488/980 nm excitation (the erbium Er3+ ion transition 4I13/2→4I15/2) than corresponding glass fibers (the batch composition 48SiO211Al2O3-7Na2CO3-10CaO-10PbO-12PbF2-1.5/0.6YbF3-0.5/0.2ErF3). Glass fibers provided as a core of standard multimode waveguide (the diameter of 62 μm) have been drawn with the mini-tower to the diameter between 50 μm and 80 μm, then annealed in the two-step regime (580oC/1h – nucleation of nano-crystals; 740oC/15 min – nano-crystals growth). This kind of heat treatment ensures the transparent glass-ceramics fibers with the microstructure of homogeneously distributed nano-crystals (lead, erbium and ytterbium enriched cubic fluorite-like crystals) embedded in a glassy host. Their transmission covers the range of 80-90% and seems to be sufficient with respect to their provided limited length (~2m). The luminesc

Fabrication and characterization of a cell electrostimulator device combining physical vapor deposition and laser ablation
Paper AO100-25
Author(s): Angel Luis Aragón, Carmen Bao-Varela, Univ. of Santago de Compostela (Spain); Daniel Nieto, Univ. of Santiago de Compostela (Spain), National Univ. of Ireland (Ireland); Eliseo Pérez, Univ. of Santago de Compostela (Spain); Antonio Pazos, Univ. of Santiago de Compostela (Spain)

We present the fabrication process of a prototype of a cell electrostimulator device combining physical vapor deposition and laser ablation. In a first step a thin layer of 200 nm of aluminum is deposited on a borosilicate glass substrate using physical vapor deposition. In a second stage the geometry design of the electrostimulator is drawn in a CAD-like software available in a Nd:YVO4 Rofin Power line 20E, operating at the fundamental wavelength of 1064 nm and with 20 ns pulse width. In order to control the electrical signal applied to the electrostimulator a digital I/O device from National Instruments (USB-6501) is used which provides 5 V at the output monitorized by a software programmed in LabVIEW. Finally the optical and electrical characterization of the cell electrostimulator device is presented.

Indoors positioning through VLC technology using an a-SiC:H photodetector
Paper AO100-26
Author(s): Paula Louro Antunes, ISEL-ADEETC (Portugal); M. A. Vieira, João Costa, CTS-UNINOVA (Portugal), ISEL-ADEETC (Portugal); M. Vieira, CTS-UNINOVA (Portugal), ISEL-ADEETC (Portugal)

In this work it is proposed an indoor navigation system based on VLC. The system includes RGB white LEDs with red and blue chips modulated at different frequencies and a pinpin photodetector with selective spectral sensitivity. The photodetector device consists two pin structures based on a-SiC:H and a-Si:H optimized for the detection of short and large wavelengths in the visible range. Its sensitivity is externally tuned by steady state optical bias. The localization algorithm makes use of the Fourier transform to identify the frequencies and the wavelength filtering properties of the sensor to detect the existing red and blue signals.

Photoluminescence decay kinetics in CdSe QDs structured films: measurement and statistical analysis
Paper AO100-27
Author(s): Cesar R. Bernardo, Michael Belsley, Mikhail Vasilevskiy, Eduardo Pereira, Univ. do Minho (Portugal); Peter Schellenberg, MackGraphe – Graphene and Nanomaterials Research Ctr. (Brazil); Hugo Gonçalves, Univ. do Minho (Portugal)

Here we present a study of the energy transfer between different populations of CdSe QDs embedded in a thin film polymeric matrix by fitting the time correlated single photon counting data obtained using a Epi-Fluorescence Illumination system as well as a Total Internal Reflection Fluorescence system. Evaluation of the fluorescence lifetimes by fitting decay kinetics for these systems is far from straightforward. The key problems are that these systems are heterogeneous and the overall fluorescence decay is not at all well described by a single exponential function, since the emission can occur through numerous diverse decay mechanisms. We will present a study using several models (probability distribution functions of decay rates) and discuss how well they describe the obtained experimental data and the degree to which one can draw conclusions regarding the suitability of the physical assumptions underlying these models.

Critical discussion on the UV absorption properties of Earth's atmosphere
Paper AO100-28
Author(s): Thorsten Döhring, Hochschule Aschaffenburg (Germany)

Ultraviolet radiation emitted by the sun is often divided into UVA, UVB, and UVC bands. Thereby UVA passes through Earth´s atmosphere, while most of UVB is absorbed by atmospheric ozone. This paper discusses the limitations of the commonly accepted assumption, that solar UVC radiation is always completely absorbed by Earth´s atmosphere. Therefore the atmospheric absorption is considered in more detail: In the wavelength range between 125 nm and 200 nm the extraterrestrial solar spectrum is strongly absorbed by molecular oxygen. The ozone layer in the stratosphere has strong absorption characteristics between 200 nm and 300 nm, named Hartley band. It is already verified that the observed ozone layer depletion increases UVB radiation below 300 nm. However, the ozone layer depletion should also open a small transmitting atmospheric window in the UVC regime around 210 nm at the overlap

region between oxygen absorption and ozone absorption. This hypothesis should be proved experimentally.

Energy transfer between silver clusters and europium Eu^{3+} ions in photo-thermo-refractive glasses
Paper AO100-30
Author(s): Moeen Ghafoor, Univ. of Eastern Finland (Finland), ITMO Univ. (Russian Federation); Yevgeniy Sgibnev, Nikolay Nikonorov, Victor Dubrovin, ITMO Univ. (Russian Federation)

Luminescent silver clusters (SCs) in glasses reveal a broadband and intensive luminescence in the visible and near-infrared ranges. These silver clusters also are a useful and novel tool for improving the spectroscopic properties of rare-earth ions in glasses for functional applications. Photo-thermo-refractive PTR glasses can be classified as polyfunctional materials having, properties of different monofunctional materials. In this work we present the results of studies into energy transfer between SCs and Eu3+ ions in PTR glasses. The effective energy transfer from silver clusters to Eu3+ ions is observed under excitation at any wavelength in the range of 250-430 nm, this was evidenced by the presence of sharp characteristic emission bands of europium Eu3+ ions in the luminescence spectra of the samples. These results can be used for developing warm white LEDs and down converters for solar cells.

Indirect gonioscopy system for imaging iridocorneal angle of eye
Paper AO100-35
Author(s): Sandeep Menon Perinchery, Chan Yiu Fu, Nanyang Technological Univ. (Singapore); Mani Baskaran, Tin Aung, Singapore Eye Research Institute (Singapore); Murukeshan V. Matham, Nanyang Technological Univ. (Singapore)

Current clinical optical imaging systems do not provide sufficient structural information of trabecular meshwork (TM) in the iridocorneal angle (ICA) of the eye due to their low resolution. Increase in the intraocular pressure (IOP) can occur due to the abnormalities in TM, which could subsequently lead to glaucoma. Here, we present an indirect gonioscopy based imaging probe with significantly improved visualization of structures in the ICA including TM region, compared to the currently available tools. Imaging quality of the developed system was tested in porcine samples. Improved direct high quality visualization of the TM region through this system can be used for Laser trabeculoplasty, which is a primary treatment of glaucoma. This system is expected to be used complementary to angle photography and gonioscopy.

An inherently gain flattened three-core erbium doped fiber amplifier
Paper AO100-45
Author(s): David Benedicto, Univ. of Zaragoza (Spain); Juan Antonio Vallés, Univ. of Zaragoza (Spain), i3A- Aragon Institute of Engineering Research (Spain)

Erbium Doped Fiber Amplifiers (EDFAs) are widely used in optical communication. However, its gain spectrum is not uniform. Coupling between adjacent cores can be used in order to flatten the gain spectrum. In this contribution, the proposed design consists of three aligned, parallel, non-identical cores, the central one doped with Er3+ ions. The parameters of the side cores have been optimized so that the modes of the isolated cores phase match that of the central core at two different wavelengths nearby the Erbium emission peak one. In order to calculate the gain of the asymmetric Er-doped 3-core fiber and optimize the amplifier design, we have used a home-made computer code which evaluates the power propagation equations of the structure supermodes coupled to the rate equations of the involved active ions.

Ultrabroadband YCOB optical parametric chirped pulse amplifier
Paper AO100-47
Author(s): Hugo A. Pires, Victor Hariton, Celso P. João, Gonçalo M. Figueira, Univ. de Lisboa (Portugal)

Femtosecond laser systems operating at high average and peak powers are usually based on Ti:sapphire technology and conventional laser amplification. This approach, however, lacks the inherent broad

bandwidth, tunability, and efficiency that parametric amplification can offer. In this work, we report a large bandwidth, tunable, 10 Hz laser system based on optical parametric chirped pulse amplification (OPCPA). The nonlinear crystal is yttrium calcium oxyborate (YCOB), the pump is an Yb-based multi-pass amplifier and the broadband seed is a white-light continuum generated from a fused silica plate. The OPCPA chain has two stages operating at sub-ps pulse durations. The system's performance at different repetition rates, wavelength tunability and compression of the output pulses are shown.

Modeling of multi-core integrated structures in highly-doped glass
Paper AO100-50
Author(s): David Benedicto, Univ. of Zaragoza (Spain); Juan Antonio Vallés, Univ. of Zaragoza (Spain), I3A- Aragon Institute of Engineering Research (Spain)

Owing to the 3D capabilities of femtosecond laser waveguide writing, integrated multi-core structures (IMCS) can be produced in glass samples. However, when modelling active IMCS significant differences arise compared to multi-core fibers. When the core is highly doped, supermodes profile may experiment appreciable changes due to strong variations in the gain coefficient. Furthermore, in active integrated fs-laser written structures in glass the substrate is also doped, therefore the unconfined signal field experiences strong absorption in absence of pump. In addition, fs-laser waveguide writing generates a depressed refractive index area that influences the mode field distributions. Finally, signal beatings between quasi-phase-matched cores can be neglected. In this contribution, we present a quantitative study of how the supermodes formalism must be adapted for modeling 3-core and 7-core IMCS.

Aberration correction in confocal microscopy using ray tracing simulations to determine the sample induced aberrations
Paper AO100-52
Author(s): Pieter Smid, Georges Janes, John Vaughan-Hirsch, Anthony Bishopp, Darren Wells, Chung See, Amanda Wright, Univ. of Nottingham (United Kingdom)

In optical microscopy, imaging through thick and complex samples gives rise to optical aberrations which reduce image quality at depth. Confocal detection can be used to remove bulk scatter and out of focus light and Adaptive Optics (AO) can correct for aberrations. The challenge with AO is that it requires the wavefront aberrations present to be known. We investigated whether ray tracing simulations can be used to estimate sample induced aberrations prior to imaging and if they can provide accurate wavefront corrections for 3D confocal imaging. We studied root samples of the Arabidopsis Thaliana plant. Ray tracing simulations results of root samples will be presented. This will be supported with experimental data and confocal microscopy images. Simulations can provide useful corrections without the necessity of using a wavefront sensor. It was found that for high numerical apertures lens (> 1.0) correction of high order aberrations is also necessary.

Electronic band structure and optical response of $Sr_xZn_{1-x}O$ ternary alloy through modified Becke-Johnson potential
Paper AO100-55
Author(s): Salima Labidi, Annaba Univ. (Algeria)

First principles calculations have been performed within the framework of density functional theory to investigate the structural, electronic and optical properties of SrxZn1-xO ternary alloys. The exchange-correlation potential for structural properties was calculated by the standard local density approximation (LDA) and GGA (PBE), a more accurate nonempirical density functional generalized gradient approximation (GGA), as proposed by Wu and Cohen [Phys. Rev. B 73, 235116 (2006)], while for electronic properties, the Engel and Vosko GGA (EVGGA) and the modified Becke-Johnson (MBJ) schemes were also applied. The MBJ band gaps values agree well with the available experimental results. In addition optical properties were calculated and compared to the available experimental data and previous theoretical works.

Laser scanners and handheld probes for optical coherence tomography: fundamentals and applications
Paper AO100-57
Author(s): Virgil-Florin Duma, Aurel Vlaicu Univ. of Arad (Romania); George Dobre, Univ. of Kent (United Kingdom); Dorin Demian, Aurel Vlaicu Univ. of Arad (Romania); Cosmin Sinescu, Victor Babes Univ. of Medicine and Pharmacy of Timisoara (Romania); Adrian Bradu, Adrian Podoleanu, Univ. of Kent (United Kingdom)

Some of our main results in optical scanning are presented, with a focus on galvanometer-based scanning (GSs) applied in Optical Coherence Tomography (OCT): (i) the experimental demonstration of the best commonly used scanning function, i.e., triangular – with regard to sinusoidal and sawtooth ones (from which rules-of the thumb for the optimal use of GSs in OCT were extracted); (ii) mathematical models of sawtooth and triangular scanning with regard to scan frequency, amplitude, and input duty cycle (from which the optimal algorithm for collating individual images in OCT is obtained); (iii) the most efficient custom-made scanning input signals to determine a maximum duty cycle of GSs (which we demonstrated to be linear with parabolic non-linear stop-and-turn portions, and not linear with sinusoidal portions, as it has been considered previously in the literature). The handheld probes we have developed for OCT are presented, as well as some of their applications in dental medicine.

Electromagnetic properties of a monolayer of polarisable particles deposited on graphene
Paper AO100-59
Author(s): André Souto, Rui Pereira, Jaime Santos, Nuno Peres, Mikhail Vasilevskiy, Univ. do Minho (Portugal)

The plasmonic and THz optical properties of a system composed of a monolayer of small polarisable particles on top of a graphene sheet will be discussed in this presentation, taking into account, beyond the usual dipole-dipole interactions, interactions between polarisation charges induced in the graphene by each particle. Such a system possesses some interesting properties, for instance, a reflection minimum for a broad range of angles, whose spectral position can be tuned by changing the Fermi energy in graphene via electrostatic gating.

Definition of characteristics of silicon (Si) in conditions of strong thermodynamic non-equilibrium
Paper AO100-62
Author(s): Alexander V. Mazhukin, Olga N. Koroleva, Vladimir I. Mazhukin, Alexander V. Shapranov, Keldysh Institute of Applied Mathematics (Russian Federation)

Ultrashort (10-12-10-15 s) high power (109-1015 W/cm2) laser irradiation on Si is accompanied by the emergence of highly non-equilibrium states. In the case of a strong deviation from local thermodynamic equilibrium (LTE) the irradiated material (Si) is represented as a two subsystems, electron and phonon (lattice) with the energy exchange between them. Using mathematical modeling based on continuum models associated with the problem of determining the thermophysical, thermodynamic, optical, mechanical and other characteristics of the material for each of subsystems. In the present work suggest methods for determining of thermophysical and thermodynamic characteristics of Si in a wide range of pressures and temperatures for each of subsystems. Characteristics of the electronic subsystem is calculated from the thermodynamic and kinetic concepts, using the technique of the Fermi-Dirac integrals. Properties of silicon phonon subsystem were determined from a series of computational experim

Simulation of amorphous silicon waveguides
Paper AO100-63
Author(s): Paulo Lourenco, ISEL-ADEETC (Portugal); Alessandro Fantoni, CTS-UNINOVA (Portugal), ISEL (Portugal); Pedro Pinho, IT-ISEL (Portugal)

This paper presents some results, obtained by a set of FDTD (Finite-Difference Time-Domain) simulations, about the characteristics of amorphous silicon waveguides embedded in a SiO2 cladding. Light absorption dependence on the material properties and waveguide curvature radius are analysed for

wavelengths in the IR (infrared) spectrum. Wavelength transmission efficiency is determined analysing the decay of the light power along the waveguides and the obtained results show that radiation losses should remain within acceptable limits when considering curvature radius as small as 3 μm at its most and that hydrogenated amorphous silicon based waveguides are highly dependent of operating wavelength, with its extinction coefficient rapidly increasing as operating wavelength goes into visible and beyond spectrum range, namely within the 1st optical transmission window. When the operating wavelength is within the 2nd or 3rd optical transmission windows, a-Si:H is practically transparent.

Scattering, absorption and transmittance of experimental graphene dental nanocomposites
Paper AO100-68
Author(s): Maria del Mar Pérez Gómez, Marianne Salas, Univ. de Granada (Spain); Marioara Moldovan, Babes Bolyai Univ. (Romania); Diana Dudea, Univ. of Medicine, Pharmacy Iuliu Hatieganu (Romania); Ana Yebra, Razvan Ghinea, Univ. de Granada (Spain)

This study aimed to evaluate the optical properties of experimental graphene dental nanocomposites. Spectral reflectance was measured against white and black background and S and K coefficients as well as transmittance of samples were calculated using Kubelka-Munk's equations. The spectral behavior of S, K and T experimental graphene exhibited different trends compared with the commercial nanocomposites and they were statistically different. Experimental nanocomposites show higher scattering and lower transmittance when compared with commercial nanocomposite, probably, due to the shape, type and size of the filler. K coefficient for short wavelength of the pre-polymerized experimental nanomposites was very low. According to our results, hidroxypatite with graphene used in dental composites needs to be improved to reproduce esthetic properties of natural dental tissues and to have potentially clinical applications.

The analogue quantum mechanical of plasmonic atoms
Paper AO100-74
Author(s): Rúben Azinheira Alves, João C. Costa, Miguel T. Gomes, INESC TEC, Ctr. of Applied Photonics (Portugal), Univ. of Porto (Portugal); Nuno A. Silva, INESC-TEC (Portugal), Univ. of Porto (Portugal); Ariel R. N. S. Guerreiro, INESC TEC, Ctr. of Applied Photonics (Portugal), Univ. of Porto (Portugal)

Localized plasmons in metallic nanostructures present strong analogies with Quantum Mechanical problems of particles trapped in potential wells. In this paper we take this analogy further using the Madelung Formalism of Quantum Mechanics to express the fluid equations describing the charge density of the conduction electrons and corresponding interaction with light in terms of an effective generalized nonlinear Schrödinger equations. Within this context, it is possible to develop the analogy of a plasmonic atom and molecule that exhibits Rabi oscillations, Stark effects, among other Quantum Mechanical effects.

Research and development of optical fibres coated with thin films for sensing applications
Paper AO100-75
Author(s): Luis Coelho, INESC TEC, Ctr. of Applied Photonics (Portugal); José L. Santos, INESC TEC, Ctr. of Applied Photonics (Portugal), Univ. do Porto (Portugal); Pedro Jorge, INESC TEC (Portugal), Univ. do Porto (Portugal); José M. M. M. de Almeida, INESC TEC, Ctr. of Applied Photonics (Portugal), Univ. de Trás-os-Montes e Alto Douro (Portugal)

The outcome of optical fibre sensors started a new class of sensing devices for a large variety of parameters either physical or chemical entities. The addition of specific thin film coatings over fibre structures surface could open new possibilities in fibre optic sensors particularly at two levels, tailoring and enhancement. The majority of the fibre sensors are refractometers where the external refractive index changes the optical properties of the spectral response. Coating these structures with metals, plasmonic effects, or with high refractive index materials, the sensing response is enhanced and adding sensitive coatings to the surface it is possible to detect specific targets. This detection is accomplished by measuring the changes of the coating optical properties or through the surface functionalization

processes. In this work, new guided wave sensors that have been developed will be discuss, based mostly on metallic and dielectric thin film deposition.

High-energy diode-pumped laser for OPCPA pumping
Paper AO100-76
Author(s): Celso Paiva João, Victor Hariton, Hugo Pires, Nuno Gomes, Gonçalo Figueira, Instituto Superior Técnico (Portugal)

The latest developments on the diode-pumped laser system at the Laboratory of Intense Laser (L2I) and its applications are presented. Currently, the laser delivers 60 mJ, 1 ps pulses at repetition rate of 2 Hz with high-energy stability. The output pulses are used for high harmonic generation, OPCPA pumping and laser material ablation experiments.

Development of a quantum particle in cell algorithm in GPU for solving Maxwell-Bloch equations
Paper AO100-79
Author(s): Miguel B. T. Gomes, João C. Costa, Rúben A. Alves, INESC TEC, Ctr. of Applied Photonics (Portugal); Nuno A. Silva, Ariel R. N. S. Guerreiro, INESC TEC (Portugal)

In this paper we report on the development of a numerical solver of the Maxwell-Bloch equations based on heterogeneous supercomputing using GPGPUs. The solver adapts techniques from many-body simulation, namely the particle-in-cell approach, to describe the interaction between the electromagnetic field and atomic gas whose internal state is described by the multilevel Bloch equations. We also present the benchmark and performance analysis of the code. We investigate the interaction between two coherent light beams, as a case of study to demonstrate the validation of the code.

Special home-made microstructured optical fibers for engineered SFWM photon pair sources
Paper AO100-82
Author(s): Vladimir P. Minkovich, Ctr. de Investigaciones en Óptica A.C. (Mexico); Francisco Dominguez-Cerna, Karina Garay-Palmett, Ctr. de Investigacion Cientifica y Educacion Superior de Ensenada (Mexico); Roberto Ramirez-Alarcon, Ctr. de Investigaciones en Óptica A.C. (Mexico)

Measurements of spontaneous four wave mixing (SFWM) spectra in special home-made microstructured optical fibers (MOFs) together with information of the transverse modes in which generated wavepackets propagate inside the fiber, are analyzed by means of a genetic algorithm. As a result, it is possible to identify the SFWM-interaction giving rise to a particular energy conserving peak, and to fully characterize the fiber, i.e. the fiber dispersion properties can be inferred. We have implemented SFWM sources in fabricated special MOFs with different geometries in order to get the full chromatic dispersion properties of each fiber, and identify optimal experimental conditions for the generation of two-photon states with engineered entanglement properties.

Low cost intrinsic Fabry-Perot interferometric optical fiber strain and pressure sensor
Paper AO100-83
Author(s): Maria F. Domingues, Instituto de Telecomunicações (Portugal); Joana Martins, Univ. of Aveiro (Portugal); Camilo A. Rodriguez, Federal Univ. of Espirito Santo (Brazil); Catia Tavares, Nelia Alberto, Instituto de Telecomunicações (Portugal); Paulo S. André, Technical Univ. of Lisbon (Portugal); Paulo Antunes, Instituto de Telecomunicações (Portugal)

In this paper, a cost effective procedure to manufacture strain and pressure intrinsic optical fiber sensors is presented. The proposed sensing elements are based on Fabry-Perot interferometric micro-cavities created from the recycling of optical fibers destroyed by the catastrophic fuse effect. The sensitivities determined were 8.4 pm/με and 6.5 pm/kPa, for the strain and pressure sensors, respectively. The repeatability of the sensors' response is also demonstrated.

Pinching optical potentials for spatial nonlinearity management in Bose Einstein condensates
Paper AO100-85
Author(s): Nuno A. Silva, João Costa, Miguel Gomes, Ruben Alves, Ariel Guerreiro, INESC TEC, Ctr. of

Applied Photonics (Portugal), Departamento de Física e Astronomia da Faculdade de Ciências da Universidade do Porto (Portugal)

Spatiotemporal management of nonlinearities is emerging as a new tool for the manipulation of soliton dynamics. In particular, for the case of matter-wave solitons of Bose Einstein Condensates, these so called “collisionally inhomogeneous media” has been a playground for novel nonlinear phenomena, which include for example the adiabatic compression of matter waves, atomic soliton lasers and interferometers and the observation and control of Faraday waves. Unfortunately for many interesting experiments involving spatial varying nonlinearities, the standard approach of the Feshbach resonance management has proven to be unsuitable due either to length scale mismatches or additional parasitic effects. Here we explore the possibility of controlling the inhomogeneities in quasi-1D Bose Einstein condensates using a spatial variation of the transverse confinement potential and explore different optical strategies to realize these pinched traps.

Wavefront coding for visual optics
Paper AO100-87
Author(s): Eva Acosta, Univ. of Santago de Compostela (Spain); Justo Arines, Citlalli Almaguer, Univ. of Santiago de Compostela (Spain)

Wavefront coding (WFC) enables the depth of field of incoherent optical systems to be extended. This method involves a cubic-phase plate in the system yielding a blurred image nearly invariant to defocus. It was recently demonstrated invariance to also small amount of astigmatism and high order aberrations. In visual optics there is a big interest in improving solutions in two different problems: Presbyopia correction and high resolution retinal images with low cost devices. In WFC based systems the blur is removed by image postprocessing. In the case of contact or intraocular lenses for presbyopia correction, the very brain is the one who makes the decoding process. High-resolution retinal images can be obtained by proper post processing, avoiding thus all the optics needed to sense and correct ocular aberration, i.e., wavefront sensors and deformable mirrors, what reduces considerably the complexity and cost of the device. Experimental results for both applications will be shown.

The extended Kubelka-Munk theory and its application to colloidal systems
Paper AO100-92
Author(s): Rodrigo Alcaraz de la Osa, Andrea Fernández Pérez, Univ. of Cantabria (Spain); Yael Gutiérrez, Dolores Ortiz, Univ. de Cantabria (Spain); Franciso González, Fernando Moreno, Jose M. Saiz, Univ. of Cantabria (Spain)

The Kubelka-Munk (K-M) theory is one of the main theories of light flux through homogeneous isotropic media [1]. It has been recently extended to the case of a specimen on top of an arbitrary substrate [2]. In this research, we propose to use the extended K-M theory to perform a colorimetric study of colloidal systems, connecting absorption and scattering cross-sections calculated with Mie theory [3], with absorption and scattering parameters associated with the K-M theory [4]. Trajectories in the color space are calculated from both reflection and transmission spectra, either as we vary the radius of the particles or the proportion of different radii in a polydisperse sample, comparing results with those from effective medium theories, such as the Maxwell-Garnett theory [3].

Modeling metal-dielectric core-shell nanoparticles with effective medium theories
Paper AO100-93
Author(s): Yael Gutiérrez Vela, Dolores Ortiz, Rodrigo Alcaraz de la Osa, Juan Marcos Sanz, Univ. of Cantabria (Spain); Jose Maria Saiz, Univ. de Cantabria (Spain); Francisco Gonzalez, Fernando Moreno, Univ. of Cantabria (Spain)

Extending nanoplasmonics to the UV-range has awaken new interest due to challenges arising in some important areas like chemistry (photocatalysis) or biology. Two of the more promising metallic materials in this range are aluminum (Al) and magnesium (Mg). However, nanoparticles (NPs) made of these two metals suffer from the formation of a native oxide layer whose thickness strongly depends on the ambient

conditions. These oxidized NPs can be theoretically modeled as metal-oxide core-shell NPs. Some authors have proposed to treat this type of NPs with effective medium theories. Effective medium theories (EMTs) allow to obtain an effective dielectric function of the whole core-shell NP. Here, we propose a new procedure to obtain the effective dielectric constant of a nano-shell outside the electrostatic approximation and we compare it with other existing EMTs. We believe that the proposed procedure can be helpful for predicting the electromagnetic response of spherical core-shell NPs.

Image encryption scheme based on computer generated holography and time-averaged moiré
Paper AO100-94
Author(s): Paulius Palevicius, Giedrius Janusas, Arvydas Palevicius, Minvydas Ragulskis, Kaunas Univ. of Technology (Lithuania)

A technique of computational image encryption and optical decryption based on computer generated holography and time-averaged moiré is proposed. Dynamic visual cryptography (a visual cryptography scheme based on time-averaging geometric moiré), Gerchberg–Saxton algorithm and 3d microstructure manufacturing techniques are used to construct the scheme. The secret is embedded into a cover image by using a stochastic moiré grating and can be visually decoded by a naked eye if the amplitude of harmonic oscillations in the Fourier plane corresponds to an accurately preselected value. The process of the production of 3D microstructure is given. Electron beam lithography is exploited for physical 3D patterning. A phase data of a complex 3D microstructure is obtained by Gerchberg-Saxton algorithm which is used to produce a computer generated hologram. Physical implementation of microstructure is performed by using a single layer polymethyl methacrylate as a basis for 3D microstructure.

Effect of cooling water on ablation efficiency in Er-YAG laserosteotome of hard bone
Paper AO100-95
Author(s): Hamed Abbasi, Lina M. Beltran B., Azhar Zam, Univ. of Basel (Switzerland)

This paper aims to examine the effect of immersion water on ablation efficiency of hard bone. Fresh hard pig bones were ablated using pulsed Er-YAG laser and ablation efficiency was measured with and without presence of cooling water. The laser worked in 2940 nm wavelength and 10 Hz repetition rate in microseconds pulse duration regime. Immersion water was added to the sample container with different volume for preventing carbonization. Several areas of samples were ablated with fixed deposited energy to investigate the effect of immersion cooling water on ablation efficiency of bones. Ablation efficiency was measured by observing the amount of cut area per seconds and it was observed that ablation efficiency was reduced in presence of cooling water.

Mueller matrix imaging and analysis of cancerous cells
Paper AO100-97
Author(s): Andrea Fernández Pérez, Jose María Saiz Vega, Fernando Moreno Gracia, Univ. de Cantabria (Spain); José Luis Fernández Luna, Hospital Universitario Marqués de Valdecilla (Spain)

Imaging polarimetry has become a field of increasing interest in diagnosis because of its non-invasive nature and its potential to identify abnormal tissues. When light interacts with matter its polarimetric properties are affected by the nature of the material. Consequently, the analysis of polarimetric parameters should give information about the tissue. Some methods have been widely used to extract the information given by the Mueller matrix, transforming it into useful parameters that may contribute to providing a physical interpretation. The experimental device used for the measurement of the Mueller matrix consists of a Dynamic Rotating Compensator Polarimeter. We have performed imaging polarimetry and measured the transmission Mueller matrix of several samples of tumor cells. We have applied three different methods for its analysis: polar decomposition, Mueller matrix transformation and differential decomposition. We want to compare the results provided by all of them.

Evaluation of FEL lamp seasoning behavior for use as a spectral irradiance standard
Paper AO100-98
Author(s): Antonio F. Gentil Ferreira, Instituto de Pesquisas Tecnológicas (Brazil), Lab. de Engenharia

Biomédica, Escola Politécnica da Univ. de São Paulo (Brazil); José Carlos T. B. Moraes, Lab. de Engenharia Biomédica, Escola Politécnica da Univ. de São Paulo (Brazil)

This work presents seasoning result from a set of 1000 W FEL-type lamp concerning its qualification to be used as a secondary spectral irradiance standard. The lamps from the set were made from two different manufactures and were seasoned for a period of 40 hours. During the seasoning, relative drift of the lamp irradiance, lamp current and voltage were measured at each 5 minutes. The lamp irradiance was measured in a narrow spectral band with a full width half maximum of 35 nm in the blue range of spectrum with peak wavelength of 460 nm. The visible spectrum was measured four times for each lamp during the seasoning period using a commercial spectroradiometer and a PTFE diffusion plate in the configuration 0º/45º. The irradiance was measured using a 4 ½ digits radiometer with thermal stabilized detector head, the lamp current was measured using a 6 ½ digits voltmeter associated with a standard resistor of 0.1 Ohm and the lamp voltage was measured using a 6 ½ digits voltmeter.

Correlative optical imaging in the far-field and near-field regimes: architecture and applications
Paper AO100-101
Author(s): Stefan G. Stanciu, Catalin Stoichita, Denis E. Tranca, Radu Hristu, George A. Stanciu, Univ. Politehnica of Bucharest (Romania)

Correlative imaging assays are often challenging as investigating corresponding sample regions using different systems can be cumbersome, and sometimes impossible in the case of samples with time-dependent properties. For facilitating such correlative studies, we have recently developed a multimodal imaging system which allows the acquisition of optical data using a variety of complementary techniques operating in the far-field and near-field regimes. In this contribution we present the architecture of this system, and discuss a series of connected experiments focused on imaging biological samples and advanced materials.

Studying tunability of some NIR semiconductor lasers by external cavity setup
Paper AO100-103
Author(s): Mohammad Amin Bani, Majid Nazeri, Univ. of Kashan (Iran, Islamic Republic of); Hamed Abbasi, Univ. Basel (Switzerland)

In this paper, tunability of three near-infrared semiconductor lasers which typically lase at 808 nm, 892 nm and 980 nm is studied. Both Littrow (wavelength dependent beam direction setup) and Littman (wavelength independent beam direction setup) configurations have been used in this experiment. A 1200 l/mm diffraction grating, a plane front surface mirror, a collimating convex lens, a power supply and opto-mechanical components have been used to tune these lasers in the external cavity setup. The wavelength of the output beam of the laser and the power of the output beam of the laser have been measured by means of a compact CCD spectrometer and a power meter, respectively. In all three cases, Littrow configuration shows a little better tuning range. In both Littrow and Littman configurations the wavelengths near the main wavelength of the laser had more power. The highest achieved power of these lasers in the Littrow setup was more than that of the Littman setup.

Spiropyran polymeric films as NLO functional materials: experiments and DFT calculations
Paper AO100-105
Author(s): Ilona Radkowska, Piotr Bragiel, Izabela Fuks-Janczarek, Zygmunt Bak, Jan Dlugosz Univ. in Czestochowa (Poland)

Spiropyrans could form promising functional materials applicable in NLO field due to their special properties connected with a photochromism phenomenon. Research was done for two different spiropyran molecules and their open forms. Three polymers were tested: poly(vinyl alcohole) (PVA), polystyrene (PS) and poly(methyl methacrylate) (PMMA). Calculations were performed in Gausssian 09 v.C1 program, using three DFT functionals – B3LYP hybrid functional and two long-range functionals: CAM-B3LYP and LC-BLYP ones – and three basis sets: 6-31G(d), 6-311++G(2d,2p) and NLO-V basis sets. Geometry parameters, energies, absorption and oscillation spectra were calculated as well as the components of the polarizability and hyperpolarizability tensors. Experiments were focused on

spiropyran-polymer films preparation – two different forms were made, namely polymer foils and thin layers on quartz or cuprum substrate. They were studied with UV-VIS, RAMAN spectroscopies, SEM and Z-scan techniques.

Interoccular suppression
Paper AO100-108
Author(s): Ana Rita Ramos Tuna, Amélia Maria Fernandes Nunes, Univ. of Beira Interior (Portugal)

Parameters such as suppression and ocular dominance are fundamental to evaluate the quality of binocular fusion. Techniques recently proposed and used to evaluate these parameters are based on the movement of optical coherence, or manipulation of interocular luminance. The objective of this work is to quantify the interocular dominance or suppressive imbalance, based on the manipulation of ocular luminance, between a group of subjects with normal binocular vision and a group of subjects diagnosed with amblyopia. Participants included 25 subjects with normal binocular vision and 11 subjects with amblyopia, aged between 8 and 35 years. The suppressive imbalance was quantified for each of the volunteers and the results were compared between the two groups.

Quasi-distributed optical fiber sensor for simultaneous vibration and temperature measurement in stator bars of a 370 MVA electric generator
Paper AO100-110
Author(s): Uilian José Dreyer, Federal Univ. of Technology - Paraná (Brazil); Erlon V. da Silva, Tractebel Energia (Brazil); Cicero Martelli, Jean Carlos Cardozo da Silva, Federal Univ. of Technology - Paraná (Brazil)

In this paper, we present the results obtained from a new multiparametric optical fiber transducer applied to an electric generator of 370 MVA. The obtained results are from temperature and vibration measurement of the stator bars over a 23 h test. The temperature results have a maximum difference of 2 °C between all the installed FBG's. The vibration measurement shows the 2 Hz mechanical component and 120 Hz electromagnetic component during the electric generator operation.

Nonlinear optics in kagomé microstructured optical fibres
Paper AO100-111
Author(s): Sílvia M. G. Rodrigues, Margarida M. R. V. Facão, Mário F. S. Ferreira, Univ. of Aveiro (Portugal), i3N-Institute of Nanostructures, Nanomodelling and Nanofabrication (Portugal)

The microstructured optical fibres (MOFs) are a class of optical fibres that have a microstructured design. They can be divided in two categories: solid-core MOFs which usually guide light by modified total internal reflection, or hollow-core MOFs which usually guide light by photonic bandgap effect or other correlated effects. Amongst the HC-MOFs we have the kagomé fibres. In this work we are going to study nonlinear effects in those gas-filled kagomé fibres. We will study various fibre properties including the guided modes, the group-velocity dispersion, and the nonlinear parameter. After that we will present numerical results of light propagation in those fibres.

Structural, electronic and thermodynamic properties of $Sr_xCa_{1-x}Te$: a first-principles study
Paper AO100-112
Author(s): Malika Labidi, Ecole Préparatoire aux Sciences et Techniques (Algeria); Salima Labidi, Kalthoum Klaa, Lab. des Nanomatériaux, Corrosion et Traitements de Surfaces (Algeria)

First principles calculations have been performed within the framework of density functional theory to investigate the structural, electronic and thermodynamic properties of SrxCa1-xTe ternary alloys. The exchange-correlation potential for structural properties was calculated by the standard local density approximation (LDA) and GGA (PBE), a more accurate nonempirical density functional generalized gradient approximation (GGA), as proposed by Wu and Cohen [Phys. Rev. B 73, 235116 (2006)], while for electronic properties, the Engel and Vosko GGA (EVGGA) and the modified Becke-Johnson (MBJ) schemes were also applied. Deviation of the lattice constants from Vegard’s law and bulk modulus from linear concentration dependence (LCD) were observed for the ternary alloys. The MBJ band gaps values

agree well with the available experimental results. In addition the thermodynamic stability of the alloys was investigated by calculating the critical temperatures of alloys.

Advances in holographic techniques for experimental generation of 3D images and optical nondiffracting beams
Paper AO100-113
Author(s): Marcos R. R. Gesualdi, Univ. Federal do ABC (Brazil)

This work presents the optical generation of 3D images and optical nondiffracting beams via computational and photorefractive holographic techniques. The optical realization of 3D images and nondiffracting beams was made in a computational and photorefractive holography setup, using a photorefractive silenite crystal (BSO and BTO) as holographic recording medium, where the 3D images and nondiffracting beams (Bessel, Airy, Mathieu and Parabolic), the nondiffracting beam arrays and superposition of co-propagating nondiffracting beams were obtained experimentally. The experimental results are in agreement with the theoretically predicted presenting excellent prospects for implementation of these techniques for static and dynamic systems in optics and photonics applications.

Effect of laser pulse duration on ablation efficiency of hard bone in microseconds regime
Paper AO100-115
Author(s): Lina Beltran, Hamed Abbasi, Azhar Zam, Univ. of Basel (Switzerland)

The aim of the present paper is to investigate the effect of laser pulse duration on ablation efficiency of hard bones. The bones were ablated using microsecond pulsed Er-YAG laser with different pulse durations. The laser works in 2.94 micrometer wavelength with 10 Hz repetition frequency with microseconds pulse durations. Hard porcine bones were used as a sample and several areas were ablated with fixed applied energy and different pulse durations to investigate the effect of pulse duration on ablation efficiency of bone samples. Ablation efficiency was measured by observing the amount of cut area per seconds. Moreover, effect of different pulse duration in microsecond regime on carbonization was investigated.

Perfect optical vortices generation using a spatial light modulator
Paper AO100-117
Author(s): Nelson Anaya Carvajal, Cristian H. Acevedo Cáceres, Yezid Torres Moreno, Univ. Industrial de Santander (Colombia)

Experimental perfect optical vortices with topological charges less than m=10 are generated using computerized holograms with a combination of axicon and spiral functions. The computerized holograms are displayed onto a transmission liquid-crystal spatial light modulator working with two-phase levels that is binary holograms. We also investigated numerically and experimentally the free space diffraction of a perfect optical vortex afterward the Fourier plane. It is found that the perfect optical vortices have not the ring width size and average ring diameter invariant with propagation distance.

Automatization of the Foucault knife-edge quantitative test
Paper AO100-118
Author(s): Gustavo Rodríguez, Univ. Autónoma de Madrid (Mexico); Jesús Villa, Univ. Autónoma de Zacatecas (Mexico); Geminiano Martínez, Ctr. de Investigaciones en Óptica (Mexico); Ismael de la Rosa, Univ. Autónoma de Zacatecas (Mexico)

Given the necessity of economical and reliable methods for performing quality tests of optical surfaces, we resumed the study of the Foucault test achieving a closed formulation that relates the knife-edge position with the irradiance pattern, which allowed us to propose a quantitative methodology for estimating the wavefront error of an aspherical mirror with precision akin to interferometry. In this work is presented an improved version of the algorithm in which the transient slope-point calculation and gradient integration processes have been considerably simplified and enhanced, thus remarkably increasing the accuracy and efficiency of the methodology. This revised algorithm can be easily implemented in most

microcontrollers, hence enabling the arrangement of a fully automatized test apparatus and opening a realistic path for the proposal of an optical mirror analyzer prototype.

Simulation of partially coherent light propagation using parallel computing devices
Paper AO100-120
Author(s): Tiago E. C. Magalhães, José M. Rebordão, Instituto de Astrofísica e Ciências do Espaço (Portugal)

Light acquires or loses coherence and coherence is one pf the few optical observables. Spectra can be derived from coherence functions and understanding any interferometric experiment is also relying upon coherence functions. Beyond the two limiting cases (full coherence or incoherence) the coherence of light is always partial and it changes with propagation. We have implemented a code to compute the propagation of partially coherent light from the source plane to the image plane using parallel computing devices (PCDs). To this end, we used the Open Computing Language (OpenCL) and the open-source toolkit PyOpenCL, which gives access to OpenCL parallel computation through Python. We tested our implementation for several systems with different devices and compared it with the usual one in Python. When using powers of two for the dimensions of the cross-spectral density matrix (e.g. 16^4, 32^4), a speed increase is observed in the PyOpenCL implementation when the matrix dimension is 64^4.

Variable structure and sliding modes nonlinear control system applied to a fiber optic interferometer
Paper AO100-124
Author(s): Roberta I. Martin, Univ. Estadual Paulista - UNESP (Brazil); João M. S. Sakamoto, Instituto de Estudos Avançados (Brazil); Marcelo C. M. Teixeira, Cláudio Kitano, Univ. Estadual Paulista - UNESP (Brazil)

In this work, we present the application of a nonlinear control system, based on variable structure control and sliding modes, to a fiber optic Mach-Zehnder interferometer. We showed that this control system is able to keep the interferometer in quadrature, suppress the signal fading, lead to high accuracy control, featuring ease of implementation and high robustness. Thus, the controlled interferometer was employed for the measurement of frequency response and mechanical resonances of a cylindrical piezoelectric actuator, showing its capability to properly detect mechanical vibrations. The advantages of an all-fiber interferometric sensor combined with the proposed nonlinear control features compactness, light weight, alignment free, electromagnetic immunity, high sensitivity, geometric versatility, robustness, real-time high precision measurement, and possibility of operation in harsh environments.

Cavity ring-down technique for refractive index sensing using multimodal interference
Paper AO100-131
Author(s): Susana Silva, INESC TEC, Ctr. of Applied Photonics (Portugal), Univ. of Porto (Portugal); Orlando Frazao, INESC TEC (Portugal), Univ. of Porto (Portugal)

This work presents a cavity ring-down (CRD) system using a multimode interference-based fiber sensor for refractive index (RI) measurement. The fiber sensor is inserted inside the fiber loop cavity of the CRD and it is used for sensing temperature-induced RI changes of water. A modulated laser source was used to send pulses down into the fiber loop, inside of which an erbium-doped fiber amplifier (EDFA) was placed in order to provide an observable signal with a reasonable decay time. The behavior of the sensing head to temperature was studied due to its intrinsic sensitivity to said parameter – a sensitivity of -1.6x10-9 us/ºC was attained. This allowed eliminating the temperature component from RI measurement of water and a linear sensitivity of 580 us/RIU in the RI range of 1.324-1.331 was obtained.

Optical properties of Au/CuO nanoplasmonic thin films
Paper AO100-133
Author(s): Joel Borges, Rui S. S. Pereira, Univ. do Minho (Portugal); Manuela Proença, Marco S. Rodrigues, Ctr. de Fisica, Univ. do Minho (Portugal); Mikhail I. Vasilevskiy, Filipe Vaz, Univ. do Minho (Portugal)

In this work, the LSPR characteristics of Au/CuO films were studied experimentally and theoretically. Using Monte Carlo methods, different distributions of Au NPs were modeled and their optical susceptibility inside a CuO matrix was calculated numerically using the coupled dipole equations. The effect of different parameters (such as the concentration and size of the NPs) was analysed in order to compare with the experimentally observed optical behaviour of Au/CuO films.

Maritime environment effect on underwater image restoration
Paper AO100-135
Author(s): Fatah Almabouada, Ctr. de Développement des Technologies Avancées (Algeria), Univérsité Kasdi Merbah, Faculté Mathématiques & des Sciences de la Matière, Département de physique (Algeria); Kamal Eddine Aiadi, Univ. Kasdi Merbah (Algeria)

Nowadays, laser sources are widely used in a maritime environment for mobile robot, imaging and optical communication [1,2]. In general, there are only the blue and green wavelengths which propagate easily in water [3]. Depending on the type of water, such as clear water, coastal water and turbid harbor the propagation of these two wavelengths can be strongly attenuated. This attenuation is the result of the increase of the absorption and the scattering effects. This paper describes the effect of the maritime environment on image restoration using a laser source to illuminate an object. An underwater imaging system allows to restore an image of an object in a water body at a certain distance.

Using DSLR cameras in digital holography
Paper AO100-137
Author(s): Diego Hincapie Zuluaga, Univ. Nacional de Colombia (Colombia); Jorge A. Herrera-Ramirez, Instituto Tecnológico Metropolitano (Colombia); Jorge I. Garcia-Sucerquia, Univ. Nacional de Colombia (Colombia)

In digital holography (DH) the size of the bidimensional image sensor to record the digital hologram plays a key role on the performance of this imaging technique; the larger the size of the camera sensor the better the quality of the final reconstructed image. Scientific cameras with large formats are offered in the market, but their cost and availability limit their use as a first option when implementing DH. Nowadays, DSLR cameras provide an easy-access alternative that is worthwhile to be explored. The DSLR cameras are a widely commercially available option that in comparison with traditional scientific cameras offer a much lower cost per effective pixel over a large sensing area. However, in the DSLR cameras, with their RGB pixel distribution, the sampling of information is different to the sampling in monochrome cameras usually employed in DH. This fact has implications in their performance. In this work, we discuss why DSLR cameras are not extensively used for DH.

Empirical mode decomposition (EMD) with post processing and Hilbert-Huang Transform (HHT) of occipital (Oz) electrophysiological signal correlated with our feelings as what see is like when we see
Paper AO100-139
Author(s): Vitor Pereira, Univ. de Lisboa (Portugal)

We move from the features of the ERP (such as the amplitude and latency of peaks) of the Pereira 2015 towards the instantaneous frequency of occipital event-related changes correlated with a contrast in access and correlated with a contrast in phenomenology. Despite that the Wavelet or the Fourier Transform are the methods most widely used for analysing the linear (proportionality or additivity) and stationary (the signal, and so the time series representing this signal, has the same mean and variance throughout) properties of the EEG signal, the EEG signal have nonlinear (nonproportionality or nonadditivity) and non stationary (signal's statistical characteristics change with time) properties. However, one suitable method for analyse the instantaneous change in occipital ERPs phase and accounted for a transient peak in frequency (positive or negative), if any, in the underlying structure of the occipital ERPs correlated with a contrast in access and correlated with a contrast.

Simultaneous measurement of temperature and refractive index based on microfiber knot resonator integrated in an abrupt taper Mach-Zehnder interferometer

Paper AO100-141
Author(s): André Delgado Gomes, INESC TEC, Ctr. of Applied Photonics (Portugal); Orlando Frazão, INESC TEC (Portugal)

Recently, several configurations using MZIs have been demonstrated for simultaneous measurement of temperature and refractive index. In this work, a microfiber knot resonator integrated in an abrupt taper Mach-Zehnder interferometer was used for simultaneous measurement of temperature and refractive index. This compact structure was fabricated using only CO2 laser processing. The two different components of the transmission spectrum (the microfiber knot resonator and the Mach-Zehnder interferometer components) present different sensitivities when subjected to physical or chemical parameters. A characterization in temperature and refractive index was performed. A simple matrix method is used for simultaneous measurement of temperature and refractive index.

Thermal sensitivity increase of RFBG in the visible range
Paper AO100-142
Author(s): Patricia L. Inácio, Camila C. de Moura, Valmir de Oliveira, Ismael Chiamenti, Federal Univ. of Technology - Paraná (Brazil); Hypolito J. Kalinowski, Univ. Federal Fluminense (Brazil)

The huge density of the internet traffic in the optical networks compels implementing new cost-effective solutions. One possibility is adding to links operating at the visible range, useful at short distance – like those used in the distribution (FTTH/B,PON), which will require a new class of optical devices. A widespread component is the fibre Bragg grating (FBG), due to its spectral quality. It is known that regeneration improves the FBG optical spectral characteristics, including changes in the thermal sensitivity. In this work, the increase of this parameter for FBGs in the visible range is presented after the regeneration for three different silica fibres: single-, few- and multi-mode at visible wavelengths. The FBGs are produced by direct illumination under the phase mask using UV light from two different laser sources at 248 nm. The regeneration starts with an initial heating ramp (≈ 40 min) followed by the high temperature plateau and a subsequent cooling down to room temperatu

Strain sensor based on hollow microsphere Fabry-Perot cavity
Paper AO100-144
Author(s): Catarina S. Monteiro, Susana Silva, Orlando Frazão, INESC Porto (Portugal)

Fusion splicing technique was explored for the fabrication of two sensing structures based on hollow microsphere Fabry-Perot cavity. The first sensor proposed was fabricated with a hollow microsphere tip, and works as a probe sensor. This structure was studied for lateral load pressure, yielding a 1.56 ± 0.01 nm/N sensitivity. The second sensing structure relied on an in-line hollow microsphere. This sensor allowed the detection of lateral load pressure, with a sensitivity of 2.62 ± 0.02 nm/N. Furthermore, the proposed structure enabled strain sensing, with a sensitivity of 4.66 ± 0.03 pm/με. The two sensing structures were subjected to temperature presenting low thermal cross-sensitivity.

Fiber Bragg grating on abrupt taper end for temperature independent refractive index sensing
Paper AO100-145
Author(s): André Delgado Gomes, INESC TEC, Ctr. of Applied Photonics (Portugal); Beatriz Silveira, INESC TEC (Portugal); Stephen C. Warren-Smith, Institute for Photonics and Advanced Sensing (Australia), Leibniz Institute of Photonic Technology IPHT (Germany); Martin Becker, Manfred Rothhardt, Leibniz Institute of Photonic Technology IPHT (Germany); Orlando Frazão, INESC TEC (Portugal)

Temperature independent refractive index measurements were achieved using a fiber Bragg grating inscribed in an abrupt taper end. The Bragg grating was inscribed using a phase-mask interferometer driven by a femtosecond laser. The grating period is 537.5 nm, corresponding to a Bragg wavelength of 1550.6 nm for the fundamental mode of the abrupt taper. The abrupt taper transition excites many modes with different effective refractive indices. Refractive index and temperature analysis are performed for different reflection peaks. Temperature independent refractive index sensing is performed by monitoring the difference between the wavelength shifts of two measured reflection peaks.

Antiresonant polymer capillary fibers as pressure sensors
Paper AO100-150
Author(s): Jonas H. Osório, Unicamp (Brazil); Thiago H. R. Marques, Instituto de Física "Gleb Wataghin", Unicamp (Brazil), Instituto de Filosofia e Ciências Humanas, Unicamp (Brazil); Igor C. Figueredo, Unicamp (Brazil); Cristiano M. B. Cordeiro, Instituto de Física "Gleb Wataghin", Unicamp (Brazil)

Recently, antiresonant optical fibers reacquired importance due to the study of very interesting properties as low dispersion and high damage threshold. Among antiresonant fibers, the capillaries emerge as the simplest structure which can provide opportunities in sensing. When light is transmitted through a capillary central hole, some wavelengths experiences high loss, appearing as dips in the transmitted spectrum. Dip's spectral positions are dependent on waveguide refractive indexes and capillary wall thickness which, in turn, are sensitive to pressure. Here, we studied capillary fibers sensitivity to hydrostatic pressure changes. An analytical model was used for describing the capillary wall thickness variation due to pressure application. Preliminary experimental measurements were performed by submitting a PMMA capillary fiber to increasing pressure variations between 0 and 18bar. Experimental sensitivities range from (39±2)pm/bar to (55±2)pm/bar.

Influence of a perturbation in the gyrator domain for a joint transform correlator-based encryption system
Paper AO100-153
Author(s): Juan M. Vilardy Ortiz, Univ. de la Guajira (Colombia); María S. Millán, Elisabet Pérez-Cabré, Univ. Politècnica de Catalunya (Spain)

We present the results of the noise and occlusion tests in the Gyrator domain (GD) for a joint transform correlator-based encryption system. This encryption system was recently proposed and it was implemented by using a fully phase nonzero-order joint transform correlator (JTC) and the Gyrator transform (GT). The decryption system was based on two successive GTs. In this paper, we make several numerical simulations in order to test the performance and robustness of the JTC-based encryption-decryption system in the GD when the encrypted image is corrupted by noise or occlusion. The encrypted image is affected by additive and multiplicative noise. We also test the effect of data loss due to partial occlusion of the encrypted information. Finally, we evaluate the performance and robustness of the encryption-decryption system in the GD by using the metric of the RMSE between the original image and the decrypted image when the encrypted image is degraded by noise or modified by occlusion.

Electro-kinetic phenomena in liquid crystals for THz photonics
Paper AO100-159
Author(s): Sergey V. Pasechnik, Olga Semina, Alex Dubtsov, Valentin Tsvetkov, Andey Bluzhin, Dina Shmeliova, Moscow Technological Univ. (Russian Federation)

In this work we consider electro-kinetic phenomena in Liquid Crystals for elaboration of new terra fluidic devices.

Recent Vulcan laser facility upgrades
Paper AO100-162
Author(s): Alexis Boyle, Marco Galimberti, Pedro Oliveira, Dave Pepler, Ian Musgrave, Rutherford Appleton Lab. (United Kingdom)

Here we present planned upgrades to the Vulcan laser to increase its capabilities as a user facility. Vulcan's existing shaped long pulse (SLP) will be augmented by a secondary, independently timed SLP system. This will provide an additional two long pulse beam lines capable of generating pulses from 300 picoseconds to 10 nanoseconds and up to 500 joules, to complement the existing six long pulse beam lines. Implementation of a new timing system means it will be possible to time the SLPs with respect to each other and to the short pulse, picosecond time scale, with an rms error of 25 picoseconds. We also present the planned upgrade of the diagnostics network, including a gigabit camera network and new adaptive optics capabilities.

Criterion for single photon sources
Paper AO100-170
Author(s): Juan Camilo López Carreño, Eduardo Zubizarreta Casalengua, Elena del Valle, Univ. Autónoma de Madrid (Spain); Fabrice Laussy, Univ. of Wolverhampton (United Kingdom), Russian Quantum Ctr. (Russian Federation)

We propose a new criterion that takes into account the N-photon correlation, rather than just the 2-photon correlation. With this criterion, we measure the distance in the Hilbert space between the SPS being tested and an ideal one. Such a distance is small as long as all the nth-order correlation functions are antibunched. We show that for most sources, the criterion converges at the 4th-order correlation function, which is accessible with modern experimental configurations.

An exploratory study of temporal integration in the peripheral retina of myopes
Paper AO100-171
Author(s): Antonio F. Macedo, Univ. of Minho (Portugal), Linnaeus Univ. (Sweden); Tito J. Encarnação, Ctr. de Diagnóstico da Visão (Portugal); Daniel Vilarinho, Univ. of Minho (Portugal); António M. G. Baptista, Univ. do Minho (Portugal)

The visual system takes time to respond to visual stimuli, neurons need to accumulate information over a time span in order to fire. Visual information perceived by the peripheral retina might be impaired by imperfect peripheral optics leading to myopia development. This study explored the effect of eccentricity, moderate myopia and peripheral refraction in temporal visual integration. Myopes and emmetropes showed similar performance at detecting briefly flashed stimuli in different retinal locations. Our results show evidence that moderate myopes have normal visual integration when refractive errors are corrected with contact lens; however, the tendency to increased temporal integration thresholds observed in myopes deserves further investigation.

Nonlinear optical fiber refractive index characterization using the acousto-optic interaction
Paper AO100-174
Author(s): Emmanuel Rivera-Pérez, Univ. de Valencia (Spain); Antonio Díez, Univ. de València (Spain); Erica P. Alcusa-Sáez, Miguel V. Andrés, Univ. de Valencia (Spain)

The in-fiber acousto-optic interaction enables the measurement of the nonlinear refractive index in single-mode optical fibers. In our experiments, acoustic waves were launched along a section of bare fiber. The transmission spectrum exhibits a notch, corresponding to the coupling between the LP01 core mode and an asymmetric LP1m cladding mode. The increase of refractive index induced by high peak power pump pulses produce the shift of the notch towards longer wavelengths, which was measured by tuning the wavelength of a probe laser to match the side-edges of the acousto-optic induced notch.

Ultra-high bit rate mm-wave photonic-wireless links employing digital equalization
Paper AO100-175
Author(s): Maria do Carmo Raposo de Medeiros, Instituto de Telecomunicações (Portugal); Paulo A. F. Almeida, IT-Instituto de Telecomunicações-Pólo de Coimbra (Portugal); Henrique J. A. Silva, Instituto de Telecomunicações, Univ. of Coimbra (Portugal); Paulo M. Monteiro, Instituto de Telecomunicações (Portugal); Beatriz M. Oliveira, Instituto de Telecomunicações, Univ. of Coimbra (Portugal)

It is expected that 5G networks will require backhaul supporting networks with data rates beyond 100 Gbit/s. In some segments of the network, when the deployment of optical fiber infrastructures is not possible or it is very expensive, it is expected that high capacity point-to-point wireless links operating at millimeter wave (mm-Wave) (30-300GHz) will be an essential part of the backhauling infrastructure. When 5G modulated signals are transmitted through analog photonic link, these signals suffer additional nonlinear distortion due to nonlinear distortion of the analog photonic links. In this paper, we focus on analyzing the performance of multiband digital adaptive pre-distortion technique to enable the efficient usage the high bandwidth available at the mm-Wave range. The referred pre-distortion technique will be

assessed, by simulation, taking into account the specificity of the mm-Wave link and the optoelectronic devices used.

MIMO processing based on higher-order Poincaré spheres
Paper AO100-177
Author(s): Gil Gonçalo Martins Fernandes, Instituto de Telecomunicações (Portugal), Department of Electronics, Telecommunications and Informatics, University of Aveiro (Portugal); Nelson J. Muga, Instituto de Telecomunicações (Portugal), Department of Electronics, Telecommunications and Informatics, University of Aveiro (Portugal), i3N (Portugal); Armando N. Pinto, Instituto de Telecomunicações (Portugal), Department of Electronics, Telecommunications and Informatics, University of Aveiro (Portugal)

A multi-input multi-output (MIMO) algorithm based on higher-order Poincaré spheres is demonstrated for space-division multiplexing systems. The MIMO algorithm is modulation format agnostic, robust to frequency offset and does not require training sequences. In this approach, the space-multiplexed signal is decomposed in sets of two tributary signals, with each set represented in a higher-order Poincaré sphere. For any arbitrary complex modulation format, the samples of two tributaries can be represented in a given higher-order Poincaré sphere with a symmetry plane. The crosstalk along propagation changes the spatial orientation of this plane and, therefore, it can be compensated by computing and realigning the best fit plane. We show how the transmitted signal can be successfully recovered using this procedure for all possible combinations of tributaries. Moreover, we analyze the convergence speed for the MIMO technique considering several optical-to-noise ratios.

Optical properties of an anterior lamellar human cornea model based on fibrin-agarose
Paper AO100-179
Author(s): Ana María Ionescu, Juan Cardona, Razvan Ghinea, Ingrid Garzón Bello, Miguel González-Andrades, Miguel Alaminos, María del Mar Pérez, Univ. de Granada (Spain)

The optical properties of the biomaterial based on fibrin with 0.1% agarose concentration, used for the generation of a bioengineered human corneal stroma by tissue engineering, after using a nanostructuring technique, were analyzed and compared with a native cornea. The temporal evaluation of the properties of these biomaterials is essential for the design of functional biological human corneal replacements. This optical evaluation was carried out using the inverse adding-doubling (IAD) method. The bioengineered human corneal stromas shared many similarities with native control cornea after four weeks of development in culture. Moreover, the fact that no significant differences were found between the transmittance values of the control cornea and the fourth week artificial sample encourages us to recommend a period of four weeks for the development of artificial fibrin-agarose human cornea before it can be considered for several clinical purposes.

2.05-μm Holmium-doped all-fiber continuous-wave laser at in-core diode pumping at 1.125 μm
Paper AO100-180
Author(s): Alexander V. Kir'yanov, Yuri O. Barmenkov, Ctr. de Investigaciones en Óptica AC (Mexico)

A Holmium-doped all-fiber laser oscillating at ~2.05 μm in continuous-wave, in-core pumped by a 1.125-μm laser diode, is reported. Two Holmium-doped alumino-germano-silicate fibers (HDF), differentiated in Ho^{3+} doping degree, were fabricated to get lasing and to reveal effect of Ho^{3+} content upon laser output. The fibers were characterized from material, optical spectroscopy, and laser action viewpoints. Particularly, lasing with both HDFs was assessed in the simplest Fabry-Perot cavity, composed of spectrally adjusted fiber Bragg gratings. In the best case, when using the lower doped HDF of proper length (1.4 m), low threshold (~370 mW) and moderate slope efficiency (~13%) of ~2.05-μm lasing were obtained at 1.125-μm diode pumping. Long-term stable, high brightness, low-noise, purely-CW operation is shown to be the laser's attractivities. In the case of the heavier doped HDF, laser output is in overall worse, with a possible reason being deterdeteriorating Ho^{3+} concentration effects.

Data multiplexing using the orbital angular momentum of photons.
Paper AO100-191

Author(s): João Sabino, Instituto de Telecomunicações (Portugal); Gonçalo Figueira, Instituto de Plasmas e Fusão Nuclear (Portugal); Paulo André, Instituto de Telecomunicações (Portugal)

Future market perspectives demand that telecommunication networks support higher data volumes. For this to become achievable, an increase of the spectral efficiency of the transmission network is needed. The Orbital Angular Momentum (OAM) of light is a property which offers a new orthogonal degree of freedom to modulate or multiplex information. In this work, a proof-of-concept communication link is implemented using OAM to multiplex/demultiplex light beams, with different topological charges, and propagation in free space. The simulation of the propagation and diffraction of OAM carrying beams was also developed, showing precise results when spiral phase computer generated holograms are used (Figure 1a and 1b). The use of Spatial Light Modulators allowed a partial modulation of the beam's wavefront which was sufficient to retrieve the information of a specific channel (Figure 1c), revealing the feasibility and robustness of OAM to be used in communication links.

Temperature sensing using an embedded-core capillary fiber filled with indium
Paper AO100-192
Author(s): Giancarlo Chesini, Jonas H. Osório, Unicamp (Brazil); Valdir A. Serrão, Marcos A. R. Franco, Instituto de Estudos Avançados (Brazil); Cristiano M. B. Cordeiro, Instituto de Física "Gleb Wataghin", Unicamp (Brazil)

We report the fabrication of an embedded-core capillary fiber and its employment for temperature sensing. The fiber consists of a silica capillary with a germanium-doped core region within the capillary wall. Post-processing was done by filling the fiber with indium, chosen because of its low melting point and reasonable large thermal expansion coefficient compared to silica. When the indium-filled fiber is heated, thermal expansion induces stresses variations within the capillary and alters core's birefringence. Analytical simulations were performed to explore the temperature-induced birefringence changes and their dependence on fiber parameters. Sensor interrogation was performed and a (14.4±0.7)nm/ºC sensitivity was measured. For comparison, the measured sensitivity of an unfilled fiber is (1.09±0.03)nm/ºC. Both these values are considerably higher than the usually found in Bragg gratings-based sensors (0.01nm/ºC) and are similar to the ones obtained with more sophisticated fibers.

White light spectral interferometry for measuring dispersion of the thermo-optical coefficient of liquids
Paper AO100-196
Author(s): Damian Rodriguez, Yago Arosa, Bilal S. Algnamat, Elena López-Lago, Raul de la Fuente, Univ. de Santiago de Compostela (Spain)

White light spectral interferometry is a well known technique applied to measure the refractive index of solid and liquids samples over a wide spectral band. In this work, we report the measurement of the refractive index of four solvents at different temperatures in the VIS-NIR spectral range. Based in these data the thermo-optical coefficient of the liquids is calculated for the whole spectral band and dispersion relations are established. The spectral interferogram is taken in a region including the stationary phase point, where the phase varies slowly. This allows to track the change in phase when temperature varies and locates for 2pi phase jumps, thus avoiding the ambiguity associate to the interference order. The obtained result are compared with available data in the literature.

White light spectral interferometer for measuring dispersion in the visible-near infrared
Paper AO100-199
Author(s): Yago Arosa, Univ. de Santiago de Compostela (Spain); Damian Rodríguez, Univ de Santiago de Compostela (Spain); Bilal S. Algnamat, Elena López-Lago, Raul de la Fuente, Univ. de Santiago de Compostela (Spain)

We have designed a spectrally resolved interferometer to measure the refractive index of transparent samples over a wide spectral band from 400 to 1600 nm. The measuring device consists of a Michelson interferometer whose output is analyzed by means of three fiber spectrometers. The first one is a homemade prism spectrometer, which obtains the interferogram produced by the sample over 400 to

1000 nm; the second one is a homemade transmission grating spectrometer thought to measure the interferogram in the near infrared spectral band from 950 to 1550 nm; the last one is a commercial Czerny-Turner spectrometer used to make high precision measurements of the displacement between the Michelson mirrors also using white light interferometry. The whole system is illuminated by a white light source with an emission spectrum similar to black body. We have tested the instrument with solid and liquids samples achieving accuracy to the fourth decimal on the refractive index after fitting it to a C

Impact of different environmental conditions on lithium-ion batteries performance through the thermal monitoring with fiber sensors
Paper AO100-200
Author(s): Micael S. Nascimento, Marta S. Ferreira, Joao L. Pinto, Univ. de Aveiro (Portugal)

In this work, an optical fiber sensing network has been developed to assess the impact of different environmental conditions on lithium batteries performance through the thermal monitoring in real time. In total, the temperature variations that occur in three different locations of a lithium battery were monitored. The battery is submitted to constant current charge and different discharge C-rates, under normal and abusive operating conditions. A lab-scale experimental signal conditioning and processing system was designed and implemented. It was based on a multichannel data acquisition system with high computational capabilities. An analysis of the thermal behavior of lithium batteries under different environmental conditions through the temperature and humidity variations in a controlled environment is presented. The results show that the FBGs are a useful tool for real time monitoring of the battery temperature as well as for failure detection and optimized management in batteries.

Phase contrast imaging of red blood cells using digital holographic interferometric microscope
Paper AO100-202
Author(s): Varun Kumar, Gufran S. Khan, Chandra Shakher, Indian Institute of Technology Delhi (India)

In this paper, digital holographic interferometric microscope (DHIM) in conjunction with Fresnel reconstruction method is demonstrated for phase contrast imaging of red blood cells (RBCs). The advantage of using the DHIM is that the distortions due to aberrations in the optical system are avoided by the interferometric comparison of reconstructed phase with and without the object.

Fourier transform phase difference method optimization for supersonic gas flow characterization
Paper AO100-203
Author(s): Francisco Rodríguez Lorenzo, José Benito Vázquez Dorrío, Jesús Blanco García, Univ. de Vigo (Spain)

We propose a complete characterization method for supersonic gas flow provided by a Laval nozzle. The optical phase of fringe patterns acquired in a simple Mach Zehnder interferometer is directly extracted with a differential phase evaluation method based on Fourier Transform (without translation to the frequency origin); reducing the computation steps and decreasing the errors due to the unwrapping process. We obtain optical phase, gradient and laplacian maps that allow detailed analysis of the pressure distribution, and shock wave patterns. We also study effects of different pass band filters on phase evaluation process for phase maps quality optimization.

Fabry-Perot cavity based on air bubble for high sensitivity lateral load and strain measurements
Paper AO100-204
Author(s): Susana Novais, Marta S. Ferreira, João L. Pinto, Univ. de Aveiro (Portugal)

A Fabry-Perot air bubble microcavity fabricated between a section of single mode fiber and a multimode fiber is proposed. The study of the microcavities growth with the number of applied arcs is performed. The sensors are tested for lateral load and strain. For the lateral load measurements, sensitivities of 0.32 nm/N and 2.11 nm/N are obtained for the 47 μm and 161 μm long cavities, respectively. For strain measurements, the sensitivities obtained for the same cavities are of 4.49 pm/με and 9.12 pm/με, respectively. Moreover, given the low temperature sensitivity (<1 pm/ºC), the proposed cavity should be adequate to perform temperature independent measurements. The accurate technique control leads to

the fabrication of reproducible cavities with the sensitivity required for the application. The way of manufacturing using a standard fusion splicer and given that no oils or etching solutions are involved, emerges as an alternative to the previously developed air bubble based sensors.

Polymer and tapered silica fiber connection for polymer fiber sensor application
Paper AO100-205
Author(s): Miguel F. S. Ferreira, INESC TEC, Ctr. of Applied Photonics (Portugal); André Gomes, INESC-TEC (Portugal); Dominik Kowal, Gabriela Statkiewicz-Barabach, Wroclaw Univ. of Science and Technology (Poland); Orlando Frazão, INESC TEC, Ctr. of Applied Photonics (Portugal)

A new type of polymer and silica connection is proposed. A tapered SMF-28 silica optical fiber point is fabricated using a C02 laser by focusing and stretching the fiber. The tapered silica point is inserted in one of the holes of a microstructured polymer optical fiber using a 3D alignment system. Using a supercontinuum, the spectrum is observed after one and two connections. The polymer fiber is characterized in curvature while using the previous connection.

Onion cell imaging by Talbot effect
Paper AO100-208
Author(s): Shilpi Agarwal, Varun Kumar, Chandra Shakher, Indian Institute of Technology Delhi (India)

In this paper the three-dimensional imaging of onion epidermis cell is demonstrated by using the self-imaging capabilities of a grating in visible light region. In the proposed method, second grating is removed from Talbot interferometer and the intensity pattern of the first grating is resolve directly with an image detector. The Fresnel diffraction pattern from the first grating and object is recorded at self-image plane. Fast Fourier Transform (FFT) is used for extracting the 3D amplitude and phase image of onion epidermis cell. The stability of the proposed system, from environmental perturbation as well as its compactness and portability give the proposed system a high potential for several clinical applications.

Modeling long period gratings inscribed by CO_2 laser irradiation
Paper AO100-210
Author(s): Ana I. C. Machado, Univ. of Aveiro (Portugal), Instituto de Telecomunicações (Portugal); Telmo Almeida, Instituto de Telecomunicações (Portugal), Department of Physics, University of Aveiro (Portugal); Rogério N. Nogueira, Instituto de Telecomunicações (Portugal); Margarida Facão, Univ. of Aveiro (Portugal), i3N (Portugal); Ana M. Rocha, Instituto de Telecomunicações (Portugal), i3N (Portugal)

Long period gratings (LPGs) are a type of optical fiber gratings, with a period ranging from 100 μm to 1 mm, that promote the efficient coupling between the guided mode and the cladding modes in the resonant wavelength. LPGs can be produced with several methods, such as laser irradiation (CO2 or UV irradiation), electrical arc discharge or mechanically induced. In this work, we present a model to simulate the mode coupling in LPGs inscribed by a CO2 laser. We developed a numerical model based on the coupled mode theory which was used to estimate the variations of the refractive index induced by CO2 laser radiation.

Study of dipolar SERS structures for environmental sensing
Paper AO100-213
Author(s): Henrique Vilhena, Scott G. McMeekin, A. Sheila Holmes-Smith, Glasgow Caledonian Univ. (United Kingdom); Nigel P. Johnson, Univ. of Glasgow (United Kingdom)

Nanoantennas consisting of dipole pairs with small gaps between them have been widely used in surface-enhanced Raman spectroscopy (SERS). However, large intercell distance between them is normally used to prevent cross-coupling resulting in a reduction of the overall enhanced Raman signal. In this work we use this cross-coupling effect as an additional tool for fine-tuning in SERS technology. We demonstrate that it is possible to increase the reflected signal of an array of nanoantennas by reducing the distance between them in the direction both perpendicular and parallel to the orientation of the incident electric field. Raman measurements at low analyte concentrations have shown an increase in the enhanced signal as the intercell distance is decreased. We believe that these results will enable the

design and fabrication of structures possessing a greater degree of tunability joined with an overall strong enhanced Raman signal.

Analytical transient analysis of Peltier device for laser thermal tuning
Paper AO100-221
Author(s): Yahya Sheikhnejad, Zoran Vujicic, Álvaro Almeida, Ricardo Bastos, Ali Shahparia, António Teixeira, Instituto de Telecomunicações (Portugal)

Current industry trends strongly favor the concepts of high density, low power consumption and low cost applications of Datacom and Telecom pluggable transceiver modules. Hence, thermal management plays an important role, especially in the design of high-performance compact optical transceivers. Extensive care should be taken on wavelength drift for thermal tuning lasers using thermoelectric cooler and indeed, accurate expression is needed to describe transient characteristics of the Peltier device to achieve maximum controllability. In this study, the exact solution of the governing equation is presented, considering Joule heating, heat conduction, heat flux of laser diode and thermoelectric effect in one dimension. In addition, the separation of variables method and Sturm-Liouville theorem along with the completeness features of eigenfunctions are employed to obtain time-dependent electrical potential and temperature distribution of the Peltier device.

Influence of probing conditions in functional optical diagnosis of human skin
Paper AO100-222
Author(s): Alexey Popov, Evgeny Zherebtsov, Alexander Bykov, Igor Meglinski, Univ. of Oulu (Finland)

Presently, sensors are extensively used in many applications in healthcare, sports, wellness and others. We present the results of our studies dedicated to the development of a variety of sensors for functional monitoring of human skin in vivo. The particular interest includes an assessment of skin blood oxygenation, melanin and water content, as well as measurements of blood microflows. The skin is a highly heterogeneous medium with a random spacial distribution of collagen fibers, complex vascular bed allocation and a topical localization of melanosomes and melanin granules. The accurate monitoring of actual physiological parameters and/or their functional changes require a careful selection of the source-detector configuration. To find the optimal probing conditions of a particular parameter mentioned above, we considered the influence of the source-detector separation, pressure of the probe on the skin surface and blood flow pulsations due to heart beating. Thus, the results of the

Fractional Fourier operators applied to a nonlinear image encryption system
Paper AO100-223
Author(s): Juan M. Vilardy Ortiz, Cesar O. Torres, Univ. Popular del Cesar (Colombia); Carlos J. Jimenez, Univ. de La Guajira (Colombia)

We present a nonlinear image encryption-decryption system using random phase masks, truncation operations and the following fractional Fourier operators: the fractional Fourier transform (FrFT), the fractional traslation and the fractional correlation. The encryption-decryption system utilizes nonlinear operations, such as phase encoding and truncation operations, in order to increase the security of the encrypted image. The security system (encryption and decryption) has five security keys, and all the right values of these security keys are very important in order to obtain the right decrypted image at the output of the decryption system.

Wavelength tuning of polymer optical fibre Bragg grating at longer wavelengths permanently
Paper AO100-224
Author(s): Georgios Sagias, Univ. Carlos III de Madrid (Spain)

Permanent wavelength tuning of polymer optical fibre Bragg grating (POFBG) to longer wavelengths has been demonstrated for the first time. Until now, the Bragg wavelength was able to be tuned permanently only to shorter wavelengths by utilizing thermal annealing; exposing the polymer material above the β-transition temperature, the fibre shrinks and the Bragg period becomes shorter. In this work, a positive tuning of Bragg wavelength has been shown to be feasible when the fibre is stretched during the thermal

exposure. In this paper, we demonstrate a permanent positive Bragg wavelength tuning of 12 nm when the fibre is strained up to 2% during its annealing. The work presented here can be used to multiplex POFBGs over a wide range of desired wavelengths.

Post-thermal annealing process in organic bulk-heterojunction solar cells to efficiency improve: a physical study
Paper AO100-226
Author(s): Luiz R. Pereira, Univ. de Aveiro (Portugal), i3N - Institute of Nanostructures, Nanomodelling and Nanofabrication (Portugal); António Califórnia, João Gomes, CeNTI – Ctr. for Nanotechnology and Smart Materials (Portugal)

Organic photovoltaics (OPVs) have seen significant progress. Understanding the relationship between the morphology and the electrical process is a pre-requisite for device optimization. OPVs with 25 mm2 active area were fabricated by spin-coating on glass substrates with an active layer (200 nm tick) composed of P3HT and PCMB on a ratio 1:1. After fabrication, the OPVs was submitted to several post-thermal treatments in a temperature range from 150 – 190ºC. The efficiency increases from 2% to 4% but after 180ºC decreases. The experimental data was fitted to the physical equivalent circuit, using genetic algorithms. Morphology was analyzed by AFM under current sensing modes getting a micro-electrical image. The electrical current increasing throughout OPVs and homogeneity of the electrical field guarantees a high efficiency suggesting a re-conformation of the polymer / nanostructures. The process was analyzed by impedance spectroscopy.

Electro-thermal effects in large area white-organic light emitting diodes
Paper AO100-230
Author(s): Luiz R. Pereira, Manish Kumar, Univ. de Aveiro (Portugal), i3N – Institute of Nanostructures, Nanomodelling and Nanofabrication (Portugal); João Gomes, André Pinto, CeNTI – Ctr. for Nanotechnology and Smart Materials (Portugal)

Solid State Lighting based on OLEDs became the focus of a huge scientific and technological research. Although several well succeeded results, one of the most important challenges is the uniformity / homogeneity in large area emission related with the thermal effects. WOLEDs was made by thermal evaporation (16 cm² area). A wide range of CCT was obtained, (3200 - 10500K). The CRI is almost 90 and the CIE color coordinates are stable with changes of ± 0.004. Thermal images, in a static model, shows a high temperature in the center (50ºC) decreasing in a radially to 35ºC at border. A scalar photo-electro-thermal model was developed considering the effects of electrical current, thermal convection and optical radiation. The model was developed in both electrical and thermal-scalar domain. The extracted thermal changing ratio in the series resistance and forward voltage (approx. -40 m./ºC and -10 mV/ºC respectively) can reproduces the experimental data and describes the physical phenomena.

Dielectrical and optical properties of a double doped tellurium-bismuth glass
Paper AO100-231
Author(s): Piotr Brągiel, Michał Piasecki, Jan Dlugosz Univ. in Czestochowa (Poland); Radosław Belka, Kielce Univ. of Technology (Poland); Manuel A. Valente, Univ. of Aveiro (Portugal); Adam Ingram, Marek Kostrzewa, Opole Univ. of Technology (Poland)

The tellurium glasses due to their durability are among most widely applied. Here the properties of the double doped glasses of this type, namely (70-x-y) TeO2 - 10 Bi2O3 - 20 BaCO3-xEr2O3-yYb2O3 are reported. The structural, optical and dielectrical properties of the material are analyzed. Data from UV-VIS, Raman, PL, PLE spectra as well as from dielectric measurements – 305K-633K, 3Hz – 100kHz- are used. The glasses exhibit up-conversion, 4S3/2 to 4I15/2 and 4F9/2 to 4I15/2 , effect. There are no systematic dependence of a ε' value on Er+3 or Yb+3 ions content An average value was found to be 29.6+/- 1/8. From the analysis of the complex impedance behavior two type of activation processes are revealed. In the first one the activation energy practically does not depend on dopant content and is about 1.1 eV; in the second, higher temperature region, activation energy change with variation of the dopant concentration.

3D reconstruction with texture of coleoptera using structured light
Paper AO100-232
Author(s): Nilssen Steban Marin Rojo, Carlos Andrés Madrigal González, Instituto Tecnológico Metropolitano (Colombia); Alejandro Restrepo Martinez, John Willian Branch Bedoya, Univ. Nacional de Colombia (Colombia); Viviana Marcela Calderon Marin, Instituto Tecnológico Metropolitano (Colombia)

The preservation of insect specimens in museums is a complex task. For this reason, in the largest museums in the world have chosen to digitize insect collections using 2D images or in some cases using 3D reconstruction systems. In this work, we propose the use of a structured light system to obtain textured 3D reconstruction of some samples from the Coleoptera collection of the ITM Museum. Calibration of our structured light is done to find intrinsic, extrinsic parameters and transformation matrices. Coded patterns are projected using a Digital Light Processing DLP; with them, depth data of specimens are measured. Finally, using a texture overlay technique, color information is integrated into the 3D model. In the experimental tests, five models of Coleoptera of the family of the coprophagous are analyzed. The qualitative evaluation shows that our methodology can be useful for the digitization of these and other specimens.

Diffuse reflectance spectroscopy for crops diagnosis and monitoring
Paper AO100-234
Author(s): Aldemar Reyes, Richar Pomeo, Carlos A. Galindez, Efrain Solarte-Rodriguez, Univ. del Valle (Colombia)

The spectral properties of plants are mainly defined by their leaves components which have spectral responses depending on their involvement in plant metabolism and physiology. Pest or disease, Nitrogen deficiency and water content in the leaves, change the overall spectral response or specific absorption bands. Diffuse reflectance spectroscopy in VIS-NIR range, offers an analytical technique for biophysical and chemical characterization of leaves, and to monitor the physiological state of a crop. This study was conducted on Tabasco Pepper (Capsicum frutescens) leaves, living or cut from the plant, to determine their diffuse spectral response response and to calibrate the measurement systems. CCD cameras and spectrometers were used to achieve hyperspectral data. The RGB planes were determined from leaf images using low coherence light (LEDs) in a diffuse uniform illumination system, and a VIS-NIR source was used for reflectance Lab measurements.

Usage of CISS and Conlon surveys for eye accommodation studies
Paper AO100-241
Author(s): Karola Panke, Aiga Svede, Univ. of Latvia (Latvia); Wolfgang Jaschinski, Leibniz Research Ctr. for Working Environment and Human Factors (Germany); Gunta Krumina, Univ. of Latvia (Latvia)

The purpose of this study was to investigate two different surveys – CISS and Conlon scores for the same subject group and analyse also critical visual function parameters. We found positive exponential growth relationship between CISS and Conlon scores ($R^2 = 0.7$), but separation between symptomatic and asymptomatic group differed significantly depending of which survey was used. We found positive correlation between Conlon score and exophoria at 30 cm ($r=0.41$, $p=0.01$) and 24 cm ($r=0.27$, $p=0.03$). We recommend to use subjective symptom surveys as a part of case history instead of using them for clinical trials as a criteria to divide symptomatic and asymptomatic group.

AOP2017' Poster Papers

Interchannel collisions of strong dispersion-managed solitons with different energies in the presence of higher-order effects
Paper AO100-2
Author(s): Francisco J. Diaz-Otero, Univ. of Vigo (Spain); Laura Pedrosa-Rodriguez, OHB System AG (Germany)

Dispersion management (DM) is a well-established technique which has provided a substantial progress of soliton data transmission systems. When compared to conventional constant-dispersion soliton communication links, its usage introduces an improvement in signal-to-noise ratio and a reduction of the Gordon-Haus timing jitter and four-wave mixing (FWM) [1]. Due to the high bit rates involved in the transmission and to the reduction of the pulse width, an accurate modeling of these systems needs to take into account higher-order effects both in the single-channel and in the multiple channel case. We study the interaction properties of a two-channel wavelength-division multiplexed (WDM) strongly dispersion managed (DM) communication system. By means of a variational approach [2] to the Generalized Nonlinear Schrödinger Equation we obtain an ordinary differential equations model for the main parameters of the propagating pulses including third-order dispersion (TOD), Raman scattering and

Spectroscopy of Eu^{3+} ions in bulk and nano crystal $Gd_3Ga_3Al_2O_{12}$ (GGAG) garnet
Paper AO100-17
Author(s): Piotr Solarz, Paweł Głuchowski, Radosław Lisiecki, Institute of Low Temperature and Structure Research (Poland); Michał Głowacki, Institute of Physics (Poland); Robert M. Kowalski, Tomasz Niedźwiedzki, Bogusław Macalik, Institute of Low Temperature and Structure Research (Poland); Marek Berkowski, Institute of Physics (Poland); Witold Ryba-Romanowski, Institute of Low Temperature and Structure Research (Poland)

Obtained single europium crystals via Czochralski technique possesses violet color, probably to oxygen vacancies, that disappears when they are calcinated in the air. Contrary, nanopowders of GGAG are colorless. The host absorption is about 37000 cm-1 (270 nm). Lifetime for single crystal is 3.1 ms, whereas for nonopowders it is 5.2 ms. All decay curves are exponential. It was found that optimal concentration of europium ions in this phosphor is about 1.6 at.%. The luminescence spectra are consisted of narrow lines, contrary to analog samarium doped GGAG, published early. The nanopowders were analyzed versus concentration and temperature of annealing. Measurements temperatures were taken in the region of 5 – 300 K. Calcination temperatures of nanopowders were in the region of 800-1200 °C. It was found that the best luminescence properties possesses GGAG:Eu calcined at 1000 °C.
Acknowledgements: This work was supported by the NCN under grant number DEC-2014/15/B/ST5/05062.

Goos-Hänchen shift of Cosine-Gaussian Schell-model beams with rectangular symmetry
Paper AO100-19
Author(s): Rosario Martínez-Herrero, Miguel Angel Berbel, Alejandro Cunillera, Univ. Complutense de Madrid (Spain)

The Goos-Hänchen (GH) shift is the lateral displacement by a totally reflected beam at a dielectric surface due to the angular dependence of the complex Fresnel coefficients. This phenomenon has been extensively studied over the last years in both theoretical and experimental aspects. On the other hand, partially coherent beams have found a wide range of applications and have consequently received an increasing attention in the literature. In this contribution we consider a recently introduced type of partially coherent beams, the Cosine-Gaussian Schell-model beams with rectangular symmetry, and we theoretically study the dependence of the GH shift with the coherence of the beam for both, p and s polarization.

Nanoemulsion structural design for cancer delivery of hybrid fluorophores
Paper AO100-32
Author(s): Urszula Bazylinska, Dominika Wawrzyńczyk, Wroclaw Univ. of Science and Technology (Poland); Julita Kulbacka, Medizinische Univ. Wien (Poland)

Biocompatible polyesters have been used in nanoemulsion embedding process for co-encapsulation luminescent lanthanide-doped nanocrystals - NaYF4:Tm3+,Yb3+ and photosensitizing dyes, to applied them as multifunctional hybrid agents for theranostic purposes in human malignant melanoma (MEWO or Me45) cells. After the optimization process by means of dynamic light scattering, ζ-potential, transmission electron microscopy, atomic force microscopy and fluorescent spectroscopy, spherical polyester nanocarriers with average size < 200 nm were chosen for evaluation of the therapeutic effect based on, cytotoxicity and bioimaging studies on the skin cancer cells.

Investigation of THz waveguiding features of microstructured fibers with metallic inclusions
Paper AO100-34
Author(s): Markos Paulo Cardoso, Federal Univ. of Pará (Brazil); Anderson Oliveira Silva, Federal Ctr. for Technological Education Celso Suckow da Fonseca (CEFET - RJ) (Brazil); João C. W. A. Costa, Federal Univ. of Pará (Brazil)

In this work, we investigate the guidance features of a fiber microstructured by alternating arrays of air holes and silver inclusions for THz operation. This structure consists of a rod of TOPAS (a polymer with refraction index n=1.5258) with a hexagonal lattice of subwavelength air holes. The modal characteristics are analyzed as function of the arrangement of silver particles deposited in some air holes on the fiber cross-section. Our final aim is to depict the impact of the excitation of surface plasmons on the mode effective index and propagation losses.

In vivo probe for imaging behind opaque obstacle
Paper AO100-36
Author(s): Anant Shinde, Sandeep Menon Perinchery, Murukeshan V. Matham, Nanyang Technological Univ. (Singapore)

We describe an in vivo fiber probe that performs optical imaging behind an opaque obstacle in real-time. Our probe method is based on a simple real time optical imaging concept using an axicon lens to view, image and record the object kept behind thick opaque obstacles in free space. This work is an improvement upon an earlier demonstration of axicon lens based imaging behind obstacle. The flexible fiber optic imaging bundle is used in combination with the axicon lens to achieve in vivo imaging behind obstacle. We demonstrate the performance of our system with images and videos of a fluorescently labelled mouse kidney cells imaged from behind an obstacle. The in vivo probe for imaging behind obstacle is a candidate technique for injury free minimally invasive surgeries.

Impact of the activators concentration on up-conversion phenomena and emission efficiency of the Er,Yb co-doped oxyfluoride glasses and glass-ceramics.
Paper AO100-37
Author(s): Radoslaw Lisiecki, Institute of Low Temperature and Structure Research (Poland), ILTSR PAS (Poland); Witold Ryba-Romanowski, Institute of Low Temperature and Structure Research (Poland); Elwira Czerska, Michał Żelechower, Silesian Univ. of Technology (Poland)

The erbium and ytterbium co-doped oxyfluoride glasses were manufactured at T=1460oC. The heat treatment in the wide range of temperatures was used up to 750 oC to obtain the glass-ceramic systems. The processes attributed to depletion of pump and luminescent levels have been assessed based on experimental data attained during measurement of up-converted luminescence, steady state emission and dynamics of excited states as a function of excitation power and activator concentration. It was discerned that the spectroscopic properties of the glass-ceramic samples were substantially different in relation to as-melted glasses. Furthermore, the different peculiarities of the up-conversion phenomena and relaxation dynamic of activators excited states were observed and studied in details.

On the behavior of linear polarizers on highly focused radially polarized beams
Paper AO100-39
Author(s): David Maluenda, Univ. Complutense de Madrid (Spain); Artur Carnicer, Ignasi Juvells, Univ. de Barcelona (Spain); Rosario Martinez-Herrero, Univ. Complutense de Madrid (Spain)

In this communication we analyze the light field distribution of a highly focused radially polarized beam when passes through a linear polarized. Analytical results and numerical calculations are provided.

Laser based manufacturing of channels and improvement of their lifetime with sol-gel coatings
Paper AO100-40
Author(s): María Aymerich, Ana Isabel Gómez Varela, Univ. de Santiago de Compostela (Spain); Ezequiel Álvarez, Instituto de Investigación Sanitaria de Santiago de Compostela (IDIS) (Spain); María Teresa Flores-Arias, Univ. de Santiago de Compostela (Spain)

The fabrication of preclinical devices for performing bioassays has aroused a huge interest in the past years due to the fact that some pathologies are a main cause of morbidity worldwide. We have developed a preclinical device that mimics half blood vessel by using laser technologies. By employing a Nd:YVO4 laser in Q-switch mode a channel has been manufactured over soda-lime glass. Using a CO2 laser combined with a roller furnace, a thermal treatment has been applied to the channel reduce its roughness and enhance its quality. The glass structure was employed as master to replicate the channel in PDMS by soft-lithography. To avoid the deterioration of the PDMS when it is exposed to organic solvents, channels were coated with three different sol-gel coatings compositions. Endothelial cells were cultured over the channels in order to determine the most suitable composition to cell growth and to study cell behaviour in each case.

Validation of a semi-automatic protocol for the assessment of the tear meniscus central area based on open-source software
Paper AO100-41
Author(s): Hugo Pena-Verdeal, Carlos García-Resúa, Eva Yebra-Pimentel, Maria Jesus Giraldez, Univ. de Santiago de Compostela (Spain)

The aim of this study was to propose and analyse the variability of a semi-automatic method for measuring lower tear meniscus central area (TMCA) by using open source software based on Java (NIH ImageJ). On images extracted from tear meniscus videos before fluorescein instillation, the TMCA was measured in the short light beam illuminated area by a manual and a semi-atomic protocol, and then results were compared. There was no statistical difference, and a positive near to perfect correlation, between both methods. This study showed a useful tool to objectively measure the frontal central area of the meniscus in photography by free open source software.

Absolute flatness measurement with a Twyman-Green interferometer
Paper AO100-42
Author(s): Benito Vázquez-Dorrío, Samuel Costa, Javier Diz-Bugarin, Jesus Blanco-Garcia, Univ. de Vigo (Spain)

The measure of absolute flatness has an undoubted technical interest in different types of applications. All of them take as a common basis the use of an interferometer in Fizeau configuration. The objective of the present work is to explore the advantages and disadvantages that could lead to the realization of measures of absolute flatness through the use of a different configuration, specifically Twyman-Green. For this we have implemented an interferometer of this type in vertical configuration and with an automatic phase evaluation system. In order to process the obtained images we have developed a software that applies the matrix algorithms corresponding to the rotational method, in which three surfaces are compared two to two, plus an additional comparison with one of them in a rotated position. The results obtained confirm the viability of the measurement of absolute flatness in the interferometric configuration mentioned.

Ferrofluids with high dynamic ranges of optical transmission
Paper AO100-43
Author(s): Ángel Sanz-Felipe, Juan Carlos Martín, Zaragoza Univ. (Spain)

We present two ferrofluids in which huge transmission variations can be induced by application of magnetic fields up to 70G. For ferrofluid 1, the presence of a magnetic field multiplies its transmission by a factor up to 50. For ferrofluid 2, its transmission increases up to 50% or decreases up to 70% by applying it perpendicular or parallel to the incident light respectively. The transmission dependence on the applied magnetic field shows an acceptable linearity, which is a very interesting feature face to eventual sensing applications. The time evolution of both ferrofluids' transmission after DC magnetic field switch on and off has also been analyzed. For small enough magnetic fields, the behavior is relatively simple. With a magnetic field greater than a measured critical value, a growing complexity appears which suggests several reorganization stages such as particle orientation, and chain formation. The scattered light evolution observed matches with the above-mentioned stages.

Photonic integrated circuits for NG-EPON
Paper AO100-48
Author(s): Carla Rodrigues, Instituto de Telecomunicações (Portugal); Francisco Rodrigues, Instituto de Telecomunicações (Portugal), PICadvanced SA (Portugal); Mário Lima, Telecomunicações e Informática (Portugal); António Teixiera, Instituto de Telecomunicações (Portugal), PICadvanced SA (Portugal)

This paper intends to propose a monolithic photonic integrated transceiver in the context of Next Generation of Ethernet Passive Optical Network (NG-EPON). This new architecture aims to be used as an Optical Network Unit (ONU) considering a four channel approach. Photonic Integrated Circuits (PICs) are a technology that emerged to address the growing complexity of the hardware that exists nowadays. It consists of integrating numerous optical components in a single chip, leading to reduced complexity, size and power consumption as well as a cost decrease of optical-to-electrical-to-optical (OEO) conversions. These are important characteristics that make PICs a powerful tool to use in several applications. The concept behind the proposed transceiver architecture will be presented together with the steps necessary to deploy the proposed solution. The paper starts by presenting the modeling of Array Waveguide Gratings (AWG), the most important component of this solution. This is followe

Special microstructured fibers with irregular and regular claddings for supercontinuum generation
Paper AO100-49
Author(s): Vladimir P. Minkovich, Marcelo Vaca Pereira Ghirghi, Ctr. de Investigaciones en Óptica A.C. (Mexico); Joel Villatoro, Univ. of the Basque Country (Spain); Alexander B. Sotsky, Mogilev State A. Kuleshov Univ. (Belarus); Maria Asuncion Illarramendi, Joseba Zubia, Univ. of the Basque Country (Spain)

In this report, we inform in detail on fabrication of a special (3 rings of air-holes) nonlinear, index-guiding, air-silica microstructured optical fiber (IG MOF) with different air-hole diameters in the cladding (irregular cladding) and its application for a broadband supercontinuum (SC) generation by femtosecond laser pulses. Our IG MOF has a constant pitch Λ and air-holes with different diameters d. For comparison, supercontinuum generation in a special nonlinear air-silica IG MOF with regular cladding is also investigated. The structure of modes and dispersion properties of the investigated fibers were numerically predicted and experimentally verified. Broadband SC generation from visual wavelengths up to 1600 nm in such fibers, both with the length of 1 m, was observed. Optimal pumping conditions were identified by tuning the center wavelength of the pump. Optimal pump wavelengths agreed well with zero GVDs obtained from numerical analysis.

Clinical performance of an objective methodology to categorize tear film lipid layer patterns
Paper AO100-51
Author(s): Carlos García-Resúa, Hugo Pena-Verdeal, Maria Jesus Giraldez, Eva Yebra-Pimentel, Univ. de Santiago de Compostela (Spain)

Purpose: The aim of this study was to compare the performance of a new objective application designated iDEAS (Dry Eye Assessment System) with 4 experienced observers to categorize different zones of LLPs in one image, by using the Tearscope-plus and a digital camera attached to a slit-lamp. 50 images were captured and analyzed by 4 experienced optometrists. The categorization made by the 4 optometrists was compared with the automatic system and it was found that the automatic system was abble to provide zones similar to the annotations made by experienced optometrists.

$SrMoO_4$:Ho^{3+}:Tm^{3+} crystals for laser application in 2 μm region
Paper AO100-53
Author(s): Elizaveta Dunaeva, Liudmila Ivleva, Maxim Doroshenko, Petr Zverev, Vjatcheslav Osiko, Prokhorov General Physics Institute (Russian Federation)

Solid state lasers, which operate in the spectral region around 2 μm, have great market potential for the use in LIDAR and gas sensing systems. Crystalline materials doped with Tm3+ and Ho3+ ions for developing 2 μm laser are based on the 3F4 →3H6 optical transition of Tm3+ (1.9μm) and the 5I7 →5I8 transition of Ho3+ (2.1μm). Tm3+ ions can also be used as a sensitizer to transfer an absorbed pump energy to Ho3+ ions, so that high power commercial laser diodes at 790 nm can be used to pump Tm3+/Ho3+ co-doped systems.We have developed the growth technology of high optical quality SrMoO4 crystals doped with Ho3+/Tm3+ ions by Czochralski method from the melt in the air. Spectral luminescent characteristics were investigated for as-grown SrMoO4:Ho3+/ Tm3+ crystals. Efficient room temperature lasing under 1700 nm laser diode pumping was obtained in the Tm3+:SrMoO4 crystal with slope efficiency up to 18%. Broad oscillation wavelength tuning within 1840-1980 nm spectral range was obtained.

Experimental study of photon statistics in actively Q-switched fiber lasers and its role in supercontinuum generation
Paper AO100-54
Author(s): Yuri O. Barmenkov, Ctr. de Investigaciones en Óptica A.C. (Mexico); Josue A. Minguela-Gallardo, Centro de Investigaciones en Óptica A.C. (Mexico); Alexander V. Kir'yanov, Ctr. de Investigaciones en Óptica A.C. (Mexico); Georgina Beltran-Perez, Benemérita Univ. Autónoma de Puebla (Mexico)

In this work, we discuss the results of an experimental study of photon statistics of Q-switched pulses in actively Q-switched erbium-doped fiber lasers assembled in two common configurations: (i) Fabry-Perot (F-P) fiber laser (FL) with fiber Bragg gratings (FBGs) as selective couplers and (ii) one-directional ring laser without selective elements. The photon statistics were measured separately for each sub-pulse in train being a ‘whole’ Q-switch pulse. It is shown that pulsing registered from the F-P FL is very noisy, with some peaks of instantaneous noise being approximately an order higher than an averaged pulse, whereas that observed from the loop FL is much less noisy, with difference between noise peaks and averaged pulse being no more than a few percent. We also demonstrate that noisy Q-switched pulses with duration of tens ns can effectively generate supercontinuum, covering a 1550…2000-nm range.

Real time measurement of the E. coli concentration in liquid media with a di-ureasil Mach-Zehnder interferometer sensor
Paper AO100-58
Author(s): Carlos M. S. Vicente, Univ. of Aveiro (Portugal); Rui Oliveira-Silva, Nuno J. O. Silva, Univ. of Aveiro (Portugal), CICECO - Aveiro Institute of Materials (Portugal); Marta Tacão, João P. da Costa, Univ. of Aveiro (Portugal); Rute A. S. Ferreira, Univ. of Aveiro (Portugal), Aveiro Institute of Materials (Portugal); Paulo S. André, Univ. of Lisbon (Portugal), Instituto de Telecomunicações (Portugal)

Herein, we report the fabrication and optical characterization of an E. coli concentration optical sensor based on a Mach-Zehnder interferometer (MZI) imprinted in photo-patternable organic–inorganic di-ureasil hybrids. The sensor was tested for the real-time determination of E. coli cells growth in an aqueous medium. The measured values for the refractive index (RI) of E. coli suspension, in the range of 1.330 to 1.380, are in agreement with the reported theoretical values. E. coli cells concentration was measured during an induced concentration process of the suspension from 3.9×10^9 to 5.4×10^10

cells/mL in less than 5 minutes, requiring only a small drop of suspension. The proposed sensor fabricated with a sol-gel low RI contrast waveguide platform constitutes a compact, fast and cost effective solution for monitoring the concentration of cells, namely, of E. coli, in biological fluids, without the drawback of the ambiguity of a broad measurement range associated with high resoluti

Quantification of the absorption of light in coals using fiber optic sensors
Paper AO100-60
Author(s): Leonardo Alberto Díaz Marulanda, Cesar Orlando Torres Moreno, Univ. Popular del Cesar (Colombia)

The possibility of using lasers diodes and a fiber optic trifurcated for the evaluation of the power optic absorbed on coals samples is studied. The method is based on scanning of samples using a lasers diodes with the wavelengths 632,8nm, 532nm, 405nm, and calibration plots of the reflected luminosity of the selection as function of the absorbance of coals. In this paper we showed the calibration plots and the colorimetric parameters of coals calculated from the absorption or diffuse-reflectance. The advantages of the method are its high performance for estimating the colorimetric parameters of coals samples, quality control of industrial processes, classification of coals and institutions dedicated at the investigations of the coal.

Modeling of dynamics of nanosecond laser ablation in phase explosion regime
Paper AO100-61
Author(s): Vladimir I. Mazhukin, Alexander V. Shapranov, Mikhail M. Demin, Alexander V. Mazhukin, Keldysh Institute of Applied Mathematics (Russian Federation)

Laser action with short pulses of duration from 5 to 10 ns, and high-intensity G=(0.5÷1)x109 Wcm-2 is accompanied by melting, evaporation and formation of a contact and shock wave in the surrounding gas. Modeling of dynamics of heterogeneous mechanisms of laser melting and evaporation-condensation was carried out on the basis of a continuum model that takes into account the processes of hydro- and heat transfer with kinetics of moving interfaces solid-liquid and liquid-vapor. Modeling allowed to determine the temperature and hydrodynamic fields in the target, vapor and air, the propagation velocity of the contact boundary, shock wave and interphase interfaces, taking into account their degree of overheating. Investigation of kinetics of homogeneous mechanism of laser evaporation was carried out in the framework of the atomistic approach. Using molecular - dynamic simulations were defined threshold values of fluence and the main characteristics of phase explosion: number and size of the

Surface enhanced Raman spectroscopy analysis of HeLa cells using a multilayer substrate
Paper AO100-67
Author(s): Iris Aguilar, Instituto Tecnológico y de Estudios Superiores de Monterrey (Mexico); Juan Luis Pichardo-Molina, Ctr. de Investigaciones en Óptica (Mexico); Tzarara López-Luke, Ctr. de Investigaciones en Óptica A.C. (Mexico); Nancy Ornelas-Soto, Centro de Investigaciones en Óptica, A.C. (Mexico)

Numerous cells and tissues have been analysed by normal Raman spectroscopy, but for some cells the resulting spectra can exhibit low signal-to-noise ratio due to the intrinsic low sensitivity of the technique. Surface Enhanced Raman Spectroscopy (SERS) can help overcome the above limitation, allowing the ultrasensitive detection of biomolecules. In this work a SERS active substrate formed by 3 layers of gold nanospheres and a final layer of gold nanocubes was studied for the label-free SERS analysis of a model biological matrix (HeLa cells). The substrate generated high enhancement of peaks associated with important biomolecules.

Doppler broadening effects in plasmonic quantum dots
Paper AO100-78
Author(s): Rúben Azinheira Alves, Miguel B. T. Gomes, INESC TEC, Ctr. of Applied Photonics (Portugal), Univ. of Porto (Portugal); João C. Costa, Nuno A. Silva, Ariel R. N. S. Guerreiro, INESC-TEC (Portugal), Univ. of Porto (Portugal)

In this paper we describe the inhomogeneous broadening of the energy levels of the localized plasmon modes in a moving fluid containing metallic quantum dots. The results are compared with numerical simulations.

Solving the multi-level Maxwell-Bloch equations using GPGPU computing for the simulation of nonlinear optics in atomic gases
Paper AO100-77
Author(s): João C. Costa, Miguel Gomes, Ruben A. Alves, INESC TEC, Ctr. of Applied Photonics (Portugal), Univ. do Porto (Portugal); Nuno A. Silva, INESC TEC (Portugal), Univ. do Porto (Portugal); Ariel Guerreiro, INESC TEC, Ctr. of Applied Photonics (Portugal), Univ. do Porto (Portugal)

We present a numerical implementation of a solver of the Maxwell-Bloch equations to calculate the propagation of a light pulse in a nonlinear medium composed of an atomic gas in two and three dimensional systems. This implementation solves the wave equation of light using a finite difference method in the time domain scheme, while the Bloch equations for the atomic population in each point of the simulation domain are integrated using splitting methods. We present numerical simulations of soliton propagation in coupling-probe configurations.

Fast physical ray-tracing method for gravitational lensing using heterogeneous supercomputing in GPGPU
Paper AO100-80
Author(s): João C. Costa, Miguel Gomes, Ruben A. Alves, INESC TEC, Ctr. of Applied Photonics (Portugal), Univ. do Porto (Portugal); Nuno A. Silva, INESC TEC (Portugal), Univ. do Porto (Portugal); Ariel Guerreiro, INESC TEC (Portugal)

In this work we address the development of a fast solver of the ray-tracing equations based on heterogeneous supercomputing using PyOpenCl. We apply this solver to the study of gravitational lensing and light propagation in optical systems.

Ultrasensitive detection of phenolic antioxidants by surface enhanced Raman spectroscopy
Paper AO100-81
Author(s): Nancy Ornelas-Soto, Iris A. Aguilar-Hernández, Instituto Tecnológico y de Estudios Superiores de Monterrey (Mexico); Nils Kristian Afseth, Nofima AS – Norwegian Institute of Food, Fisheries and Aquaculture Research (Norway); Tzarara López-Luke, Ctr. de Investigaciones en Óptica AC (Mexico); Flavio Contreras-Torres, Instituto Tecnológico y de Estudios Superiores de Monterrey (Mexico); Jens Petter Wold, Nofima AS – Norwegian Institute of Food, Fisheries and Aquaculture Research (Norway)

Surface-Enhanced Raman Spectroscopy (SERS) is a powerful surface-sensitive technique to study the vibrational properties of analytes at very concentrations. In this study, SERS measurements carried out evaluated for the phenolic antioxidants ferulic acid, p-coumaric acid, caffeic acid and sinapic acid. A number of SERS active Ag colloids were synthesized and characterized. A SERS method based on the Ag colloids was developed for the detection of the selected molecules. The SERS-active silver colloids showed an effective signal enhancement, reaching low concentrations (2.5x10-9M). For caffeic acid and coumaric acid, this detection limit has been reached for the first time, as well as the SERS analysis of Sinapic acid using silver colloids.

Tunable light fluids using quantum atomic optical systems
Paper AO100-84
Author(s): Nuno A. Silva, João Costa, Miguel Gomes, Ruben Alves, Ariel Guerreiro, INESC TEC, Ctr. of Applied Photonics (Portugal), Univ. do Porto (Portugal)

The propagation of light in a bulk defocusing cubic nonlinear media is well described within the framework of the Generalized Nonlinear Schrödinger equation, which through the use of the Madelung transformation can be interpreted into a hydrodynamic description of light. In this description, the laser intensity maps into the light fluid density and the fluid velocity is related with the spatial phase gradient. In this work, we will show how one can use quantum atomic optical systems to develop highly tunable

optical media based on the electromagnetically induced transparency, with spatial control of both linear and nonlinear susceptibility. Also, we will introduce the theory to explore the superfluid behavior of light in these atomic media and purpose a strategy to create connected geometries, discussing and investigating through GPU-enhanced numerical simulations the existence of quantized persistent currents.

Dissipative solitons in 4-level atomic optical systems
Paper AO100-86
Author(s): Nuno A. Silva, Miguel Gomes, João Costa, Ruben Alves, Ariel Guerreiro, INESC TEC, Ctr. of Applied Photonics (Portugal), Univ. do Porto (Portugal)

The study of the dynamics of optical systems under non-equilibrium conditions is currently a topic of increasing importance in photonics, as exploring novel regimes such as response to ultra-short pulses and dissipative processes plays an important role in the engineering of new optical materials capable of addressing the needs of modern technology. Still, the role of decoherence and dissipation processes in the optical response of atomic optical systems is under-explored. A particular interesting problem is the possibility of the existence of dissipative soliton, stable self-localized wave solutions that can be formed in non-equilibrium systems when the dissipation fades out or is counter-balanced by gain mechanisms. In this work we present a model to describe the propagation of an optical pulse in a 4-level atomic system and deduce it as an equation that allows dissipative soliton solutions, supporting the results with numerical simulations based on the Maxwell-Bloch equation.

Simulation of the interaction between an atom and a coherent ultrashort laser pulse including radiative losses
Paper AO100-88
Author(s): Miguel B. T. Gomes, João C. Costa, Rúben A. Alves, INESC TEC, Ctr. of Applied Photonics (Portugal); Nuno A. Silva, Ariel R. N. S. Guerreiro, INESC TEC (Portugal)

In this paper we describe the development of a numerical solver or the Maxwell-Schrodinger equations with radiative losses that describe the interaction of a coherent ultrashort laser pulse with an hydrogen atom. Numerical simulations are used to study the response of the atom as a function of the pulse parameters. The application of the code to study atoms with multiple electrons is also discussed.

Solver of the Einstein equations using GPUs under the gravitoelectromagnetic approximation
Paper AO100-90
Author(s): Miguel B. T. Gomes, João C. Costa, Rúben A. Alves, INESC TEC, Ctr. of Applied Photonics (Portugal); Nuno A. Silva, Ariel R. N. S. Guerreiro, INESC TEC (Portugal)

Under specific conditions, there is a formal analogy between the fundamental equations of electromagnetism and relativistic gravitation, described by the Einstein field equations of general relativity. In this paper, we report on how we have used this analogy to implement a solver of the Einstein equations adapting algorithms initially developed for electromagnetism, combined with methods of heterogeneous supercomputing, in GPU that can achieve fast computing and exhibit good performance. We also present the results of the simulations used to validate our solver.

SPR immunosensor for the detection of emerging pollutants in water samples
Paper AO100-91
Author(s): Melissa Rodríguez-Delgado, Iris A. Aguilar-Hernández, Lab. de Nanotecnología Ambiental, Ctr. del Agua para América Latina y el Caribe (Mexico); Donato Luna-Moreno, Ctr. de Investigaciones en Óptica A.C. (Mexico); Nancy Ornelas-Soto, Lab. de Nanotecnología Ambiental, Ctr. del Agua para América Latina y el Caribe (Mexico)

The continuous contamination of worldwide water bodies by the presence of emerging pollutants has raised great importance the last decades. Some of these chemicals are daily life items, such as pharmaceutical compounds; which are extensively used and constantly released into the aquatic ecosystems by human activities and direct discharges from wastewater treatment plants. These pollutants encompass human and veterinary drugs, which have been recognized as part of the hazardous

compounds able to risk public and environmental health. In this work, our interest was focused on the detection of the b-lactam antibiotics in water by a Surface Plasmon Resonance biosensor. Amoxicillin was chosen as a probe molecule to be measured by a custom-designed SPR platform based on an indirect competitive immunoassay, using highly specific monoclonal antibodies.

Physical ray-tracing method for anisotropic optical media in GPGPU
Paper AO100-99
Author(s): Ariel Guerreiro, INESC TEC, Ctr. of Applied Photonics (Portugal), Univ. do Porto (Portugal); Miguel T. Gomes, João P. Costa, Rúben A. Alves, Nuno A. Silva, Univ. do Porto (Portugal), INESC-TEC (Portugal)

In this work we address the development of a fast solver of the ray-tracing equations based on heterogeneous supercomputing using PyOpenCl. We apply this solver to the study of the propagation of light and image formation in anisotropic heterogeneous optical media.

First approach on the Haar transform using a 2 x 2 multimode interferometer
Paper AO100-100
Author(s): João Fernandes, Instituto de Telecomunicações (Portugal), Departamento de Electrónica, Telecomunicações e Informática (Portugal); Francisco Rodrigues, Telecomunicações e Informática (Portugal), Instituto de Telecomunicações (Portugal), PICadvanced SA (Portugal); Mário Lima, Telecomunicações e Informática (Portugal), Instituto de Telecomunicações (Portugal); António Teixeira, Telecomunicações e Informática (Portugal), Instituto de Telecomunicações (Portugal), PICadvanced SA (Portugal)

Nowadays, Wavelet Transforms are being used as a prime method of image processing and compression. Among all varieties of Wavelet Transforms, the Haar Wavelet Transform arises a solution which allows uncomplicated design and fast computation. Since both forward and inverse Haar Transforms require only additions and subtractions, they can be implemented by optical planar interferometry. This paper presents a Multimode Interferometer, based on the self-image principle, capable of reproducing the Haar Transform. Due to possibility of implement the Haar Transform, the device is named Magic-T.

Partially polarized pseudo Schell-model sources
Paper AO100-102
Author(s): Rosario Martinez-Herrero, David Maluenda, Univ. Complutense de Madrid (Spain); J. Carlos G. de Sande, Univ. Politecnica de Madrid (Spain); Gemma Piquero, Univ. Complutense de Madrid (Spain); Massimo Santarsiero, Franco Gori, Univ. degli Studi di Roma Tre (Italy), CNISM (Italy)

In this work a new type of partially polarized sources are proposed. These sources are partially polarized and partially coherent with coherence characteristics that are not shift invariant as occurs for Schell-model sources. The coherence and polarization characteristics of this kind of fields at the plane source and upon free space propagation are analysed in detail.

Study of an optical sensor for the measurement of hydrostatic pressure in microfluids using a bubble resonator.
Paper AO100-104
Author(s): Duber A. Avila Padilla, Cesar O. Torres Moreno, Univ. Popular del Cesar (Colombia)

In this work the properties of measurement of an optical sensor based on an optical cavity in the form of a bubble made from the polymer PMMA for the measurement of the hydrostatic pressure in microfluids were studied. During the investigation, it is proposed the design and manufacture of cavities from the polymethylmethacrylate PMMA polymer using a heating technique to achieve bubbles with an external diameter of 1950 µm and wall thickness of 23 µm achieving a sensitivity of 0.5566 nm/bar for a thin-wall bubble. The phenomenon of hydrostatic pressure measurement in fluids using the cavity can be explained by its use as an optical resonator capable of confining the field to the interior of the cavity through the approximation of a taper fiber which provides an evanescent field which is coupled to the

interior of the cavity by exciting the so-called Whispering Gallery WGMs produced by the total internal reflection phenomenon inside the device.

Theoretical analysis of a PMMA polymer capillary microresonator for measuring the relative humidity
Paper AO100-107
Author(s): Fredy Amador Donado, Duber A. Avila Padilla, Cesar O. Torres Moreno, Univ. Popular del Cesar (Colombia)

In this work, it is reported the theoretical study of a sensor based on an optical microresonator with capillary shape for measuring the hydrostatic pressure in fluids. The sensitivity of the device for measuring the hydrostatic pressure is analyzed from Maxwell's equations considering the micro-capillary as a structure of three layers with different refractive index. Along the analysis, the field confinement within the microcavity is studied through WGMs modes with independent polarization states leading to the eigenvalue equation for determining the wavelengths of resonance that can support the cavity. In this research, shifts wavelengths of resonances are studied in terms of the hydrostatic pressure inside the cavity and the geometric parameters of the cavity. In the mathematical analysis of the problem it is possible to determine the optical sensitivity of the device when it experiences changes in hydrostatic pressure within the cavity.

Theoretical analysis of the sensitivity of an optical sensor based on a capillary microresonator for measuring the hydrostatic pressure in microfluids
Paper AO100-109
Author(s): Duber A. Avila Padilla, Cesar O. Torres Moreno, Univ. Popular del Cesar (Colombia); Cristiano M. B. Cordeiro, Univ. Estadual de Campinas (Brazil)

In this work, it is reported the theoretical study of a sensor based on an optical microresonator with capillary shape for measuring the hydrostatic pressure in fluids. The sensitivity of the device for measuring the hydrostatic pressure is analyzed from Maxwell's equations considering the micro-capillary as a structure of three layers with different refractive index. Along the analysis, the field confinement within the microcavity is studied through WGMs modes with independent polarization states leading to the eigenvalue equation for determining the wavelengths of resonance that can support the cavity. In this research, shifts wavelengths of resonances are studied in terms of the hydrostatic pressure inside the cavity and the geometric parameters of the cavity. In the mathematical analysis of the problem it is possible to determine the optical sensitivity of the device when it experiences changes in hydrostatic pressure within the cavity as a function of different parameters.

Refractive index sensitivity in etched FBG on the visible range
Paper AO100-114
Author(s): Jean Filipe Kuhne, Rafael Battistella Nadas, Patrícia Loren Inácio, Ismael Chiamenti, Ricardo Canute Kamikawachi, Univ. Tecnológica Federal do Paraná (Brazil); Hypolito J. Kalinowski, Univ. Federal Fluminense (Brazil)

A visible fiber Bragg grating (Vis-FBG) was inscribed in a multimode fiber designed for infrared (IR) operation using a femtosecond (fs) laser emitting at 248nm. The VIS-FBG has its wavelength peak centered at 673.07 nm. The fiber was dipped into a 40% hydrofluoric acid (HF) solution until the wavelength shifted about 0.29 nm. After the chemical etching, the fiber’s diameter was measured with a given value of 7.00 ± 0.14 nm. The refractive index sensitivity was carried out by dipping the sensor into diluted glycerin solution at different concentrations (0.00 to 90.0%). Experimental results showed a sensitivity of 15.71 nm/RIU for a refractive index of 1.4607

Coherent Rayleigh noise sensitive OTDR for dynamic strain sensing
Paper AO100-119
Author(s): Guilherme Dutra, Uilian J. Dreyer, Rafael J. Daciuk, Guilherme H. Weber, Jean C. C. da Silva, Marco J. da Silva, Daniel R. Pipa, Cicero Martelli, Univ. Tecnológica Federal do Paraná (Brazil)

In this paper tests results of a distributed optical dynamic strain sensor using a Coherent Rayleigh Noise sensitive Optical Time-Domain Reflectometer CRN-OTDR are presented. The pulse width is 10 ns (1 m spatial resolution) at a 10 kHz repetition rate. The experimental setup consists of three fiber sections (1 m each), located at different positions on the fiber under test. Detection using three different fiber section excited at different moments is performed successfully as well and the resonant frequency to each fiber section is determined with error smaller than 4%.

The method angular spectrum for Fresnel diffraction in term of Fourier fractional transform from title in circular aperture: theory and simulations
Paper AO100-121
Author(s): Jaime Castillo Pérez, Carlos J. Jiménez Ruiz, Univ. de la Guajira (Colombia); Cesar O. Torres Moreno, Univ. Popular del Cesar (Colombia); Susana A. Salinas, Univ. del Zulia (Venezuela); Juan M. Vilardy, Univ. de la Guajira (Colombia)

We applied the method angular spectrum for the numerical computation of Fresnel diffraction in term of Fourier fractional transform from, patterns from circular aperture title at an arbitrary angle to the optical axis. Detailed theoretical formalism is developed and discussed, and then is applied for the numerical computation and simulation of the actual diffraction patterns for an arbitrary optical configuration. The generated intensity distributions images show distortion and stretching in the direction of the tilt, but not in the other orthogonal direction. Significant decrease of the intensity is also predicted and observed, the decrease being proportionate with the tilt angle. The simulated images qualitatively resemble those published in the literature. In addition to single-axis tilts, simultaneous rotations tilts of the aperture in two orthogonal coordinate axes were also briefly considered and simulated.

Real color fractional Fourier transform holograms: using fiber optics
Paper AO100-122
Author(s): Carlos J. Jiménez Ruiz, Samuel E. Zambrano Rojas, Juan M. Vilardy, Univ. de la Guajira (Colombia); Cesar O. Torres Moreno, Univ. Popular del Cesar (Colombia); Susana A. Salinas, Univ. del Zulia (Venezuela)

A new experimental setup to obtain the complex distribution in amplitude and phase of a real color image is proposed and implemented. This holographic configuration is based on fractional Fourier transform techniques and uses a bifurcated optical fiber interferometer. Three focused lasers beams, with different wavelengths (RGB), are passed through the optical system and produced two holographic images: one obtained from the reflections on the surfaces (the hologram) and other from the transmitted beam. The holographic images are recorded by a CCD camera and processed using an iterative computer algorithm based of the fractional Fourier transform. It can be shown that the obtained holographic image quality is better than those generated by traditional methods

Study of photo activation reaction of experimental graphene dental nanocomposites through dynamic laser speckle.
Paper AO100-123
Author(s): Marianne Salas, Ana Yebra, Antonio Manuel Pozo Molina, Cristina Lucena, María del Mar Pérez Gómez, Univ. de Granada (Spain)

The objective of this study was to characterize the photo activation reaction of experimental graphene dental nanocomposites and to compare this reaction between commercial nanocomposite by dynamic laser speckle patterns. One commercial nanocomposite and two experimental graphene nanocomposites were used. LED curing unit was used to produce the photo activation reaction. While this reaction occurs, speckle patterns were generated by the incident light from the laser diode. These patterns were captured with the CMOS camera at a rate of 16 images/second. Later the speckle correlations was calculated. The photo activation process originates different speckle patterns between the nanocomposites used. Speckle activity of the commercial nancocomposite increases rapidly immediately withthe exposure to curing light and continues slowly after the irradiation. The experimental graphene nanocomposites speckle activity decreases after ignition of the curing unit, without the initial increment.

A model for prediction of color change after tooth bleaching based on CIELAB color space
Paper AO100-125
Author(s): Luis Javier Herrera, Rosa Pulgar, Ana Yebra, María José Rivas, Maria del Mar Pérez Gómez, Univ. de Granada (Spain)

An experiment was performed aiming to develop a model based on CIELAB color space for prediction of color change after tooth bleaching procedure. 40 subjects were treated with a 20% carbamide peroxide tooth-bleaching agent. Subsequently, the color of teeth was determined using a spectroradiometer and these measurements were repeated to 0, 7, and 14 days. Multivariate linear regression models were obtained to predict the L*, a*,b* and W* index post-bleaching values depending on the CIELAB color coordinates values prior to bleaching. Univariate linear regression models were obtained to predict the variation in C*, h^o and W*. The models show that the most saturated and with lowest hue angle teeth obtain the best results after the tooth bleaching The models obtained can be applied to predict the color change prior to bleaching, which means a great step forward in the clinical practice.

Finite element model for the simulation of laser activated micro- and nano-scale drug delivery systems
Paper AO100-126
Author(s): Henrique Vilhena, Glasgow Caledonian Univ. (United Kingdom); João M. P. Coelho, José M. Rebordão, Univ. de Lisboa (Portugal)

This paper describes a flexible model that can be used to simulate laser-based photoactivation of drug delivery systems. It considers Gaussian beams and the heat diffusion equation is solved by the finite element method. As an example, a typical liposome geometry in the focal volume of a laser beam is simulated and the results are compared with experimental data obtained in the literature, showing a good agreement. The model has potential in the design of drug delivery systems as it can be a starting point for the development of new kinds of micro- and nano-scale drug delivery systems.

Short-length long period fiber grating for torsion sensing applications
Paper AO100-127
Author(s): Marta Nespereira, João M. P. Coelho, José M. Rebordão, Univ. de Lisboa (Portugal)

The response of short-length CO2 -induced Long Period Fiber Gratings (LPFGs) sensors to torsion is reported. While engraving, the fiber is submitted to high tension allowing to obtain gratings with shorter lengths, one order of magnitude lower than the usual. Also, the fiber was only irradiated in one side, creating an asymmetrical profile leading to highly birefringent gratings. Good sensitivity to axial twists is demonstrated, with values from 0.11 to 0.99 nm/(rad/m) for the resonant wavelength shift, and 0.03 to 0.10 dBm/(rad/m) for the variation in the intensity. Discrimination between rotation direction, clockwise and counterclockwise, can be obtained.

Semiconductor quantum dots in optical fibers
Paper AO100-134
Author(s): Sindi Horta, Duber A. Avila, Cesar O. Torres, Univ. Popular del Cesar (Colombia); José Sierra Ortega, Univ. del Magdalena (Colombia)

This research highlights the potential use of semiconductor quantum dots QDs as an optical field source for fiber based telecommunications systems or through dielectric waveguides. During the investigation, it is proposed to study the use of light emitted by a quantum dot assembly QDs em-bedded in SiO2 as a mechanism to improve coherence and reduce the losses of the transmitted wave along an optical fiber. In the work, a simulation is performed to study the propagation characteris-tics of a soliton profile wave emitted by a quantum dot through a nonlinear optical fiber solving the nonlinear Schrödinger equation using the Fourier Split Step method.

Full Poincaré beams obtained by means of uniaxial crystals
Paper AO100-140

Author(s): Juan Carlos G. de Sande, Univ. Politécnica de Madrid (Spain); Massimo Santarsiero, Univ. degli Studi di Roma Tre (Italy); Gemma Piquero, Univ. Complutense de Madrid (Spain)

The generation of non-uniformly totally polarized beams and the study of their applications is a subject of increasing interest in the last years. A particular class of these beams are the so-called full Poincaré beams that have the property of presenting all possible polarization states across its transverse section, perpendicular to the propagation direction. Several methods have been proposed to generate such kind of beams as, for example, the use of symmetrically stressed windows or spatial light modulators. Here we present a simple and easy way to obtain a full Poincaré beam. This method is based on the use of an initially linearly polarized beam that propagates along the optics axis of a uniaxial crystal. When slight divergence of the beam is considered, both ordinary and extraordinary waves propagate through the crystal and, at the ouput of the crystal, a non-uniformly polarized beam is obtained. In this work it will be shown that this ouput beam is a full Poincaré beam. Differe

Fiber Bragg grating embedded in polymer 3D printed material for acceleration measurement
Paper AO100-143
Author(s): Rita Lima, INESC TEC, Ctr. of Applied Photonics (Portugal); Rafael Tavares, LAETA-INEGI (Portugal); Susana Silva, INESC-TEC (Portugal); Paulo Abreu, Maria T. Restivo, LAETA-INEGI (Portugal); Orlando Frazão, INESC-TEC (Portugal), Porto Univ. (Portugal)

We propose a fiber optic accelerometer, based on fiber Bragg grating (FBG) sensors, in a 3D printed cubic geometry. Three FBG sensors were embedded in 3D printed coating, placed in three different axis position on the cubic face structure. The first tests with the cubic structure were characterized. The FBG sensors were submitted to displacement (mm) and temperature (ºC). After appropriate signal processing, it will be possible to obtain the velocity (mm/s) and the acceleration (G) of the cubic structure.

Infrared light sensor applied to early detection of tooth decay.
Paper AO100-148
Author(s): Eberto Benjumea, José Espitia, Leonardo Díaz, César Torres, Univ. Popular del Cesar (Colombia)

The approach dentistry to dental care is gradually shifting to a model focused on early detection and oral-disease prevention; one of the most important methods of prevention of tooth decay is opportune diagnosis of decay and reconstruction. The present study aimed to introduce a procedure for early diagnosis of tooth decay and to compare result of experiment of this method with other common treatments. In this setup, a laser emitting infrared light is injected in core of one bifurcated fiber-optic and conduced to tooth surface and with the same bifurcated fiber the radiation reflected for the same tooth is collected and them conduced to surface of sensor that measures thermal and light frequencies to detect early signs of decay below a tooth surface, where demineralization is difficult to spot with x-ray technology. This device will can be used to diagnose tooth decay without any chemicals and rays such as high power lasers or X-rays.

Optoelectronic implementation of a nonlinear joint transform correlator-based encryption system
Paper AO100-151
Author(s): Juan M. Vilardy Ortiz, Univ. Popular del Cesar (Colombia); María S. Millán, Elisabet Pérez-Cabré, Univ. Politècnica de Catalunya (Spain)

In this work, an experimental validation of a nonlinear joint transform correlator-based encryption system is presented. The fully phase input plane of the joint transform correlator (JTC) architecture is composed by two non-overlapping data distributions. The first distribution is the input image information encoded in phase and placed against the first random phase mask (RPM-I), and the second distribution contains the second random phase mask (RPM-II) key. The encrypted image is obtained in the Fourier domain by introducing nonlinear operations in the joint power spectrum (JPS). The nonlinear encryption system is implemented using an optoelectronic setup. We obtain the encrypted image by using an experimental

two-step JTC. The decryption system is implemented using computational simulations. We present experimental and digital results that support our proposal.

Images encryption and authentication systems based on the photon-counting technique and a nonlinear joint transform correlator
Paper AO100-152
Author(s): Juan M. Vilardy Ortiz, Univ. de la Guajira (Colombia); María S. Millán, Elisabet Pérez-Cabré, Univ. Politècnica de Catalunya (Spain)

The integration of the photon-counting technique with the nonlinear encryption system based on a joint transform correlator (JTC) in order to authenticate and verify a primary image and a random phase code, respectively, in a secure and simultaneous manner is presented. The encryption system uses the double random phase encoding (DRPE) in the Fourier domain (FD). The DRPE is implemented using a nonlinear nonzero-order JTC architecture. The integration of the photon-counting technique in the information processing system increases the security of the encryption system and also, makes the authentication system more robust against unauthorized attacks. The simultaneous authentication process of the primary image and the random phase code is performed by means of the nonlinear correlation in the FD. Numerical simulations show the validity and feasibility of these new security and authentication systems.

The USC-OSA-EPS section activities in optics
Paper AO100-154
Author(s): María Aymerich, Ferran Cambronero, Ángel Aragón, Tamara Delgado, Ana I. Gómez-Varela, Ana Gargallo, Ángel Sánchez, Sandra Williamson, Adán Amorín, María Teresa Flores-Arias, Facultade de Óptica e Optometría (Spain)

The USC-OSA Student Chapter and USC-EPS Young Minds Section is a group financed by OSA and the EPS formed by PhD and Physics degree students from the Universidade de Santiago de Compostela and one supervisor of the Faculty of Physics. Its main goal is to promote Optics in the society. The group carries out several activities in the academic and non-academic community. One of them consists on visiting schools located in our city and its surroundings to explain to primary and secondary students the basic principles of Optics by means of simple and visual experiments.It has been performed for several years in different schools with good acceptance among both children and teachers.The group is also committed to the professional development of our members, organising conferences and bringing lecturers to our Faculty to explain their research.Moreover, the chapter motivates the exposition of our work into the scientific community.

Direct formation of nanostructures by focused electron beam on a surface of thin metallic films
Paper AO100-156
Author(s): Jānis Sniķeris, Vjaceslavs Gerbreders, Daugavpils Univ. (Latvia)

This paper describes the method, which allows obtaining the metallic nanostructures (MN) with a focused electron beam irradiation in a scanning electron microscope (SEM) in one fabrication step and without the use of additional chemicals. MN – nanodots were obtained by 30kV SEM on the surface of various metallic thin films (Al, Cr, Cu, Mo, Ag). The thin films were prepared by direct current magnetron sputtering on the Si substrate with 500 nm thickness. The size and shape of the obtained MN were measured with an atomic force microscope. The height of the nanodots was up to 500 nm and their width at half height was in range from 100 to 500 nm. The size of the obtained MN depends on the parameters of the electron beam and the properties of the metal. The possible mechanisms of MN forming under the influence of focused electron beam are discussed.

Real-time measurement of ocular wavefront aberrations in accommodative disorders
Paper AO100-160
Author(s): Sandra M. Franco, Univ. do Minho (Portugal); Jessica Gomes, Univ. of Minho (Portugal)

From ocular aberrations it is possible to compute several accommodation parameters like the lag of accommodation. The ocular aberrations were measured in 5 subjects, with different accommodative

disorders, during several cycles of accommodation/disaccommodation and for different accommodative stimulus. The measurement was done continuously and in real-time during different accommodative stimulus. From the ocular aberrations, the lag of accommodation was compute for all the subjects.The measurement of wavefront ocular aberrations can be a tool to diagnose accommodative disorders. In some subjects with complains, this method showed anomalies before the usual clinical exams did it.

Assessing the wavefront aberrations of the emmetropic eye after a reading task
Paper AO100-161
Author(s): Sandra M. Franco, Cristina M. Oliveira, Univ. do Minho (Portugal)

Purpose: The main goal of this study was to investigate the effect of performing a near task on eye's optical quality. Methods: Wavefront aberrations data of 35 young emmetropic eyes were measured with the L80 Wave+: (1) ocular aberrations were measured with the wavefront sensor, (2) corneal wavefront aberrations were computed from the Placido disk system's data and (3) the internal wavefront component of the eye were determined as the difference between ocular and corneal wavefront aberrations. The measurements were performed before and after a reading task was completed. Results: Several corneal and internal aberration terms changed in opposite directions with the reading task, most of them changing its sign relative to the pre-task condition. The opposite sign between the cornea and the internal optics produced a partial balance that leaved the eye with less aberrations than the individual components. Furthermore, the optical quality of the eye and the retinal image quality changes

Lateral light polarization in lenses
Paper AO100-165
Author(s): Lázaro J. Miranda Díaz, CEADEN (Cuba)

When a linearly polarized light beam incident on a lens are made to manifest the algebraic properties of geometric shapes, such as the intersection between a plane and a spherical surface, a polarized light beam is composed of electromagnetic waves to oscillate in planes parallel to each other and in the same direction. Taking one of these planes to affect orthogonally on the spherical surface of a convex lens, the light is reflected and refracted without leaving the plane which belongs, Now if the polarization plane of polarized light beam is rotate, not the lens, then also changes the direction of the rays reflected and refracted as they remain within the plane of polarization of light.

Changes in the optical properties of the eye with the use of computers
Paper AO100-167
Author(s): Sandra M. Franco, Univ. do Minho (Portugal); Andreia Gonçalves, Univ. of Minho (Portugal)

It is estimated that today that about 75% of professional occupations involve the use of computers. In the last years several studies have been carried out on Computer Visual Syndrome, most of which have found that there is a decrease in blinking, a greater percentage of incomplete blinking, and a decrease in the lipid layer. In addition to tear change, some studies have concluded that there are alterations in binocular vision and accommodation, although there is some controversy regarding this topic. Several studies report that after computer use there is an increase in exophoria, an increase in convergence insufficiency, lower fusional convergence, and less accommodative range, while others say that people with exophoria have fewer symptoms. On the other hand, changes in the optical properties of the eye were found with paper reading. Therefore, it is important to realize if there are also changes with the accomplishment of tasks with computers and if these are identical or not to t

FAB-Laser: femtosecond ablation with shaped laser pulses
Paper AO100-168
Author(s): Victor Hariton, Gonçalo Figueira, Hugo Pires, Univ. de Lisboa (Portugal); Celso Paiva João, Univ. de Lisboa, Instituto Superior Técnico (Portugal)

Femtosecond pulses are typically employed for high precision microprocessing of high quality materials on the micro/nanoscale, but they are also able to probe and shape delicate living structures without damaging them. In this work, we propose to investigate the mechanism of ultrafast laser ablation for

biological applications by employing simultaneous spatial and temporal shaping of the laser beam. Our goal is to investigate whether we can design laser pulses that enable better, faster, more precise interaction with matter. We present the design of the pulse and beam shaping stations as well and discuss their effects under a range of different parameters.

Organic semiconductor rubrene thin films prepared by matrix-assisted pulsed laser evaporation
Paper AO100-176
Author(s): Natalia Majewska, Gdansk Univ. of Technology (Poland); Gerard Sliwinski, Rafał Jendrzejewski, Miroslaw Szawczak, Szewalski Institute of Fluid-Flow Machinery (Poland); Sayani Majumdar, Univ. of Turku (Finland)

Organic semiconductor rubrene belongs to most preferred spintronic materials because of the highest charge carrier mobility up to 40 cm2(V·s)-1. In this work the preparation and properties of rubrene thin films deposited with use of matrix-assisted pulsed laser evaporation (MAPLE) are reported. The frozen rubrene solutions (0.23-1% wt) in aromatic solvents such as toluene, xylene, dichloromethane and 1,1-dichloroethane (DCE) serve as target ablated by a pulsed (2-20 Hz) 1064 nm or 266 nm laser operated at fluence of 0.22-10.37 J/cm2. Films are deposited on Si, SiO2/ITO and Si/SiO2 substrates in vacuum (10-6 mbar). The Raman and AFM data for deposited thin film how presence of the mixed crystalline and amorphous rubrene phases. Agglomerates of rubrene crystals are revealed by SEM observation and the UV-vis absorbance spectra of the films correspond closely to those of the genuine rubrene sample.

Optical design for ultra intense, high bandwidth laser systems
Paper AO100-178
Author(s): Alexis Boyle, Marco Galimberti, Ian Musgrave, Rutherford Appleton Lab. (United Kingdom)

The next generation of high power, short pulse lasers require optical propagation systems and techniques to allow them to maintain high bandwidth, >150nm, high fluence beam line. In order to achieve the ultra-intense pulses, the beam must be compressed to sub 30fs, this requires good spatial quality over a large bandwidth. Here we present optical designs for beam propagation and beam expansion in such laser systems.

Evaluating polarization diversity for speckle reduction in retinal images
Paper AO100-183
Author(s): Diego Hincapie Zuluaga, Univ. Nacional de Colombia (Colombia); Jorge Herrera, Instituto Tecnológico Metropolitano (Colombia); Nelson Correa, ITM (Colombia); Raul Castañeda, Univ. Nacional de Colombia (Colombia); J. Gaviria, ITM (Colombia); Mikel Aldana, Univ. Politecnica de Cataluña (Spain)

Retinal imaging quality measurements (double-pass & Hartmann-Shack) using spatially coherent light sources like lasers or superluminescent diodes suffer from the presence of speckle in the final images. This well-known phenomenon diminishes the performance of those systems. Although solutions to this problem have been proposed, there still exist room to implement effective methods to face this challenge. We evaluate the influence of changing the polarization states of a laser beam in a double-pass system in order to reduce the speckle noise. By rotating the linear polarization state during the exposure time of the camera the speckle changes and partially averages out. We use the speckle contrast metric to evaluate the performance of the proposed method over experimental results.

Effects of photochromic furan-based diarylethenes on gold/silver nanoparticles aggregation
Paper AO100-185
Author(s): Alina Khodko, Khomenko Vadim, Olexander Mamuta, Valeriy Voitsekhovich, Institute of Physics (Ukraine); Iuliia Mukha, Chuiko Institute of Surface Chemistry (Ukraine); Nataliya Kachalova, Institute of Physics (Ukraine)

The diarylethene derivatives (DAEs) - photochromic molecules that can be reversibly switched between open-ring (OF) and closed-ring (CF) forms by external optical and/or electrical stimulation, attract considerable attention since these molecular switches grafted on metal nanoparticles are the promising base for optoelectronic elements and smart materials. The photochromic cyclization dynamics of furan-

based diarylethenes was studied by femtosecond transient absorption spectroscopy and their interaction with gold/silver nanoparticles were investigated by ultraviolet/visible absorption spectroscopy and transmission electron microscopy. Nanoparticles coupled with diarylethene derivatives exhibit a new surface plasmon resonance band coming from their aggregation. We analyzed the effects of functional side-chain groups on aggregation process. These results can be considered as a basis for further designing of novel hybrid nanomaterials and optoelectronic elements.

Modeling and possible implementation of self-learning equivalence-convolutional neural structures for auto-encoding-decoding and clusterization of images
Paper AO100-187
Author(s): Vladimir G. Krasilenko, Vinnitsa Social Economy Institute (Ukraine); Alexander A. Lazarev, Vinnitsa National Technical Univ. (Ukraine); Diana V. Nikitovich, Vinnitsa Social Economy Institute (Ukraine)

Self-learning equivalence-convolutional neural structures (SLECNS) for auto-encoding-decoding and clusterization of images will be discussed. We shall consider these SLECNS and their spatial-invariant equivalental models (SIEMs) based on the corresponding matrix-matrix (or tensor) procedures using as basic operations of continuous logic and nonlinear processing. We show that these SIEMs have several advantages, such as the ability to recognize of image fragments with best efficiency and strong mutual correlation. The proposed clustering method of fragments with regard to their structural features is suitable not only for binary, but also color images and combines self-learning and the formation of weight clustered matrix-patterns. Its model is constructed and designed on the basis of recursively processing algorithms and to k-average method. The experimental results confirmed that larger images and 2D binary fragments with a large numbers of elements may be clustered. For the first

Photo-induced ultrasound microscopy for photo-acoustic imaging of non-absorbing specimens
Paper AO100-189
Author(s): Elena Tcarenkova, Sami Koho, Pekka E. Hänninen, Univ. of Turku (Finland)

Photo-Acoustic Microscopy (PAM) has raised a special interest in pre-clinical imaging of different animal models due to its ability to preserve the near-diffraction limited spatial resolution of optical microscopes, whilst extending the penetration depth to the mm-range. Another advantage of PAM is that it is a label-free technique -- any substance that absorbs light at the excitation wavelength can be viewed with PAM. However, not all samples absorb light sufficiently to provide contrast for imaging. This work describes a novel imaging method that makes it possible to visualize optically semi-transparent samples that lack intrinsic photoacoustic contrast, without the addition of contrast agents. A thin, strongly light absorbing layer is used to generate a strong ultrasound signal that can be used to obtain an ultrasound image on any PAM.

3D printed THz sieves
Paper AO100-195
Author(s): Walter D. Furlan, Univ. de València (Spain); Federico Machado, Ctr. de Tecnologías Físicas, Univ. Politècnica de València (Spain); Przemysław Zagrajek, Institute of Optoelectronics, Military Univ. of Technology (Poland); Juan A. Monsoriu, Ctr. de Tecnologías Físicas, Univ. Politècnica de València (Spain)

Imaging at terahertz (THz) frequencies are every day more frequent in many applications including: security screening, iodetection, telecommunications and spectroscopy. In many cases these applications need specially designed lenses with customized characteristics that are not commercially available. In this work we present a new concept of THz diffractive lenses with advantageous properties: The THz sieves. These leneses are the counterpart of the photon sieves, introduced here for the first time to focus THz radiation. We show that these diffractive lenses can be constructed by 3D printing. Nimerical and experimental results show that these lenses have improved resolution and therefore can be useful in THz imaging systems and other applications in which focusing THz radiation is needed.

A method to produce HHG with multicycle lasers using cross polarized wave generation on solid targets
Paper AO100-197
Author(s): Ferran Cambronero-López, Manuel Blanco, Univ. de Santiago de Compostela (Spain); Camilo Ruiz, Instituto Universitario de Fisica Fundamental y Matemáticas (Spain); Maria Teresa Flores-Arias, Carmen Bao-Varela, Univ. de Santiago de Compostela (Spain)

The generation of ultrashort attosecond pulses arouses the attention of the community due to its capability to extend our understanding of the ultrafast atomic and molecular dynamics. To produce this attosecond pulses, a femtosecond laser pulse is focused on either a gas or a solid target. For circular polarization the HHG is partially suppressed while for linear polarization the generation is optimized. Hence, it is possible to control the HHG by tailoring the polarization of the ultrashort laser pulse. This idea can be implemented through a several complex experimental techniques. It usually requires the use of few cycle laser pulses [], which are expensive. However during the last years different schemes propose to use multicycle lasers, which are the most common femtosecond laser system. In this communication we propose the use of the Cross Polarized Wave Generation (XPWG) nonlinear effect to produce a temporal polarization axis on an input pulse. Due to its nonlinear nature, only

Multimodal texture analysis of OCT images as a diagnostic application for skin tumors
Paper AO100-198
Author(s): Oleg O. Myakinin, Dmitry S. Raupov, Ivan A. Bratchenko, Valery P. Zakharov, Alexander G. Khramov, Samara Univ. (Russian Federation)

Optical coherence tomography (OCT) is an effective tool for determination of pathological topology that reflects structural and textural metamorphoses of tissue. In this paper, we propose a report about our examining of the validity of OCT in identifying changes using a skin cancer texture analysis compiled from Haralick texture features, fractal dimension, complex directional field features and Markov random field method from different tissues. Finally, the Boosting has been used to combine all heterogeneous texture method introduced before to single multimodal texture analysis method for the quality enhancing of the diagnosis method. We obtained sensitivity about 96% and specificity about 99% for a task of discrimination between malignant melanoma and nevus.

An efficient method for classifying skin tumors based on the two-dimensional Fourier fractal analysis
Paper AO100-201
Author(s): Wei Gao, Ningbo Univ. of Technology (China); Dmitry S. Raupov, Oleg O. Myakinin, Samara Univ. (Russian Federation); Hui Huang, Chunji Zhuang, Xinlong Zhou, Ningbo Univ. of Technology (China); Ivan A. Bratchenko, Valery P. Zakharov, Samara Univ. (Russian Federation)

Optical coherence tomography (OCT) is employed in the diagnosis of the skin tumors. The fractal dimension was extracted from OCT images and was used as indicators to classify the skin tumors. The two dimensional Fourier fractal analysis was performed on OCT images for classifying the melanomas, basal cell carcinomas and pigment nevi. Our results suggested that the two dimensional Fourier fractal analysis could provide a more efficient method to differentiate skin tumors as compared to the two dimensional differential box-counting method.

The electromagnetic induced transparency effect in hollow-core microstructured optical fibres
Paper AO100-207
Author(s): Sílvia M. G. Rodrigues, Margarida Facão, Mário F. S. Ferreira, Univ. de Aveiro (Portugal)

The electromagnetic induced transparency (EIT) is a phenomenon that can be observed in which a medium becomes transparent for a probe field due to interactions between a pump field with the medium. In this phenomenon, the light turns out to have special features, such as the possibility of being slow-light. Here, we study the effects of fibre guidance on the probe field under the EIT effect, and we have found some conditions, in an incoherent medium, where we predict gains on the light propagation.

Thermal effects in LPG generated by moderate power signals
Paper AO100-214
Author(s): Xavier Roselló-Mechó, Univ. de València (Spain); Martina Delgado-Pinar, Luis Poveda-Wong, Univ. de Valencia (Spain); José Luis Cruz, Antonio Díez, Univ. de València (Spain); Miguel V. Andrés, Univ. de Valencia (Spain)

Resonances of optical fiber whispering gallery modes (WGM) exhibit high Q and are sensitive to small variations of material properties and geometrical parameters. In this paper we report the characterization of thermal effects induced in UV-irradiated photo-sensitive fibers and in long period gratings (LPG) recoded with UV irradiation, when they are illuminated with an optical signal of moderate power, ~1 W. Our results show that the UV radiation increases the absorption coefficient of the fibers in more than one order of magnitude. In the case of LPG, the heating is not uniform resulting in a thermally induced chirp. The comparison of our results with direct measurement of the losses induced by the UV-irradiation gives information on the relative contribution of absorption and scattering to the overall fiber losses.

Long period fiber gratings of subnamometric bandwidth: fabrication with a UV laser
Paper AO100-215
Author(s): Luis Poveda-Wong, Univ. de Valencia (Spain); José Luis Cruz, Univ. de València (Spain); Martina Delgado-Pinar, Univ. de Valencia (Spain); Xavier Roselló-Mechó, Antonio Díez, Univ. de València (Spain); Miguel V. Andrés, Univ. de Valencia (Spain)

This paper reports on the fabrication of long period fiber gratings (LPG) having subnanometric bandwidth in the 1500 nm spectral region. Selecting high numerical aperture photosensitive fibers we demonstrate the fabrication of LPG with a full width at half maximum (FWHM) of 0.83nm and 0.68nm for gratings 15 and 20 cm long respectively. Polarization effects and excitation of quasy-degenerated modes are discussed. The sensitivity of the gratings to the surrounding refractive index, temperature and strain variations is presented as well.

An advanced arrangement of the optical spectrograph based on acousto-optical and cross-disperser techniques for astronomical applications
Paper AO100-217
Author(s): Alexandre S. Shcherbakov, Adan O. Arellanes, Eduardo Tepichin Rodriguez, Vahram Chavushyan, Instituto Nacional de Astrofísica, Óptica y Electrónica (Mexico)

We develop a new avenue to creating the optical spectrometer for the Guillermo Haro astrophysical observatory (Mexico), which combines specifically progressed prism spectrometer with modern acousto-optical approach in the frame of a joint instrument. This schematic arrangement includes two principal novelties. First, we exploit recently developed acousto-optical nonlinearity of the two-phonon light scattering in crystals with linear acoustic losses, which admits an additional physical degree of freedom. This effect allows us to use nonlinear acousto-optical effect for linear processing of optical signals in parallel regime within all the visible range. Similar effect is based on the possibility for tuning the frequency of elastic waves and admits the nonlinear apodization improving the dynamic range. Secondly, we are using the cross-disperser technique with acousto-optical processing for the first time to our knowledge.

Stationary light trapping in cold atoms
Paper AO100-218
Author(s): José-António Rodrigues, Univ. do Algarve (Portugal), Instituto de Plasmas e Fusão Nuclear (Portugal); João D. Rodrigues, António F. Vito, Hugo F. Terças, José T. Mendonça, Instituto de Plasmas e Fusão Nuclear (Portugal)

In an optically thick cloud of cold atoms, the strong attenuation of an incoming laser beam is responsible for the transfer of such photons from the laser into a multiplicity of diffusion modes, due to multiple scattering of light. In such conditions, light transport inside the medium bares strong similarities with heat transport, described by a diffusion process, which depends on the local atom density. On the other hand,

the local density of photons influences the atomic dynamics via radiation pressure effects. Here, we experimentally demonstrate that such strong coupling between light transport and atom dynamics can lead to the nucleation of stable structures where light is trapped, similar to photon bubbles, often considered in astrophysical scenarios.

Cross-spectral periocular recognition using correlational filters
Paper AO100-219
Author(s): Kiran Raja, Raghavendra Ramachandra, Norwegian Univ. of Science and Technology (Norway)

Most of the current operational iris biometric systems use Near-Infra-Red (NIR) for in constrained conditions. However, the recent use of visible spectrum for iris recognition has resulted in iris/ocular images captured in visible light. In order to have robust comparison of visible spectrum ocular images against NIR spectrum ocular images, we explore the problem of cross-spectrum recognition for biometric authentication. In order to achieve this, we employ a database of ocular images captured using two different cameras operating in visible spectrum and NIR spectrum. The database consists of ocular images captured from 120 different subjects amounting to 240 unique ocular samples. We propose a framework which leverages the ocular features using correlational descriptors with a unique way of score combination for each set of correlational descriptor.

Set-to-set distance metric learning for efficient gender classification using extended spectral images
Paper AO100-220
Author(s): Kiran Raja, Raghavendra Ramachandra, Norwegian Univ. of Science and Technology (Norway)

We explore the problem of gender classification using the spectral images captured in 9 different spectral wavelengths. In order to explore the problem, we have collected a face image database of 168 subjects with 92 male and 76 female subjects. In order to address the problem, in this work, we explore Set-to-Set Distance Metric Learning (SSDML) for classifying the gender. SSDML has been previously explored in many visual classification tasks with a great success including the gender classification in visible spectrum image domain. However, there has been no earlier works exploring the set-based metric learning to classify the genders with the images captured in extended-spectral domain. Thus, this work presents a new paradigm of using SSDML for classifying the genders in extended spectral domain. Further, we also present a comparative analysis of the proposed approach with other state-of-art gender classification approaches to demonstrate the applicability of the SSDML.

Image phase encryption and decryption schemes through Gyrator domains and chaotic random phase masks
Paper AO100-225
Author(s): Juan M. Vilardy Ortiz, Univ. de la Guajira (Colombia); Carlos J. Jimenez, Samuel E. Zambrano, Univ. de La Guajira (Colombia)

We use the double random phase encoding (DRPE) in the Gyrator domain (GD), chaotic random phase masks (CRPMs) and a random permutation of the Jigsaw transform (JT) in order to implement a system for digital images encryption-decryption. The DRPE utilizes two random phase masks (RPMs) to encode the image to encrypt (original image) into a random noise. The JT applied to the resulting image of the DRPE technique allows to obtain an encrypted image more random. We use the chaos theory with the purpose of generating the two RPMs of the DRPE, these masks are CRPMs. The generation of the CRPMs are controlled by the parameters of the chaotic function. The encryption-decryption system has the following security keys: the rotation angles of the GTs, the parameters of the chaotic function utilized to generate the two CRPMs and the random permutation of the JT. When all the proper security keys are used in the decryption system, the obtained decrypted image is a replica of the image to encrypt.

Novel multiband polarization beam splitter based on a dual-core transversally chirped microstructured optical fiber

Paper AO100-229
Author(s): Erick Estefen Reyes Vera, Institute Tecnologico Metropolitano (Colombia), Universidad Nacional de Colombia (Colombia); Freiman Gomez, Juan Usuga Restrepo, Nelson Gomez Cardona, Institute Tecnologico Metropolitano (Colombia)

A novel compact and multiband polarization beam splitter based on a dual-core transversally chirped microstructured optical fiber is proposed and analyzed using finite element method. The results show that the 2.7 mm-long polarization splitter can reach an extinction ratio lower than -10 dB in two bands with bandwidths of 52.12 nm and 62.65 nm respectively. In addition, in this work the operation of the device is analyzed when it is subjected to changes of curvature and we find that it is possible to tune the operating bands and the bandwidths with this method. Numerical calculation indicate that this novel structure may find applications in telecommunications, being capable of working in different wavelength ranges, which can be tuned through changes in the curvature.

The impact of surfactant on structural, optical and photocatalytic activity of ZnO nanostructures
Paper AO100-233
Author(s): Manish Kumar, Univ. de Aveiro (Portugal); Ritesh Soni, Indian Institute of Science (India); Shalaka Varshney, Raman Research Institute (India); Luiz Pereira, Univ. de Aveiro (Portugal)

The presence of surfactants cetyltrimethylammonium bromide (CTAB) and diethylene glycol (DEG) on the surface of zinc oxide (ZnO) nanostructures resulted in variation in their size, crystal structure, and optical properties. The spherical, rod and needle-shaped morphology of the samples are characterized. Hexagonal and cubic wurtzite crystal structures were determined by X-ray diffraction (XRD) pattern. The optical properties of each surfactant-capped zinc oxide nanostructures were investigated using UV–visible absorption techniques. The absorption spectra of ZnO prepared in mixture showed a significant blue shift compared to pure DEG and CTAB. The results indicate that the mixture of CTAB and diethylene glycol can significantly modify the shape and size of ZnO nanostructures. Time-dependent degradation of methyl orange-ZnO shows the photocatalytic activity of synthesized ZnO nanostructures.

Nonlinear joint transform correlator architectures for images encryption, decryption and authentication systems
Paper AO100-236
Author(s): Juan M. Vilardy Ortiz, Univ. de la Guajira (Colombia); María S. Millán, Elisabet Pérez-Cabré, Univ. Politècnica de Catalunya (Spain)

We present several joint transform correlator (JTC) architectures for nonlinear images encryption, decryption and authentication systems. These JTC architectures are developed in different processing domains, such as Fourier, Fractional Fourier, Fresnel and Gyrator domains. Some of these processing domains can add new security keys in order to improve the security of the images encryption, decryption and authentication systems. In this work, we review and present recent nonlinear modifications of encryption decryption and authentication systems based on JTC architecture that allow to significantly increase the quality of the retrieved image after information decryption, and to achieve a high security level against a variety of system attacks.

Design of low-loss photonic crystal fiber based on porous-core with elliptical holes in THz regime
Paper AO100-237
Author(s): Erick Estefen Reyes Vera, Institute Tecnologico Metropolitano (Colombia), Univ. Nacional de Colombia (Colombia); Juan Usuga Restrepo, Institute Tecnologico Metropolitano (Colombia); Juan Botero Cadavid, Univ. Nacional de Colombia (Colombia); Johana Zuñiga, Institute Tecnologico Metropolitano (Colombia)

In this work, we present a new design of a low loss and high birefringent THz Photonic Crystal fi-ber on TOPAS material based on porous core with elliptical holes. This configuration has a total fiber diameter of 3200 µm and a diameter of holes in the cladding (d) equal to 271 µm and the dis-tance of separation between the holes of 285 µm. The core is composed for an array of ellipses with semi-axis a and b are 12.7 µm and 19.1 µm respectively, the array of ellipses have a pitch equal to 42.4 µm. The full-vector

finite element method was employed to analyze the optical properties such as birefringence, confinement losses and dispersion and how these depend on the geometrical struc-ture. The simulation results show a confinement losses ≈1.26×10-12 dB/m when is implemented a configuration with high grade of porosity in the core. At the same time, there were obtained bire-fringence values close to 3×10-3, which can be controlled through the manipulation of geometrical parameters. Finally,

Detection of low frequency, out-of-plane vibrations by the Talbot effect and adaptive photodetectors
Paper AO100-238
Author(s): Ponciano Rodríguez-Montero, Eduardo Tepichín-Rodriguez, Nikolai Korneev, Instituto Nacional de Astrofísica, Óptica y Electrónica (Mexico)

Detection and measurement of low frequency, out-of-plane vibrations plays a very important role in several metrological applications. Classical interferometry is well suited for measuring small amplitudes of vibrations, ranging from picometers up to micrometers, but its use is limited to a laboratory environment. In this work we consider the Talbot effect and the so-called adaptive photodetectors based on the non-steady-state photo-electromotive force effect for the measuring of low frequency, out-of-plane of vibrations of flat objects with rough surfaces; with amplitudes of vibrations in the order of microns. Experimental results that verify our proposal are presented. It is worth noting that the obtained results are in very good agreement with those obtained with a Michelson interferometer.

Multi-arm spectrometer for parallel frequency analysis of radio-wave signals oriented to astronomical observations
Paper AO100-240
Author(s): Alexandre S. Shcherbakov, Miguel Chavez Dagostino, Adan O. Arellanes, Eduardo Tepichín-Rodriguez, Instituto Nacional de Astrofísica, Óptica y Electrónica (Mexico)

We describe a potential prototype of modern spectrometer based on acousto-optical technique with a few parallel optical arms for analysis of radio-wave signals specific to astronomical observations. The arrangement under development has two principal novelties. First, each individual optical arm represents an individual spectrum analyzer with its individual performances. Such an approach is conditioned by exploiting various materials for acousto-optical cells operating within various regimes, frequency ranges, and light wavelengths from independent light sources. The other novelty consists in the usage of unique acousto-optical materials for creating wide-aperture acousto-optical cells. Here, one can mention specifically selected cuts of tellurium dioxide, bastron, lithium niobate, and rutile, which overlap the frequency range from 30 MHz to 3.5 GHz. Thus one yields the united versatile instrument providing comprehensive studies of astronomical objects simultaneously.

Straight edge diffraction of OAM waves
Paper AO100-243
Author(s): Paula López, Zayda Reyes, Yezid Torres, Jesús Mendoza, Univ. Industrial de Santander (Colombia); Ángela Guzman, Univ. Nacional de Colombia (Colombia)

In this communication we will present a numerical simulation of the Fraunhofer regime propagation of a straight edge diffracted beam, described as a superposition of OAM waves.